REPORT DOCUMENTATION PAGE

1. AGENCY USE ONLY (Leave b	2. REPORT DATE	3. REPORT TYPE AND DATES COVERED
	1-Oct-00	Annual Report 10/1/99-9/30/00

4. TITLE AND SUBTITLE
Modelling Swell High Frequency Spectral and Wave Breaking

5. FUNDING NUMBERS
N00014-98-1-0070

6. AUTHOR(S)
V. E. Zakharov

7. PERFORMING ORGANIZATION NAME(S) AND ADDRESS(ES)
Department of Mathematics
617 N. Santa Rita Avenue
University of Arizona
Tucson, Arizona 85721

8. PERFORMING ORGANIZATION REPORT NUMBER

9. SPONSORING /MONITORING AGENCY NAMES(S) AND ADDRESS(ES)
Office of Naval Research, Program Officer C.L. Vincent ONR 321 CD
Ballston Centre Tower One,
Arlington, VA 22217-5660

10. SPONSORING/MONITORING AGENCY REPORT NUMBER

11. SUPPLEMENTARY NOTES

12a. DISTRIBUTION/AVAILABILITY STATEMENT
Approved for public release; distribution unlimited.

12b. DISTRIBUTION CODE

13. ABSTRACT (Maximum 200 words)

In 2000 research in framework of the grant N000 14-98-1 0070 was performed by Dr. V. E. Zakharov in collaboration with Dr. A. Pushkarev and Dr. A. Dyachenko. A part of the work was done in collaboration with our French colleague Dr. F. Dias and his graduate student P. Guyenne. The results of the research are summarized in five articles. Three of them are accepted for publication. The results were reported on five international conferences.

14. SUBJECT TERMS

15. NUMBER OF PAGES
3

16. PRICE CODE

17. SECURITY CLASSIFICATION OF REPORT	18. SECURITY CLASSIFICATI	19. SECURITY CLASSIFICATION OF ABSTRACT	20. LIMITATION OF ABSTRACT
UNCLASSIFIED	UNCLASSIFIED	UNCLASSIFIED	UL

Progress Report
N00014-98-1-0070

"Modelling Swell High Frequency Spectral and Wave Breaking"

Principal Investigator, V.E. Zakharov

1 October 1999 - 30 September 2000

In 2000 research in framework of the grant N000 14-98-1 0070 was performed by Dr. V. E. Zakharov in collaboration with Dr. A. Pushkarev and Dr. A. Dyachenko. A part of the work was done in collaboration with our French colleague Dr. F. Dias and his graduate student P. Guyenne. The results of the research are summarized in five articles. Three of them are accepted for publication. The results were reported on five international conferences. Research was performed in the following directions:

1. Constants of motion in the SNL models.

The most solidly justified approach to the description of nonlinear interaction of sea waves is the use of the kinetic equation for the spectral density of wave action first derived by K. Hasselmann in 1962. Since this time several codes for the numerical solution of the kinetic equation were developed. Different codes give qualitatively similar but quantitatively slightly different results. So far there was no universal test making it possible to estimate a quality of a given numerical code. We offer such a test based on the use of four conservative quantities preserved by the kinetic equation: wave action, energy and two components of momentum.

Using this constant of motion is not a trivial problem. The SNL is a complicated nonlinear integral operator, describing the nonlocal interaction of waves in the K-space. Due to this nonlocality there is a "leakage" of the motion constant outside of any finite domain of integration. We made estimates of this leakage and found that if the domain of integration is bounded by the wave number K, the leakage is going to the extended domain bounded by the wave number 3/2K. This result creates the theoretical foundation for development of the "clean" universal test for examination of different codes for solution of the kinetic equation. The results are summarized in the articles [1,2] and to be reported in the Workshop of Wave Prediction in Monterey (November 6-10 2000).

2. Nonlocal diffusion models of SNL.

In 1999 we offered a simple euristic model of SNL making it possible to speed up its computer simulation in four orders of magnitude. This model is based on the use of a simple nonlinear diffusion operator. It works very well for broad in angle spectra but fails for narrow in angle spectral distribution. To fix this point we offered an array of nonlocal diffusion models including averaging the spectrum over angle. The new model includes seven fitting constants which can be found by an optimal way as soon as we will have a "paragon" exact numerical model of the SNL. These results were reported on the workshops of wave modeling in Delft(March 2000), Reykjavic(June 2000) and are to be reported in Monterey (November 2000). The article on this subject is in preparation.

3. New approach to the problem of wave breaking.

In collaboration with A. Dyachenko we developed a completely new approach to the description of the dynamics of an ideal fluid with a free surface. The new exact equation describing the fluid dynamics are suitable for analytical study and numerical simulatuion. The first results of their numerical solution are very promising. We hope by the use of the new approach to soon develop a solidly justified analytical and numerical model of wave breaking.

One article is accepted for publication, another one is in preparation. The result will be reported on the workshop on singularities in classical, Quantum and Magnetic fluids. 20-23 October, 2000 in Warwick, UK.

4. One-dimensional model of wave turbulence in deep water.

In collaboration with Dr. F. Dias and P. Guyenne we performed a detailed analytical and numerical study of the MMT(Maida, McLaughlin and Tabak) model of wave interaction in one dimenstion. We established a fundamental role of the localized wave group(quasisolitons) in this turbulence. These results can be used for the explanation of the formation of the "rogue waves" dangerous for coastal construction.
They were reported on the Conference of Wave Turbulence(June 2000, Massachusetts)
Two articles are accepted for publication.

References

1. On conservation of the constant of motion in the models of nonlinear wave interaction, A. Pushkarev and V. Zakharov, to be published in the Proceedings of the Workshop of Wave Prediction, Monterey (November 2000)

2. A. Pushkarev, V. Zakharov

3. On the dynamics of ideal fluid with free surface, A. Dyachenko, to be published in Reports of Russian Academy of Science

4. Turbulence of one-dimenstional weakly nonlinear dispersive waves, V. E. Zakharov, P. Guyenne, A. N. Pushkarev and F. Dias, to be published in Proceedings of the Workshop on Wave Turbulence

5. V. E. Zakharov, P. Guyenne, A. N. Pushkarev and F. Dias, to be published in Physica D

Turbulence of one-dimensional weakly nonlinear dispersive waves

V. E. Zakharov, P. Guyenne, A. N. Pushkarev, and F. Dias

ABSTRACT. The turbulence of weakly nonlinear dispersive waves is studied by numerically integrating a three-parameter one-dimensional model equation. In particular the validity of weak turbulence theory is assessed. The predicted power-law solutions are explicitly determined and then compared with the numerical results. For both signs of nonlinearity, it is shown that the weakly turbulent regime is strongly influenced by the presence of coherent structures. These are wave collapses and quasisolitons.

1. Introduction

The weak turbulence theory developed by Zakharov [8] is a tool for obtaining the shape of frequency spectra in problems dealing with weakly nonlinear dispersive waves. The applications of this theory range from water waves in hydrodynamics to ion-acoustic waves in plasma physics. The weak turbulence theory is based on a hamiltonian formulation of the problem where only resonant interactions between weakly nonlinear waves are taken into account. It is then possible to derive approximate equations by performing perturbation expansions in terms of the nonlinearity parameter. Although the theory was developed more than thirty years ago, few proofs, either experimental or numerical, have been given to assess its validity (e.g. [7]). Recently, Majda et al. [5] proposed a one-dimensional model equation as a basis to check the validity of weak turbulence theory. Numerical computations on this model have been reported in [1], [3], [5] and [9]. In this paper we summarize the most important numerical results on this equation, which depends on three parameters, and show that the weakly turbulent regime is strongly influenced by the presence of coherent structures, namely wave collapses and quasisolitons.

1991 *Mathematics Subject Classification.* Primary 76F55; Secondary 60H15.

Key words and phrases. weak turbulence, Kolmogorov spectra, water waves, wave collapse, quasisoliton.

The first and the third authors were supported in part by US Army, under the grant DACA 39-99-C-0018, and by ONR, under the grant N00014-98-1-0439. The second and fourth authors were supported in part by DGA, under the contract ERS 981135. The four authors were supported as well by NATO, under the Linkage Grant OUTR.LG 970583.

2. One-dimensional model equation

The following three-parameter nonlinear dispersive equation was proposed by Majda et al. [5]:

$$\mathrm{i}\frac{\partial \hat{\psi}_k}{\partial t} = \omega_k \hat{\psi}_k + \int T_{123k}\,\hat{\psi}_1\hat{\psi}_2\hat{\psi}_3^*\,\delta(k_1+k_2-k_3-k)\,dk_1dk_2dk_3\,. \tag{2.1}$$

In equation (2.1), which has been written in Fourier space, $\hat{\psi}_k$ denotes the k-th component in the Fourier decomposition of the complex wave field $\psi(x,t)$ and $(*)$ stands for complex conjugation. Equation (2.1) depends on three parameters. The first parameter, α, is related to the linear frequency $\omega_k = |k|^\alpha$. The second parameter, β, is related to the interaction coefficient

$$T_{123k} = \lambda\,|k_1k_2k_3k|^{\beta/4}\,. \tag{2.2}$$

The third parameter, λ, which also appears in the interaction coefficient (2.2) and is equal to ± 1, governs the balance between dispersive and nonlinear effects. One can use the terminology *focusing* for $\lambda = -1$ and *defocusing* for $\lambda = +1$. The system possesses two important first integrals, the Hamiltonian

$$H = \int \omega_k|\hat{\psi}_k|^2dk + \frac{1}{2}\int T_{123k}\hat{\psi}_1\hat{\psi}_2\hat{\psi}_3^*\hat{\psi}_k^*\,\delta(k_1+k_2-k_3-k)\,dk_1dk_2dk_3dk$$

and the wave action (or number of particles)

$$N = \int |\hat{\psi}_k|^2dk\,.$$

Equation (2.1) describes four-wave resonant interactions satisfying

$$k_1 + k_2 = k_3 + k \tag{2.3}$$

$$\omega_1 + \omega_2 = \omega_3 + \omega_k\,. \tag{2.4}$$

It can be shown that when $\alpha < 1$ the system (2.3)-(2.4) has nontrivial solutions and that dominant interactions occur between four waves. In all computations the parameter α has been set equal to $1/2$. This case mimics gravity waves in deep water, whose dispersion relation is given by $\omega_k = (gk)^{1/2}$, where g is the acceleration due to gravity. Computations for $\lambda = +1$ were performed by Majda et al. [5]. Computations for $\lambda = \pm 1$ were recently performed by Cai et al. [1] and by Zakharov et al. [9].

3. Kolmogorov-type spectra

For a weak nonlinearity, Zakharov's theory [10] leads to a kinetic equation for the two-point correlation function $n_k = \langle|\hat{\psi}_k|^2\rangle$:

$$\begin{aligned}\frac{\partial n_k}{\partial t} &= 4\pi\int |T_{123k}|^2\,(n_1n_2n_3 + n_1n_2n_k - n_1n_3n_k - n_2n_3n_k)\\ &\quad\times\,\delta(\omega_1+\omega_2-\omega_3-\omega_k)\,\delta(k_1+k_2-k_3-k)\,dk_1dk_2dk_3\,.\end{aligned}$$

The two main hypotheses for deriving the kinetic equation are the assumptions of gaussianity and of random phases. The stationary Kolmogorov-type solutions are given by

$$n_k = a_1\,|Q|^{1/3}\,k^{-2\beta/3-1+\alpha/3} \tag{3.1}$$

$$n_k = a_2\,|P|^{1/3}\,k^{-2\beta/3-1} \tag{3.2}$$

TABLE 1. Slope and flux sign for the Kolmogorov-type solutions (3.1)-(3.2). The dispersion parameter α is equal to 1/2.

β	-1	$-3/4$	$-1/2$	$-1/4$	0	$+3$
power of k in (3.1)	$-1/6$	$-1/3$	$-1/2$	$-2/3$	$-5/6$	$-17/6$
sign of Q	$+$	$+$	0	$-$	$-$	$-$
power of k in (3.2)	$-1/3$	$-1/2$	$-2/3$	$-5/6$	-1	-3
sign of P	$-$	0	$+$	$+$	$+$	$+$

and are associated respectively with a particle flux Q and an energy flux P. The coefficients a_1 and a_2 denote the dimensionless Kolmogorov constants. It is important to emphasize that these solutions do not depend on the sign of nonlinearity λ. Such solutions can be written for all values of β and $\alpha < 1$. But there is a physical argument which plays a crucial role in deciding the realizability of the Kolmogorov-type spectra. Suppose that pumping is performed at some frequencies around $\omega_k = \omega_f$ and damping at ω_k near zero and $\omega_k \gg \omega_f$. Weak turbulence theory then states that the energy is expected to flow from ω_f to higher ω_k's (direct cascade with $P > 0$) while the particles mainly head for lower ω_k's (inverse cascade with $Q < 0$). Accordingly, we need to evaluate the fluxes in order to select, among the rich family of power laws (3.1) and (3.2), those which are likely to result from numerical simulations of equation (2.1) with damping and forcing. Only the cases

$$\beta < -3/2 \quad \text{and} \quad \beta > 2\alpha - 3/2$$

i.e.

$$\beta < -3/2 \quad \text{and} \quad \beta > -1/2 \quad \text{if} \quad \alpha = 1/2$$

are relevant because they correspond to a particle flux towards large scales ($Q < 0$) and to an energy flux towards small scales ($P > 0$). The signs of the fluxes are shown in Table 1 for $\alpha = 1/2$ [9]. Computations are performed in the range $\beta > -1/2$, which includes the case of simple cubic nonlinearity ($\beta = 0$) and the case of gravity waves ($\beta = 3$).

4. Solitons, collapses and quasisolitons

The numerical results presented below show that the weakly turbulent regime is strongly influenced by the presence of coherent structures. These are solitons, quasisolitons or collapses. The existence of solitons depends on the parameter λ. Looking for soliton solutions of (2.1) of the form

$$\hat{\psi}_k(t) = e^{i(\Omega - kV)t}\hat{\phi}_k$$

with Ω and V constant leads to

$$\hat{\phi}_k = -\frac{1}{\Omega - kV + \omega_k} \int T_{123k}\, \hat{\phi}_1 \hat{\phi}_2 \hat{\phi}_3^* \, \delta(k_1 + k_2 - k_3 - k)\, dk_1 dk_2 dk_3 \,. \tag{4.1}$$

For $\alpha < 1$, the condition $\Omega - kV + |k|^\alpha \neq 0, \forall k \in \mathbb{R}$, implies that the propagating speed V is zero. Rewriting equation (4.1) in variational form:

$$\delta(H + \Omega N) = 0$$

one can conclude that 'stationary' solitons can exist only if $\lambda = -1$. In that case an equilibrium between nonlinear and dispersive effects is possible. As for nonlinear Schrödinger-type equations, the linear stability criterion for solitons is given by $\partial N/\partial\Omega > 0$ [4]. In our case this gives

$$\beta < \alpha - 1$$

i.e.

$$\beta < -1/2 \quad \text{if} \quad \alpha = 1/2\,.$$

Therefore the solitons are unstable in the regime of interest.

In view of this result, it is natural to look at the formation of collapses. They are typically described by self-similar solutions of the form

$$\hat{\psi}_k(t) = (t_0 - t)^{p+i\epsilon}\,\chi(\xi)$$

where

$$\xi = k\,(t_0 - t)^{1/\alpha}, \quad p = \frac{\beta - \alpha + 2}{2\alpha}, \quad \epsilon = \text{arbitrary constant}\,.$$

An analysis of the convergence of the Hamiltonian and of the wave action integral as $t \to t_0$ shows that necessary conditions for collapses to exist when $\alpha = 1/2$ are $\beta > -1/2$ for $\lambda = -1$, which coincides with the soliton instability criterion, and $\beta > 0$ for $\lambda = +1$. In spectral space, the self-similar solution behaves at $t = t_0$ like

$$n_k \simeq k^{-\beta+\alpha-2} \tag{4.2}$$

which is analogous to Phillips spectrum for deep water gravity waves [6].

In the case $\lambda = +1$, quasisolitons can exist. These are approximate solutions of equation (4.1) which look like envelope solitons. In the limit of a narrow spectrum centered at $k = k_m$, such as $\Omega - k_m V + k_m^\alpha \neq 0$, these quasisolitons are given by

$$\psi(x,t) \simeq \phi(x - Vt)\,e^{i\Omega t + ik_m(x-Vt)}$$

with ϕ, Ω and V given by

$$\phi(\xi) = \sqrt{\frac{\alpha(1-\alpha)}{k_m^{\beta-\alpha+2}}}\,\frac{\kappa}{\cosh(\kappa\,\xi)}\,, \quad \kappa = |k - k_m| \ll k_m$$

$$\Omega = -(1-\alpha)\,k_m^\alpha - \frac{1}{2}\alpha\,(1-\alpha)\,k_m^{\alpha-2}\kappa^2\,, \quad V = \alpha\,k_m^{\alpha-1}\,.$$

When κ/k_m is small, the quasisolitons look almost like true solitons and can persist for a long time. They can play an important role in weak turbulence. When κ/k_m is large, the quasisolitons can become unstable and develop into wave collapse.

5. Numerical results

The numerical computations are performed by adding to equation (2.1) a source term in a narrow spectral band as well as a damping term containing a wave action sink at large scales and an energy sink at small scales:

$$\mathrm{i}\frac{\partial\hat{\psi}_k}{\partial t} = \omega_k\hat{\psi}_k + \int T_{123k}\,\hat{\psi}_1\hat{\psi}_2\hat{\psi}_3^*\,\delta(k_1 + k_2 - k_3 - k)\,dk_1dk_2dk_3 + \mathrm{i}\,(F_k + D_k)\,\hat{\psi}_k \tag{5.1}$$

with

$$F_k = \sum_j f_j\delta(k - k_j) \quad \text{and} \quad D_k = -\nu^-\,|k|^{-d^-} - \nu^+\,|k|^{d^+}\,.$$

FIGURE 1. Level of nonlinearity as a function of time. The parameters are $\alpha = 1/2, \beta = 0$ and $\lambda = +1$ (solid line); $\lambda = -1$ (dashed line).

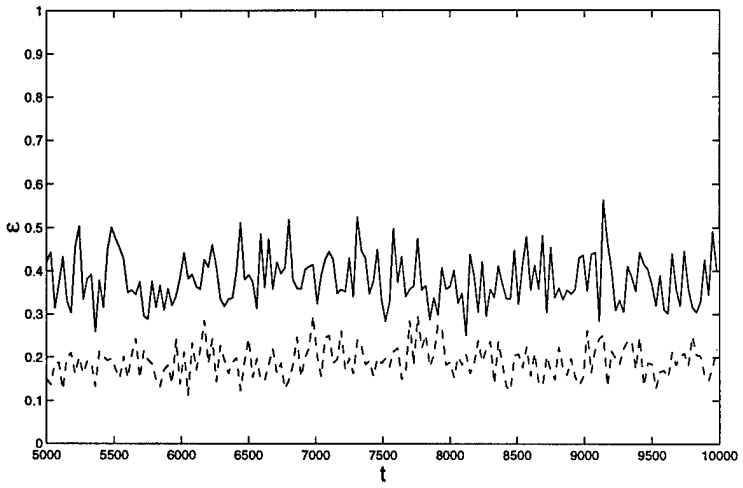

A pseudospectral code is used to integrate equation (5.1). Details can be found in [9].

5.1. Numerical results for $\beta = 0, \lambda = \pm 1$. The study is restricted to the direct cascade. Typical initial conditions are given by random noise. Simulations are run until a quasi-steady regime is established which is characterized by small fluctuations of the energy and the number of particles around some mean value. Then time averaging begins and continues for a length of time which significantly exceeds the characteristic time scale of the slowest harmonic from the inertial range (free of the source and the sink). In turn, the time-step of the integration has to provide, at least, accurate enough resolution of the fastest harmonic in the system. As our experiments show, one has to use an even smaller time-step than defined by the last condition: the presence of fast nonlinear events in the system requires the use of a time-step $\Delta t = 0.005$, which is 40 times smaller than the smallest linear frequency period. Time averaging with such a small time step leads to a computationally time-consuming procedure despite the one-dimensionality of the problem. Figure 1 shows the time evolution of the average nonlinearity ϵ, which is defined as the ratio of the nonlinear part to the linear part of the Hamiltonian, each part being calculated over the whole field. Of course, this definition does not really make sense when external forces are applied but it provides a relatively good estimation of the level of nonlinearity once the system reaches the steady state. The mean values of ϵ are 0.4 when $\lambda = +1$ and 0.2 when $\lambda = -1$. They are relatively small. Thus, the condition of small nonlinearity required by the theory holds for both systems. However the theory cannot explain the difference in the values of ϵ, since the same forcing is imposed in both systems.

The difference between the focusing and the defocusing cases is even more obvious when one looks at the dissipation rates of particles and quadratic energy

TABLE 2. $\alpha = 1/2, \beta = 0$. Time-averaged values of the wave action, quadratic energy and corresponding fluxes in the stationary state.

λ	N	E	Q^-	Q^+	P^-	P^+
$+1$	3	19	0.1957	0.0090	0.276	0.258
-1	1	9	0.0098	0.0478	0.014	1.430

for small wavenumbers:

$$Q^- = 2\int_{k<k_f} \nu^- |k|^{-d^-} |\hat{\psi}_k|^2 \, dk\,, \quad P^- = 2\int_{k<k_f} \nu^- |k|^{-d^-} \omega_k |\hat{\psi}_k|^2 \, dk$$

and for large wavenumbers

$$Q^+ = 2\int_{k>k_f} \nu^+ |k|^{d^+} |\hat{\psi}_k|^2 \, dk\,, \quad P^+ = 2\int_{k>k_f} \nu^+ |k|^{d^+} \omega_k |\hat{\psi}_k|^2 \, dk$$

where k_f is the characteristic wavenumber of forcing. Their time-averaged values in the stationary state are collected in Table 2.

The stationary isotropic spectra of turbulence are displayed in Figures 2 and 3. Again the results depend on the value of λ. For both cases the theoretical spectrum provides a higher level of turbulence than the observed one. In the focusing case ($\lambda = -1$) this difference is almost of one order of magnitude but the slope fits the predicted value -1 well. For $\lambda = +1$, the observed spectrum almost coincides with the weak turbulence one at low frequencies and then decays faster at higher wavenumbers. In this range, the slope is close to $-5/4$ as found in [5]. Note that a new derivation of the Majda et al.'s spectrum is proposed in [9].

Comparison of the turbulence levels and fluxes of particles Q^+ for both signs of nonlinearity leads to a paradoxal result. At $\lambda = -1$ the total number of particles is three times less than at $\lambda = +1$, while the dissipation rate of particles is higher by one order of magnitude. It can be explained only by the presence in this case of a much more powerful mechanism of nonlinear interactions, which provides very fast wave particles transport to high frequencies. In our opinion, this mechanism is wave collapse. Sporadic collapsing events developing on top of the weak turbulence background could send most of particles to high wavenumbers without violation of energy conservation, because in each self-similar collapse structure the amount of total energy is zero. Such a collapsing event is shown in Figure 4. Note that the contribution of collapses to the high-frequency spectrum is weak because they produce a Phillips-type spectrum which decays very fast as $k \to +\infty$. In our case, equation (4.2) becomes

$$n_k \simeq k^{-3/2}\,.$$

Hence, only the weakly turbulent component k^{-1} survives at large wavenumbers. The coexistence of wave collapse and weak turbulence was also observed in [2] for the nonlinear Schrödinger equation.

FIGURE 2. $\beta = 0, \lambda = -1$. Stationary and isotropic spectra n_k vs. wavenumber. We compare the computed spectrum with the predicted one of Kolmogorov-type $n_k = c\,k^{-1}$ with $c = a_2 P^{1/3}$ (straight line).

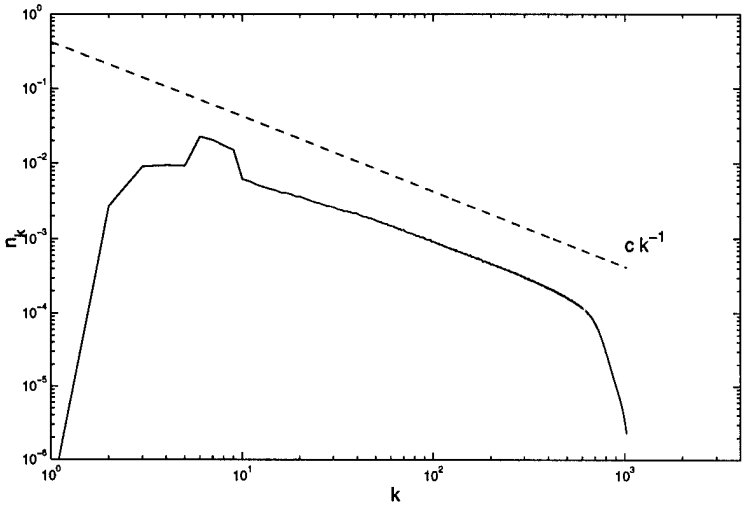

FIGURE 3. $\beta = 0, \lambda = +1$. Stationary and isotropic spectra n_k vs. wavenumber. We compare the computed spectrum with the predicted one of Kolmogorov-type $n_k = c\,k^{-1}$ with $c = a_2 P^{1/3}$ (straight line).

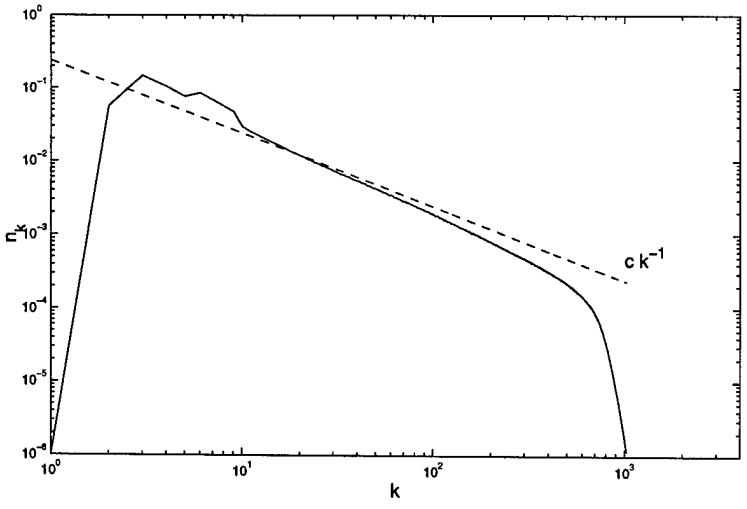

FIGURE 4. $\beta = 0, \lambda = -1$. Evolution towards collapse at $x \simeq 1$ between $t = 4999.980$ and $t = 5000.205$.

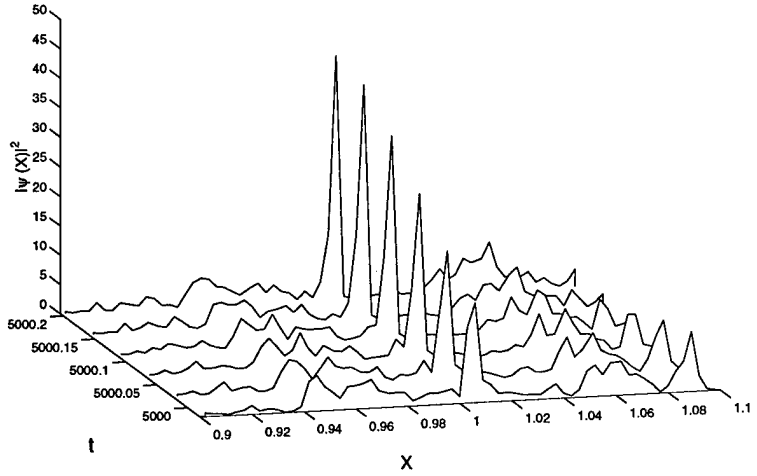

5.2. Numerical results for $\beta = 3, \lambda = +1$. At $\lambda = +1$ the picture of turbulence matches the weak turbulence prediction both quantitatively and qualitatively. Meanwhile, the spectrum at high k's is steeper than the theoretical one. So far we cannot give a consistent explanation of this fact. We can just guess that it is somehow connected with quasisolitons. As an illustration, Figure 5 shows the evidence of the presence of quasisolitons. More precisely, the system is first separated into several soliton-like structures and low-amplitude quasi-linear waves. Processes of mutual interactions slowly redistribute the number of waves in a way leading to the growth of initially bigger quasisolitons and the decay of initially smaller quasisolitons. The final state then consists of one big quasisoliton moving in a sea of small quasi-linear waves. This phenomenon is similar to the 'droplet' effect observed in the non-integrable nonlinear Schrödinger equation [**11**]. The soliton solution turns out to be a statistical attractor for the system: long time evolution leads to the condensation of the number of particles into a single soliton which minimizes the Hamiltonian.

6. Conclusions

In conclusion, the numerical results show two types of localised coherent structures: collapses in the focusing case ($\lambda = -1$) and quasisolitons in the defocusing case ($\lambda = +1$). Their role in the statistical properties of the system can be seen in the spectra. It leads to a discrepancy between numerics and theory. The fact that weak turbulence is not reached may be due to the sparsity of resonances in one dimension and to the numerical discretization. Four-wave interactions are not as efficient, while localised structures become dominant. Therefore equation (2.1) is not such a good model to assess the validity of weak turbulence theory.

FIGURE 5. $\beta = 3, \lambda = +1$. Snapshot of a quasisoliton at $x \simeq 3.7$ and $t = 10880$.

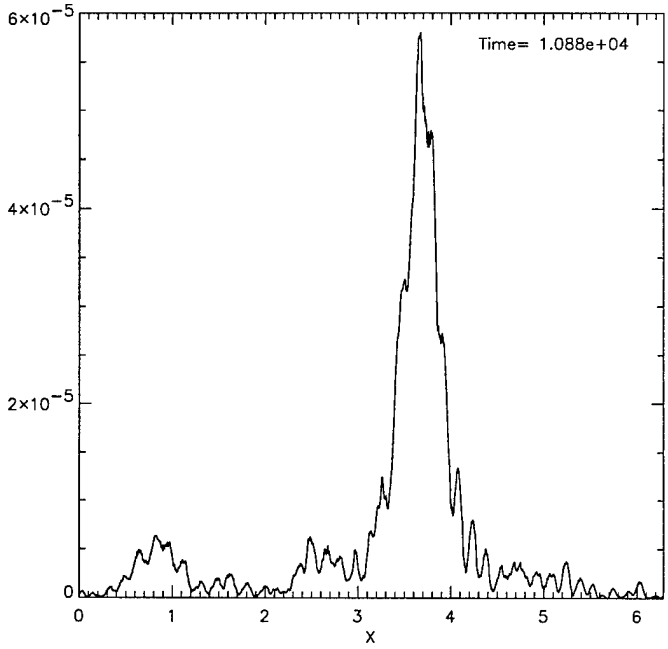

References

[1] D. Cai, A. J. Majda, D. W. McLaughlin, E. G. Tabak, *Spectral bifurcations in dispersive wave turbulence*, Proc. Nat. Acad. Sci. **96** (1999), 14216–14221.

[2] S. Dyachenko, A. C. Newell, A. Pushkarev, V. E. Zakharov, *Optical turbulence: weak turbulence, condensates and collapsing filaments in the nonlinear Schrödinger equation*, Physica D **57** (1992), 96–160.

[3] P. Guyenne, V. E. Zakharov, A. Pushkarev, F. Dias, *Turbulence d'ondes dans des modèles unidimensionnels*, C. R. Acad. Sci. Paris, Série IIb **328** (10) (2000), 757–762.

[4] E. A. Kuznetsov, A. M. Rubenchik, V. E. Zakharov, *Soliton stability in plasmas and hydrodynamics*, Phys. Rep. **142** (1986), 103–165.

[5] A. J. Majda, D. W. McLaughlin, E. G. Tabak, *A one-dimensional model for dispersive wave turbulence*, J. Nonlinear Sci. **6** (1997), 9–44.

[6] O. M. Phillips, *The dynamics of the upper ocean*, Cambridge Univ. Press, 1977.

[7] A. N. Pushkarev, V. E. Zakharov, *Turbulence of capillary waves*, Phys. Rev. Lett. **76** (1996), 3320–3323.

[8] V. E. Zakharov, *Stability of periodic waves of finite amplitude on the surface of deep fluid*, J. Appl. Mech. Tech. Phys. **2** (1968), 190–194.

[9] V. E. Zakharov, P. Guyenne, A. Pushkarev, F. Dias, *Wave turbulence in one-dimensional models*, Physica D (to appear).

[10] V. E. Zakharov, V. S. L'vov, G. Falkovich, *Kolmogorov Spectra of Turbulence I*, Springer-Verlag, 1992.

[11] V. E. Zakharov, A. N. Pushkarev, V. F. Shvets, V. V. Yankov, *Soliton turbulence*, JETP Lett. **48** (2) (1988), 83–87.

LANDAU INSTITUTE FOR THEORETICAL PHYSICS, MOSCOW, RUSSIA AND DEPARTMENT OF MATHEMATICS, UNIVERSITY OF ARIZONA, USA
E-mail address: **zakharov@itp.ac.ru**

INSTITUT NON LINÉAIRE DE NICE, 1361 ROUTE DES LUCIOLES, 06560 SOPHIA ANTIPOLIS, FRANCE
E-mail address: **guyenne@cmla.ens-cachan.fr**

LANDAU INSTITUTE FOR THEORETICAL PHYSICS, MOSCOW, RUSSIA AND DEPARTMENT OF MATHEMATICS, UNIVERSITY OF ARIZONA, USA
E-mail address: **andrei@imap3.asu.edu**

CENTRE DE MATHÉMATIQUES ET DE LEURS APPLICATIONS, FRANCE
E-mail address: **dias@cmla.ens-cachan.fr**

On the dynamics of an ideal fluid with the free surface

A.I.Dyachenko

Landau Institute for Theoretical Physics, 2 Kosygin str. Moscow, 117334, Russia

Abstract

Exact cubic equations are derived for two-dimensional flows of fluid with the free surface. The equations involve inverse derivative of conformal mapping of the domain occupied by fluid to the lower half-plane, and complex velocity of the fluid. They are hydrodynamic-type equations and describe transport of singularities of conformal mapping in the upper half-plane.

PACS codes: 47.10.+g, 47.15.Hg, 03.40.G, 02.60.Cb

1 Physical (natural) variables

The irrotational motion of an incompressible inviscid fluid with a free surface is a very basic problem in fluid dynamics. The equations describing the motion were first formulated by Stokes in 1845. In this article two-dimensional flows on the plane are considered, that allows to apply conformal mapping theory.

The velocity potential ϕ of the fluid satisfies the equation

$$\triangle\phi = 0$$

in the domain occupied by fluid. The domain is bounded by the free surface $y = \eta(x,t)$ with the boundary conditions for velocity potential and moving free surface:

$$\begin{aligned} \frac{\partial\phi}{\partial t} &+ \frac{1}{2}|\nabla\phi|^2 + g\eta = P, \\ \frac{\partial\eta}{\partial t} &+ \eta_x\phi_x = \phi_y \end{aligned} \tag{1.1}$$

at $y = \eta(x,t)$ and

$$\frac{\partial \phi}{\partial y} = 0, y \to -\infty,$$
$$\frac{\partial \phi}{\partial x} = 0, |x| \to \infty. \tag{1.2}$$

Here g is the gravity acceleration and P - constant pressure at the surface (Let $P = 0$). The system (1.1) and (1.2) is a Hamiltonian one with the Hamiltonian

$$\mathcal{H} = \frac{1}{2}\int_{-\infty}^{\infty} dx \int_{-\infty}^{\eta(x,t)} |\nabla\phi|^2 dy \ + \ \frac{1}{2}\int_{-\infty}^{\infty} g\eta^2(x,t)dx \tag{1.3}$$

and canonically conjugated variables
$\psi(x,t) = \phi(x,\eta(x,t),t)$ and $\eta(x,t)$ (see [1]):

$$\begin{aligned} \frac{\partial \eta}{\partial t} &= \frac{\partial \mathcal{H}}{\partial \psi}, \\ \frac{\partial \psi}{\partial t} &= -\frac{\partial \mathcal{H}}{\partial \eta}. \end{aligned} \tag{1.4}$$

Along with the Hamiltonian there are three more integrals of motion, amount of fluid:

$$\frac{\partial}{\partial t}\int_{-\infty}^{\infty} \eta(x,t)dx = 0, \tag{1.5}$$

and vertical and horizontal momenta:

$$\begin{aligned} \frac{\partial}{\partial t}\int_{-\infty}^{\infty} dx \int_{-\infty}^{\eta(x,t)} \phi_y dy &= 0, \\ \frac{\partial}{\partial t}\int_{-\infty}^{\infty} dx \int_{-\infty}^{\eta(x,t)} \phi_x dy &= 0. \end{aligned} \tag{1.6}$$

The equations (1.1) and (1.2) are functionally nonlinear and can be hardly studied. The most important known solutions were derived by Dirichlet in 1960, and they are ellipsoid (or ellipse in 2D case), hyperbola and parabola. Dirichlet solutions are described in detail in[2].

2 Conformal variables

To simplify the equations (1.1) and (1.2) let us perform conformal mapping (see[3]) of the domain in z-plane occupied by fluid to the lower half-plane of a complex variable $w = u + iv$

$$-\infty < u < \infty, \qquad -\infty < v < 0.$$

Now the shape of the surface is given parametrically by real and imaginary parts of conformal mapping given on real axis:

$$y = y(u,t), \quad x = x(u,t) = u + \tilde{x}(u,t), \tag{2.7}$$

here $\tilde{x}(u,t)$ and $y(u,t)$ are related through Hilbert Transformation

$$y = \hat{H}\tilde{x}, \qquad \tilde{x} = -\hat{H}y, \qquad \hat{H}^2 = -1$$

and

$$\hat{H}(f(u)) = P.V.\frac{1}{\pi}\int_{-\infty}^{\infty}\frac{f(u')du'}{u'-u}.$$

After conformal mapping $\phi(x,y,t) \to \phi(u,v,t)$. Let $\Psi(u,t) = \phi(u,0,t)$, the potential on the surface. It was shown in[3] that $y(u,t)$ and $\Psi(u,t)$ obey the following system of equations:

$$y_t = (y_u\hat{H} - x_u)\frac{\hat{H}\Psi_u}{J} \tag{2.8}$$

$$\Psi_t = -\frac{\Psi_u^2 + \hat{H}\Psi_u^2}{2J} + \hat{H}\left(\frac{\hat{H}\Psi_u}{J}\right)\Psi_u + \frac{\hat{H}\Psi_u}{J}\hat{H}\Psi_u - gy \tag{2.9}$$

here g is gravity acceleration, and

$$J = x_u^2 + y_u^2 = 1 + 2\tilde{x}_u + \tilde{x}_u^2 + y_u^2. \tag{2.10}$$

Another form of the equation (2.8) and (2.9) (see[3]) be

$$\begin{aligned} y_t x_u - x_t y_u &= -\hat{H}\Psi_u, \\ \Psi_t x_u - x_t\Psi_u + gyx_u &= \hat{H}\left(\Psi_t y_u - y_t\Psi_u + gyy_u\right) \end{aligned} \tag{2.11}$$

The integrals of motion acquire the following form:

$$\begin{aligned} \mathcal{H} &= -\int_{-\infty}^{\infty}\Psi\hat{H}\Psi_u du + \frac{g}{2}\int_{-\infty}^{\infty}y^2x_u du, \\ M &= \int_{-\infty}^{\infty}yx_u du, \\ P_y &= \int_{-\infty}^{\infty}\Psi x_u du, \\ P_x &= \int_{-\infty}^{\infty}\Psi y_u du. \end{aligned} \tag{2.12}$$

When dealing with conformal mapping $z(w,t)$ and velocity potential it is convenient to write down instead the real equations (2.8) and (2.9) the complex equations for $z(w,t)$ and complex velocity potential $\Phi(w,t)$. One can get these new equations applying projector operator $\hat{P}$

$$\hat{P}(f) = \frac{1}{2}(1 + i\hat{H})(f)$$

to the equations (2.8) and (2.9):

$$\begin{aligned} z_t &= iUz_u, \\ \Phi_t &= iU\Phi_u - \hat{P}(\frac{|\Phi_u|^2}{|z_u|^2}) + ig(z-u). \end{aligned} \tag{2.13}$$

Here U is a complex transport velocity:

$$U = \hat{P}(\frac{-\hat{H}\Psi_u}{|z_u|^2}).$$

It occurs that equations (2.13) can be simplified just by changing variables. Indeed, let us introduce instead of $z(w,t)$ and $\Phi(w,t)$ another functions $R(w,t)$ and $V(w,t)$ in a following way

$$\begin{aligned} R &= \frac{1}{z_w}, \\ \Phi_w &= -iVz_w. \end{aligned} \tag{2.14}$$

(V is just $i\frac{\partial\Phi}{\partial z}$, i.e. complex velocity). Note, that because of $z(w,t)$ is conformal mapping, its derivative does exist in lower half-plane and does not have zeroes in there. Thus function $R(w,t)$ is analytic in the lower half-plane and has the following boundary condition:

$$R(w,t) \to 1, \quad |w| \to \infty, \quad Im(w) \leq 0.$$

It is obvious that boundary condition for V is:

$$V(w,t) \to 0, \quad |w| \to \infty, \quad Im(w) \leq 0.$$

Then for these analytic functions equations acquire very nice form:

$$\begin{aligned} R_t &= i(UR' - U'R), \\ V_t &= i(UV' - R\hat{P}'(V\bar{V})) + g(R-1). \end{aligned} \tag{2.15}$$

Here

$$U = \hat{P}(V\bar{R} + \bar{V}R).$$

The equations are cubically nonlinear and include linear integral operator. They are similar to hydrodynamics type equations, but given in the complex plane. Important role there plays complex transport velocity U. It conveys zeroes of $R(w,t)$, which are singular points of conformal mapping $z(w,t)$. Possible types of zeroes need to be study in the next article. Here it should be just mentioned that in the numerical simulations only $\sqrt{w}$ branch points are observed.

It is easy to include surface tension in the equations (2.15), one has just to replace the second equation by

$$V_t = i(UV' - R\hat{P}'(V\bar{V}) + g(R-1)) - 2\sigma R\hat{P}'(Q'\bar{Q} - \bar{Q}'Q),$$

where σ is surface tension coefficient, and $Q = \sqrt{R}$.

Equations (2.15) keep the same form for other boundary conditions. Instead of boundary conditions (1.2) one can consider periodic boundaries as well as fluid of the finite depth.

Note that equations include now only derivatives of conformal mapping and complex velocity potential. As regards integrals of motion they acquire more complicated form. But if one restores complex velocity potential

$$\Phi = -i\int \frac{V}{R}dw$$

then Hamiltonian is equal to

$$\mathcal{H} = -\int_{-\infty}^{\infty} Re(\Phi)Im(\Phi')$$

and momenta

$$P_y = \int_{-\infty}^{\infty} Re(\Phi)Re(\frac{1}{R})du, \quad P_x = \int_{-\infty}^{\infty} Re(\Phi)Im(\frac{1}{R})du.$$

3 Conclusions

The main statement of the article is the following. The well-known equations for flows of fluid with the free surface (1.1) are equivalent to the cubic equations (2.15) written for the inverse derivative of the conformal mapping $R(w,t) = 1/z'(w,t)$ and fluid velocity $V(w,t)$. These equations are of hydrodynamic-type and describe transport of singularities of conformal mapping in the upper half-plane. And moving singularities define the shape of the surface.

Author thanks Prof. V.E. Zakharov for helpful discussion. This work was partially supported by INTAS-96-0413 Grant, by ONR Grant # N00014-98-1-0070, by RBRF Grant No.00-01-00929 and by the Grant of Leading scientific schools of Russia 00-15-96007.

References

[1] V.E. Zakharov. Prikl. Mekh. Tekh. Fiz. (in Russian) 2 (1968) 190.

[2] M.S. Longuet-Higgins. J. Fluid Mech. **73** (1976) 603.

[3] A.I. Dyachenko, E.A. Kuznetsov, M.D. Spector and V.E. Zakharov, *Phys. Lett. A,* **221** (1996) 73-79.

[4] A.I. Dyachenko and V.E. Zakharov, *Phys. Lett. A*, **221** (1996) 80.

[5] V.E. Zakharov and A.I. Dyachenko, *Physica D* **98** (1996) 652-664.

On conservation of the constants of motion in the models of nonlinear wave interaction.

A.Pushkarev, V.Zakharov

1. Introduction

One of the central problem of the development of the operational models for sea-wave prediction is an adequate description of nonlinear wave interaction. So far, the most solidly justified approach to this description is the use of the kinetic equation for the spectral density of wave action first derived by K.Hasselmann in 1962. Since this time, several codes for numerical simulation of nonlinear wave interaction were developed (Webb 1978, Masuda 1980, Hasselmann and Hasselmann 1981, Resio and Perrie 1991, Polnikov 1994, Lavrenov 1998, Komatsu and Masuda 1996, Van Vledder 1999, etc).

Nonlinear wave interaction is described by a complicated nonlinear integral operator and its numerical simulation is a tricky problem. All existing algorithms for its simulation are cumbersome and time consuming. So far, they are too slow to be directly used in practical operational models of wave prediction. Therefore, the development of faster approximate models of the nonlinear wave interaction is a very urgent problem.

The mostly common approximate model is DIA (Discrete Interaction Approximation), known also as the WAM method. Hasselmann and Hasselmann offered it in 1985. In this model, the integral operator in S_{nl} is replaced by a sum consisting of few discrete terms. Zakharov and Pushkarev proposed quite another approximate model, based on the use of the nonlinear diffusion operator in 1999.

To estimate the quality of an approximate model one should compare its prediction with the results of numerical simulation in the framework of the "exact" kinetic equation. To make this comparison reliable on should be sure that the " exact" model is good enough to be a paragon for such test. Actually, the real criteria for examination of quality of such models are absent.

Different schemes for numerical solution of the Hasselmann kinetic equation give qualitatively similar, but quantitatively slightly different results, and there was no so far a standard way for estimation of their reliability. This circumstances makes the problem of construction of fast approximate models of nonlinear wave interaction difficult and uneasy. One cannot believe in an approximate model if one cannot compare it with a real good standard for calibration.

Meanwhile there is a natural way for examination of numerical method for solution of the wave kinetic equation. This is the control of conservation of the basic constants of motion - wave action, energy, and two components of momentum. Similar approach is widely used in applied mathematics in the case when physical situation is described by conservative ordinary or partial differential equations.

In the case of nonlinear wave interaction, the situation is more complicated. It is described by not differential, but by the integral operator, which is non-local in the k-space. Any scheme of numerical integration of the kinetic equation operates in some finite domain of this space, always bounded in frequency and sometimes limited in angle. Integrals of motion, contained in any bounded domain are not conserved; the non-linear wave interaction carries them out of the domain. Due to non-locality of the S_{nl} operator, this leakage cannot be interpreted just as a flux through a boundary of the domain. The loss of the motion constants from finite domains is not a mathematical abstraction. Its is a real and a very strong physical effect. In many cases, the transport of motion constants is the major mechanism defining shape of spectra. For instance, a typical asymptotic behavior of energy spectrum at large frequency $E_f \propto f^{-4}$ is the result of constant transport of wave energy to the large frequency region.

In this article, we propose a modified method of calculation of conservation of the motion constant in finite domain making possible to take into consideration the leakage outside a domain. We call it "clean

test", which allows accurate estimation of the quality of any algorithms for numerical solution of the wave kinetic equation.

2. Are the constants of motion really conserved?

In the absence of pumping from the wind and dissipation the Hasselmann equation reads:

$$\frac{\partial n}{\partial t} = S_{nl} \tag{2.1}$$

$$S_{nl} = \int |T_{kk_1k_2k_3}|^2 \, \delta(k + k_1 - k_2 - k_3)\delta(\omega_k + \omega_{k_1} + \omega_{k_2} + \omega_{k_3}) \times (n_{k_1} n_{k_2} n_{k_3} + n_k n_{k_2} n_{k_3} - n_k n_{k_1} n_{k_2} - n_k n_{k_1} n_{k_3}) dk_1 dk_2 dk_3 \tag{2.2}$$

It is considered that equation preserves the following constants of motion

$$N = \int n d\vec{k} \text{ - Wave action} \tag{2.3}$$

$$E = \int \omega_k n_k d\vec{k} \text{ - Energy} \tag{2.4}$$

$$\vec{M} = \int \vec{k} n_k d\vec{k} \text{ - Momentum} \tag{2.5}$$

Are these constants really constant? To prove conservation of these integrals, one must prove validity of following identities:

$$\frac{\partial N}{\partial t} = \int S_{nl} d\vec{k} = 0 \tag{2.6}$$

$$\frac{\partial E}{\partial t} = \int \omega_k S_{nl} d\vec{k} = 0 \tag{2.7}$$

$$\frac{\partial \vec{M}}{\partial t} = \int \vec{k} S_{nl} d\vec{k} = 0 \tag{2.8}$$

These identities are trivial if one can change the order of integration by different k_i. If this operation is possible, one can transform, for instance, the expression (2.7) to the form

$$\int \omega_k S_{nl} dk = \int (\omega_k + \omega_{k_1} + \omega_{k_2} + \omega_{k_3}) \delta(k + k_1 - k_2 - k_3) \delta(\omega_k + \omega_{k_1} + \omega_{k_2} + \omega_{k_3}) n_{k_1} n_{k_2} n_{k_3} dk_1 dk_2 dk_3 \tag{2.9}$$

As it is known from the classical calculus, the operator of change of the integration order in improper integrals is allowed if the integrand decays fast enough at infinity. Let us consider this question in detail.

In equation (2.2), as well as in formulae (2.3)-(2.9), the integration is going on the infinite domain. In reality, both in experiment and in computer modeling the domain of integration is finite. Thus to check the identities (2.6)-2.8) we should first consider a finite domain. This is a quite nontrivial procedure. Suppose that the domain of integration is finite

$$|k| < p \tag{2.10}$$

One can denote

$$n_k^p = \begin{cases} n_k, |k| < p \\ 0, |k| > p \end{cases} \tag{2.11}$$

By plugging n_k^p instead of n_k into S_{nl} one get by definition $S_{nl} \to S_{nl}^{(p)}$. Apparently integrand in $S_{nl}^{(p)}$ has bounded support and change of order of integration is permitted at any value of p. Hence

$$\begin{aligned} \int S_{nl}^{(p)} dk &= \int_{|k|<p} S_{nl}^{(p)} dk + \int_{|k|>p} S_{nl}^{(p)} dk = 0 \\ \int \omega_k S_{nl}^{(p)} dk &= \int_{|k|<p} \omega_k S_{nl}^{(p)} dk + \int_{|k|>p} \omega_k S_{nl}^{(p)} dk = 0 \\ \int \vec{k} S_{nl}^{(p)} dk &= \int_{|k|<p} \vec{k}\omega_k S_{nl}^{(p)} dk + \int_{|k|>p} \vec{k} S_{nl}^{(p)} dk = 0 \end{aligned} \tag{2.12}$$

Let us denote

$$N^p = \int_{|k|<p} n dk\,, \quad E^p = \int_{|k|<p} \omega_k n_k dk\,, \quad \vec{M}^p = \int_{|k|<p} \vec{k} n_k dk$$

Now one can find balance of the motion constants in the domain $|k| < p$

$$\begin{aligned} \frac{\partial N^{(p)}}{\partial t} &= \frac{\partial}{\partial t} \int_{|k|<p} n_k dk = \int_{|k|<p} S_{nl}^{(p)} dk = -\int_{|k|>p} S_{nl}^{(p)} dk = -Q(p) \\ \frac{\partial E^{(p)}}{\partial t} &= \frac{\partial}{\partial t} \int_{|k|<p} \omega_k n_k dk = \int_{|k|<p} \omega_k S_{nl}^{(p)} dk = -\int_{|k|>p} \omega_k S_{nl}^{(p)} dk = -P(p) \\ \frac{\partial \vec{M}^{(p)}}{\partial t} &= \frac{\partial}{\partial t} \int_{|k|<p} \vec{k} n_k dk = \int_{|k|<p} \vec{k} S_{nl}^{(p)} dk = -\int_{|k|>p} \vec{k} S_{nl}^{(p)} dk = -\vec{K}(p) \end{aligned} \tag{2.13}$$

Last integrals in (2.13) can be calculated by the use of identity (2.11). In (2.13) Q, P and $\vec{K}$ are the values of the "losses" of the constants of motion. One can present S_{nl} in the following form

$$S_{nl}(k) = F_k - \gamma_k n_k \tag{2.14}$$

$$F_k = \int |T_{kk_1k_2k_3}|^2 \delta(\omega_k + \omega_{k_1} + \omega_{k_2} + \omega_{k_3}) \delta(\vec{k} + \vec{k}_1 + \vec{k}_2 + \vec{k}_3) \times n_{k_1} n_{k_2} n_{k_3} dk_1 dk_2 dk_3 \tag{2.15}$$

$$\gamma_k = \int |T_{kk_1k_2k_3}|^2 \delta(\omega_k + \omega_{k_1} + \omega_{k_2} + \omega_{k_3}) \delta(\vec{k} + \vec{k}_1 + \vec{k}_2 + \vec{k}_3) \times (n_{k_1} n_{k_2} + n_{k_1} n_{k_3} - n_{k_2} n_{k_3}) dk_1 dk_2 dk_3 \tag{2.16}$$

By definition

$$S_{nl}^{p}(k) = F_k^{(p)} - \gamma_k^{(p)} n_k^p \tag{2.17}$$

$$F_k^{(p)} = \int\limits_{|k_1|<p,|k_2|<p,|k_3|<p} |T_{kk_1k_2k_3}|^2 \delta(\omega_k + \omega_{k_1} + \omega_{k_2} + \omega_{k_3}) \delta(\vec{k} + \vec{k}_1 + \vec{k}_2 + \vec{k}_3) \times n_{k_1} n_{k_2} n_{k_3} dk_1 dk_2 dk_3 \tag{2.18}$$

$$\gamma_k^{(p)} = \int\limits_{|k_1|<p,|k_2|<p,|k_3|<p} |T_{kk_1k_2k_3}|^2 \delta(\omega_k + \omega_{k_1} + \omega_{k_2} + \omega_{k_3}) \delta(\vec{k} + \vec{k}_1 + \vec{k}_2 + \vec{k}_3) \times (n_{k_1} n_{k_2} + n_{k_1} n_{k_3} - n_{k_2} n_{k_3}) dk_1 dk_2 dk_3 \tag{2.19}$$

One should mention that $S_{nl}^{p}(k) \neq 0$ at $|k \rhd p$. As far as $n_k^p = 0$ at $|k \rhd p$, one has:

$$S_{nl}(k) = F_k^p, \; |k \rhd p \tag{2.20}$$

Formula (2.20) is extremely important. It expresses the following clear physical fact: the income term F_k^p is nonzero far beyond the domain of $|k \lhd p$ where the wave spectrum is concentrated. Meanwhile $F_k^p \neq 0$ only in a finite domain. Indeed, vector $\vec{k}$ satisfies the conditions

$$\vec{k} = \vec{k}_2 + \vec{k}_3 - \vec{k}_1 \tag{2.22}$$

$$\omega_k = \omega_{k_2} + \omega_{k_3} - \omega_{k_1} \tag{2.23}$$

and $|k_1 \lhd p, |k_2 \lhd p, |k_3 \lhd p$.

Conditions (2.22), (2.23) can be satisfied only for

$$|k \lhd p_{\max} \tag{2.24}$$

Here $p_{\max} = f(p)$ - some upper limit depending on a shape of ω_k. One can get some apriori estimate for $p_{\max}$. From (2.22) one can get

$$p_{\max} < 3p \tag{2.25}$$

From (2.23) one obtains

$$\omega_{p_{\max}} < 2\omega_p \tag{2.26}$$

More accurate estimate for $p_{\max}$ is defined by ω_k and depends on the depth. On the infinite depth $\omega_k = \sqrt{gk}$ and $p_{\max}$ is achieved if

$$\vec{k}_2 = \vec{k}_3,\ \vec{k}_1 = -\frac{1}{4}\vec{k}_2,\ |\vec{k}_2| = p \tag{2.27}$$

In this case

$$p_{\max} = \frac{9}{4}p \tag{2.28}$$

$$\omega_{p_{\max}} = \frac{3}{2}\omega_p \tag{2.29}$$

Introducing polar coordinates in $\vec{k}$ -pane, we have the following expressions for losses (rates of leakage) of the constants of motion from the domain $|k| > p$

$$\begin{aligned} Q(p) &= \int_p^{p_{\max}} pdp \int_0^{2\pi} F^p(p,\theta)d\theta \\ P(p) &= \int_p^{p_{\max}} p\omega_p dp \int_0^{2\pi} F^p(p,\theta)d\theta \\ K_x(p) &= \int_p^{p_{\max}} p^2 dp \int_0^{2\pi} F^p(p,\theta)\cos\theta d\theta \\ K_y(p) &= \int_p^{p_{\max}} p^2 dp \int_0^{2\pi} F^p(p,\theta)\sin\theta d\theta \end{aligned} \tag{2.30}$$

3. Clean test for integrals conservation

Now we can answer the question about real conservation of the integrals. If the domain is finite, they are never preserved. It is obvious from (2.30) that in all cases

$$Q(p) > 0,\ P(p) > 0 \tag{3.1}$$

Thus, wave action and energy always leak out of the domain $|k| < p$. In most cases, wave spectrum is concentrated in the right half-plane $-\frac{\pi}{2} < \theta < \frac{\pi}{2}$, $\cos\theta > 0$. In this situation $K_x(p) > 0$, the sign of $K_y(p)$ can be arbitrary.

Suppose again that

$$n_k = 0,\ |k| > p \tag{3.2}$$

We showed that

$$\frac{\partial n}{\partial t} = S_{nl}^{(p)}(k) = F^{(p)}(k) > 0 \tag{3.3}$$

if $|k| < p_{\max}$.

Hence, from physical viewpoint condition (3.2) is artificial. If it is satisfied in the initial moment of time, it will be immediately violated. In the close moment of time δt

$$n = n_0 + S_{nl}^p(k) \cdot \delta t \tag{3.4}$$

n becomes positive in the whole domain $|k| < p_{\max}$.

Anyway, the consideration we performed is useful. It can be used as a foundation for a "clean" test for all codes for numerical solution of the kinetic wave equation.

If condition (3.2) is satisfied

$$\frac{\partial n}{\partial t} = 0 \quad \text{if } |k| > p_{\max} \tag{3.5}$$

Hence

$$\begin{aligned}
&\frac{\partial}{\partial t} \int_{|k|<p_{\max}} S_{nl}^p dk \Big|_{t=0} = 0 \\
&\frac{\partial}{\partial t} \int_{|k|<p_{\max}} \omega_k S_{nl}^p dk \Big|_{t=0} = 0 \\
&\frac{\partial}{\partial t} \int_{|k|<p_{\max}} \vec{k} S_{nl}^p dk \Big|_{t=0} = 0
\end{aligned} \tag{3.6}$$

Conditions (3.6) can be rewritten in polar coordinates as

$$\begin{aligned}
&\frac{\partial}{\partial t} \int_0^{p_{\max}} p dp \int_0^{2\pi} S_{nl}^{(p)} d\theta \Big|_{t=0} = 0 \\
&\frac{\partial}{\partial t} \int_0^{p_{\max}} \omega_p p dp \int_0^{2\pi} S_{nl}^{(p)} d\theta \Big|_{t=0} = 0 \\
&\frac{\partial}{\partial t} \int_0^{p_{\max}} p^2 dp \int_0^{2\pi} S_{nl}^{(p)} \cos\theta d\theta \Big|_{t=0} = 0 \\
&\frac{\partial}{\partial t} \int_0^{p_{\max}} p^2 dp \int_0^{2\pi} S_{nl}^{(p)} \sin\theta d\theta \Big|_{t=0} = 0
\end{aligned} \tag{3.7}$$

Condition (3.7) can be relatively easily checked for any numerical code used for solution of the kinetic equation. To check the quality of the code one should put the initial data $n_k > 0$ at $|k| < p_{\max}$. Expansion of the integration domain is the price to be paid for nonlocality of the four-wave interactions.

Relations (2.13) can be generalized to the case when there is the interaction with wind and damping. Now kinetic equation (2.1)-(2.2) reads

$$\frac{\partial n}{\partial t} = S_{nl} + \beta_k n_k \tag{3.9}$$

where β_k is growth-rate of the instability or the damping depending on the sign. Equations (2.6)-(2.8) now should be replaced by the following relations:

$$\begin{aligned} \frac{\partial N}{\partial t} &= \int \beta_k n_k dk \\ \frac{\partial E}{\partial t} &= \int \omega_k \beta_k n_k dk \\ \frac{\partial \vec{M}}{\partial t} &= \int \vec{k} \beta_k n_k dk \end{aligned} \tag{3.10}$$

Relations (3.10) are formal and for a finite domain should be deciphered in a proper way. To do that one can assume

$$\beta_k = -A,\ A \to \infty,\ |k| > p$$

In the domain $|k| > p$ one can neglect the time derivative $\frac{\partial n}{\partial t}$ and put

$$S_{nl} - \beta_k n_k = F_k^p - (\gamma_k + A) n_k = 0$$

As far as $\gamma_k << A$, one can consider approximately ($|k| > 1$)

$$n_k = \frac{F_k^{(p)}}{A} \tag{3.11}$$

By plugging (3.11) into (3.10) one notice that the value of A is cancelled from the equations, taking the form

$$\begin{aligned} \frac{\partial N^p}{\partial t} &= -\int_{|k|<p} \beta_k n_k dk - Q \\ \frac{\partial E^p}{\partial t} &= -\int_{|k|<p} \omega_k \beta_k n_k dk - P \\ \frac{\partial \vec{M}}{\partial t} &= -\int_{|k|<p} \vec{k} \beta_k n_k dk - \vec{K} \end{aligned} \tag{3.12}$$

Equations (3.12) are the balance equations which also could be used to control numerical codes. One should either specially program the calculation of the losses $Q, P, \vec{K}$ or extend the integration domain to $|k \models p_{\max}$.

4. Estimates for integral losses.

Suppose that spectral density of wave action $n(k)$ has the maximum at $k \approx k_0$ and $p >> k_0$. Let us estimate in this limit the losses Q, P and $\vec{K}$. Integrals (2.30) consist of two parts. One part is given by integration in a small domain $p' \cong p + \delta p$, $\delta p \leq k_0$. In this domain, integration by k_1, k_2 is performed over the vicinity of the spectral maximum k_0. Thus

$$\begin{aligned} Q &= Q^{(1)} + Q^{(2)} \\ P &= P^{(1)} + P^{(2)} \\ \vec{K} &= \vec{K}^{(1)} + \vec{K}^{(2)} \end{aligned} \tag{4.1}$$

Here

$$\begin{aligned} Q^{(1)} &\cong \frac{n(p)n^2(k_0)}{\omega(k_0)} \cdot \left|T_{p,k_0,p,k_0}\right|^2 k_0^6 \\ P^{(1)} &\cong \frac{\omega(p)}{\omega(k_0)} n(p)n^2(k_0) \cdot \left|T_{p,k_0,p,k_0}\right|^2 k_0^6 \\ K^{(1)} &\cong \frac{p}{\omega(k_0)} n(p)n^2(k) \cdot \left|T_{p,k_0,p,k_0}\right|^2 k_0^6 \end{aligned} \tag{4.2}$$

Other part of contribution in (4.1) is given by integration in the domain $p' \cong p$. In this case, all wave vectors in (2.18) have the same order of magnitude. Hence

$$\begin{aligned} Q^{(2)} &\cong \frac{n^3(p)}{\omega(p)} \cdot \left|T_{p,p,p,p}\right|^3 p^6 \\ P^{(2)} &\cong n^3(p)\left|T_{p,p,p,p}\right|^3 p^6 \\ K^{(2)} &\cong \frac{p}{\omega(p)} n^3(p) \cdot \left|T_{p,p,p,p}\right|^2 p^6 \end{aligned} \tag{4.3}$$

We consider now the case of deep fluid. In this case $\omega(p) \cong g^{1/2} p^{1/2}$

$$\begin{aligned} T(p,p,p,p) &\cong p^3 \\ T(p,k_0,p,k_0) &\cong k_0^2 p \end{aligned} \qquad k_0 << p \tag{4.4}$$

We will consider that $n(k)$ is a powerlike function

$$n(k) \cong k^{-s} \tag{4.5}$$

Comparing $Q^{(1)}$ and $Q^{(2)}$ one see that for the case $S > 19/4$ $Q^{(1)} << Q^{(2)}$. The same is correct for other constants of motion. Finally, one obtains

$$\begin{aligned} Q &\cong p^{23/2-3s} \\ P &\cong p^{12-3s} \\ K &\cong p^{25/2-3s} \end{aligned} \tag{4.6}$$

Now we can answer the question about real conservation of the motion constants. All motion constants conserve if

$$n(k) < Ck^{-25/6} \text{ at } k \to \infty \tag{4.7}$$

5. Kolmogorov spectra and their experimental confirmation.

It is known since 1966 (Zakharov, Filonenko) that the stationary equation

$$S_{nl} = 0 \tag{5.1}$$

has isotropic powerlike solutions

$$n_k^{(1)} = C_1 k^{-23/6} \tag{5.2}$$

$$n_k^{(2)} = C_2 k^{-4} \tag{5.3}$$

The physical meaning of this solution becomes clear after plugging (5.2) into (4.6). For $s = 23/6$ Q is the constant while P and K grow in time. Hence, (5.2) is a Kolmogorov spectrum, corresponding to constant flux of wave action from large to small wavenumbers. For such type of asymptotic neither N, E or $\vec{M}$ are "real" constants of motion.

If $s = 4$ $Q \cong p^{-1/2}$. In this case $Q \to 0$ at $p \to \infty$, and wave action is "a real" constant of motion. Meanwhile, in this case $P = const$. Hence, (5.3) is a Kolmogorov spectrum describing permanent leakage of energy to large wavenumbers. In terms of spectral density of energy spectra (5.2)-(5.3) read

$$E_\omega^{(1)} = a_1 Q^{1/3} \omega^{-11/3} \tag{5.4}$$

$$E_\omega^{(2)} = a_2 P^{1/3} \omega^{-4} \tag{5.5}$$

Here a_1, a_2 are unknown Kolmogorov constants. One can formulate a conjecture that a general physically relevant solution equation

$$n_k = p^{1/3} k^{-4} F\left(\frac{Q}{P}(gk)^{1/2}, \frac{K}{P}(gk)^{-1/2}\right) \tag{5.6}$$

where F is an unknown function of two variables. It can be found explicitly in heuristic "diffusive" model of S_{nl} (Zakharov, Pushkarev 1999).

The spectrum ω^{-4} has the long history. Zakharov and Filonenko found it analytically as a well-hidden exact solution of equation (5.1) in 1966. Both authors lived in the USSR and were not allowed to travel abroad and report their results on international conferences. That was one reason why the paper of Zakharov and Filonenko, published in the leading Russian scientific journal (Doklady Academii Nauk) was almost not noticed.

There was another reason too. In 1958, O.Phillips offered that the spectrum of wind-driven waves is defined completely by wave breaking and has a universal form

$$\varepsilon_\omega \approx \alpha g^2 \omega^{-5} \tag{5.7}$$

Here α is the dimensionless "Phillips constant".

The very idea of Phillips was seminal and productive. A we understand now, situations when spectra of wave turbulence are defined completely by local singularities is rather common (see, for instance, Zakharov, Dias, Pushkarev, Guyenne 2000).

According to original idea of Phillips, spectrum (5.7) is automatically established at $\omega > \omega_0$, where ω_0 is a characteristic frequency of the spectral maximum. All spectral dynamics is just evolution $\omega_0 = \omega_0(t) \to 0$ at $t \to \infty$. In spite of its elegance and simplicity, the initial conjecture of Phillips is not confirmed by experiments. By definition

$$\int_0^\infty \varepsilon_\omega d\omega = \left\langle \eta^2 \right\rangle = H^2 \tag{5.8}$$

By integration of (5.7) one obtain

$$H^2 \cong \frac{\alpha g^2}{4\omega^4} \cong \frac{\alpha g^2}{4(2\pi)^4} T^4$$

or

$$H \propto T^2 \tag{5.9}$$

Here $T = 2\pi/\omega_0$ - characteristic period of energy containing waves.

Relation (5.9) can be checked experimentally. It was Yoshiaki Toba who did it. In 1972-73, he published a set of articles, summarizing his long-time experiments on the wind-wave channel in Sendai University. He found that, instead of (5.9), another relation holds:

$$H \propto T^{3/2} \tag{5.10}$$

Moreover, the Phillips constant, supposed to be universal and not depending on the wind velocity, happened to be proportional to the " friction velocity" u_*, characterizing the momentum transfer from air to sea. These facts can be naturally explained if one assume that instead of (5.7), the spectrum has a form

$$\varepsilon_\omega = \beta g u_* \omega^{-4} \tag{5.11}$$

Here β is another dimensionless constant (Toba's constant). Toba made careful measurements of the spectrum tale and found that formula (5.9) describes the spectral asymptotic very well. He found experimentally that the value of β is:

$$\beta = 6.2 \cdot 10^{-2} \tag{5.12}$$

We must stress that Toba was completely unaware about the paper of Zakharov and Filonenko.

After pioneering works of Toba experimental confirmation of ω^{-4} spectrum are mounted. Just a list of authors who observed this asymptotic is impressive: among them Kawai at al. 1977, Kahma 1981, Forristall 1981, Battjes at al 1986, Donelan, Hamilton and Hui 1985, Donelan and Pierson 1987. In 1985 O.Phillips, summarizing all experimental data, criticized his early theory (which, in our opinion, is still a sample of outstanding scientific intuition) and agreed that ω^{-4} is a reality.

Another approach for confirmation of the ω^{-4} spectrum is the numerical experiment. Several groups (see Masuda and Komatsu 1980, 1996; Resio and Perrie 1991; Polnikov 1994, 2000) observed a universal effect. If the initial data in equation (2.1)-(2.2) decay like ω^{-5}, very soon its asymptotic behavior changes to ω^{-4}.

In this connection, we would like to mention especially works of the group of D.Resio. They did not only follow formation of the ω^{-4} spectrum, but also calculated fluxes of energy at $k \to \infty$ and checked that for ω^{-4} the flux is constant in ω.

In conclusion, one can say that the spectrum ω^{-4} is definitely confirmed now by both many experiments as well as many numerical simulation arguments. The spectrum $\omega^{-11/3}$ also is confirmed quite well, but this point is beyond the scope of this article.

5. Why ω^{-4} not ω^{-5}?

The battle between ω^{-4} and ω^{-5} could look strange for a person outside of a narrow community of S_{nl} experts. Nevertheless, this argument makes a serious sense. It is enough to compare the value of the energy loss P in (4.6) for both spectra. For $\varepsilon_\omega \cong \omega^{-4}$ and $s = 4$, P is the constant. . For $\varepsilon_\omega \cong \omega^{-5}$ $s = 9/4$, $P \cong p^{-3/2} \to 0$ at $p \to \infty$.

Another words, for $\varepsilon_\omega \cong \omega^{-5}$ the energy in the wave ensemble is conserved, while in the case $\varepsilon_\omega \cong \omega^{-4}$ it leaks out with a constant rate. This is a very critical difference. Just an elementary analysis of the observational data contradicts the idea that both wave action and energy are conserved. Indeed, all experiments show that the spectral maximum moves in the process of "maturing " to the low wave numbers. At the same time, the spectrum in the asymptotic area $\omega >> \omega_0$ stays almost constant. As far as quanta of waves loose their energy, moving from high to low frequency region, the outlined facts are compatible with the fact of permanent loss of wave energy, existence of the constant flux of energy to high ω and, as a result, to the ω^{-4} asymptotic at $\omega \to \infty$.

Summarizing the facts, one can say that the asymptotic $\varepsilon_\omega \cong \omega^{-5}$ in the weak turbulent regime is a contradiction to the energy conservation law.

Said Aristotle: "You are friend Plato, but the truth is more valuable". We can say
" You are a friend Dr.... but the conservation of energy is more important".

Acknowledgments.

The authors are grateful for the support of US ARMY under the grant DACA 39-99-C-0018 and ONR, under the grant N00014-98-1-0439.

We would like to express our special gratitude to Dr. Donald Resio for numerous discussions.

References

Dias F., Guyenne P., Pushkarev A.N., Zakharov V.E. Wave turbulence in one-dimensional models, Preprint N2000-4, Centre de Mathematiques et del leur Applications, E.N.S.de CACHAN, pp.1-48, 2000

Battjes J.A., Stive M.J. Calibration and verification of a dissipation model for random breaking waves. J.Geophys.Res., 90(C5), pp.9159-9167, 1986.

Donelan M.A., Hamilton J. and Hui W.H. Directional spectra of wind-generated waves, Phil.Trans.Roy.Soc. London, A315, pp.509-562, 1985.

Forristall J.Z. Measurements of a saturated range in ocean wave spectra, J.Geophys.Res., 86, pp.8075-8084, 1981.

Hansen C., Katsaros K.B., Kitaigorodskii S.A., Larsen S.E. The dissipation range of wind-wave spectra observed on a lake, Journ. Phys.Oceanogr., 20, pp.1264-1277, 1990.

Hashimoto N., Tsukuya H. and Nakagawa Y. Numerical computations of the nonlinear energy transfer of gravity-wave spectra in finite water depth, Coastal Engineering Journal, 40, N1, pp.23-40, 1998.

Hasselmann, K. On the nonlinear energy transfer in a gravity wave spectrum. Part 1, J.Fl.Mech., 12 , pp.481-500, 1962.

Hasselmann, K. On the nonlinear energy transfer in a gravity-wave spectrum. Part 2., J.Fl.Mech., 15, pp.273-281, 1963.

Hasselmann S., Hasselmann K., Komen J., Janssen P., Ewing J. and Cardone V. The WAM model – a third generation ocean wave prediction model. J.Phys.Oceanogr., 18, pp. 1775-1810, 1958.

Hasselmann S. and Hasselmann K. , A symmetrical method of computing the nonlinear transfer in a gravity wave spectrum. Hamburger Geophys. Einzelschrifte., Hamburg, p.52-172, 1981.

Hasselmann S., Hasselmann K. and Bartnett T. Computation and parameterization of the nonlinear transfer in a gravity wave spectrum. Part II. J.Phys.Oceanogr., 15, pp.1378-1391, 1985.

Kahma K.K. A study of the growth of the wave spectrum with fetch, J.Phys.Oceanogr., 11, pp.1503-1515, 1981.

Kawai S., Okada K. and Toba Y. Field data support of three-second power law and $gu_*\sigma^{-4}$ spectral form for growing wind waves., J.Oceanog.Soc.Japan, 33, pp.137-150, 1977.

Kitaigorodskii S.A. On the theory of equilibrium range in the spectrum of wind-generated gravity waves, J.Phys.Oceanogr., 13, N5, pp.816-827, 1983.

Kitaigorodskii S.A. The equilibrium ranges in wind-wave spectra in wave dynamics and radio probing of the ocean surface, Ed. by O.M. Phyllips and K.Hasselmann. Plenum Press Corp., pp.9-40, 1986.

Komatsu K. and Masuda A. A new scheme of Nonlinear Energy Transfer among wind waves: RiAM method – algorithm and performance, Journal of Oceanography, 32, pp.509-537, 1996.

Lavrenov I.V. Mathematical modeling of wind waves in spatially inhomogeneous ocean, Gidrometeoizdat, Sankt-Petersburg, 1998.

Masuda A., Nonlinear energy transfer between wind waves. J.Phys.Oceanogr., 23, pp.1249-1258, 1980.

Phillips O.M. The equilibrium range in the spectrum of wind-generated waves. J.Fl.Mech., 4, pp. 426-434, 1958.

Phillips O.M. Spectral and statistical properties of the equilibrium range in wind-generated gravity waves. J.Fl.Mech., 156, pp. 505-531, 1985.

Polnikov V. Numerical modeling of the constant flux spectra for surface gravity waves in the case of angular anysotropy, Wave Motion, 1008, pp.1-12, 2000.

Polnikov V. Numerical modeling of the flux energy formation for surface gravity waves, J.Fl.Mech., 278, pp.289-291, 1994.

Resio D.T. and Perrie W.A. Implication of an f^{-4} equilibrium range for wind-generated waves. J.Phys.Oceanogr., 2, pp.193-204, 1989.

Resio D. and Perrie W. A numerical study of nonlinear energy fluxes due to wave-wave interactions. Part I. Methodology and basic results, J.Fl.Mech., 223, pp.603-629, 1991.

Tracy B.A. and Resio D.T. Theory and calculation of the nonlinear transfer between sea wave in deep water wave information studies. Report of US Army Engineer Waterway Experimental Station, Vicksburg, MS, 1982.

Toba Y. Local Balance in the air-sea boundary processes. I, J.Oceanog.Soc.Japan, 28, pp.109-120, 1972.

Toba Y. Local balance in the air-sea boundary processes. II, J.Oceanog.Soc.Japan, 29, pp.70-75, 1973.

Toba Y. Local balance in the air-sea boundary processes. III. On the spectrum of wind waves. J.Oceanog.Soc.Japan, 29, pp.209-220, 1973.

Zakharov V.E., Lvov V.S. and Falkovich J. Kolmogorov spectra of wave turbulence, Springer-Verlag, 1992.

Zakharov V.E. and Filonenko N.N. The energy spectrum for stochastic oscillation of a fluid surface, Doklady Akademii Nauk, 170, pp.1292-1295, 1966.

Zakharov V.E. and Zaslavskii M.M. The kinetic equation and Kolmogorov spectra in the weak-turbulence theory of wind waves, Izv.Atm.Ocean.Phys., 18, pp.747-753, 1982.

Zakharov V.E., Pushkarev A.N. Diffusion model of interacting gravity waves on the surface of deep fluid, Nonlin.Proc.Geophys., 6, pp.1-10, 1999.

Van Vledder G., Private communication

Webb D.J. Non-linear transfer between sea waves. Deep Sea Research, 25, pp.279-298, 1978.

Wave turbulence in one-dimensional models

V. E. Zakharov, Landau Institute for Theoretical Physics, Moscow, Russia
P. Guyenne, Institut Non-Linéaire de Nice, France
A. N. Pushkarev, Landau Institute for Theoretical Physics, Moscow, Russia and University of Arizona, USA
F. Dias, Ecole Normale Supérieure de Cachan, France

October 13, 2000

Abstract

A two-parameter nonlinear dispersive wave equation proposed by Majda, McLaughlin and Tabak is studied analytically and numerically as a model for the study of wave turbulence in one-dimensional systems. Our ultimate goal is to test the validity of weak turbulence theory. Although weak turbulence theory is independent on the sign of the nonlinearity of the model, the numerical results show a strong dependence on the sign of the nonlinearity. A possible explanation for this discrepancy is the strong influence of coherent structures – wave collapses and quasisolitons – in wave turbulence.

1 Introduction

A wide variety of physical problems involve random nonlinear dispersive waves. The most common tool for the statistical description of these waves is a kinetic equation for squared wave amplitudes, the so-called kinetic wave equation. Sometimes this equation is also called Boltzmann's equation. This terminology is in fact misleading because the kinetic wave equation and Boltzmann's equation are the opposite limiting cases of a more general kinetic equation for particles which obey Bose-Einstein statistics like photons in stellar atmospheres or phonons in liquid helium. It was first derived by Peierls in 1929 [1]. In spite of the fact that both the kinetic wave equation and Boltzmann's equation can be derived from the quantum kinetic equation, the kinetic wave equation was derived independently and almost simultaneously in plasma physics and for surface waves on deep water. This was done in the early sixties while Boltzmann's equation was derived in the nineteenth century! The derivation for surface waves is due to Hasselmann [2] (see also Zakharov [3]).

Once the kinetic wave equation has been derived, the shape of wave number spectra can be predicted by the so-called weak turbulence (WT) theory. It is called weak because it deals with resonant interactions between small-amplitude waves. Thus, contrary to fully developed turbulence, it leads to explicit analytical solutions provided some assumptions are made. So far, there have been only a few studies to check the results of WT theory. Recently, Pushkarev and Zakharov [4] numerically solved the three-dimensional dynamical equations for the free-surface elevation and the velocity potential in the case of capillary water waves. They obtained an isotropic spectrum close to the theoretical power-law found by Zakharov and Filonenko [5]. Majda, McLaughlin and Tabak [6] (hereafter referred to as MMT) considered four-wave interactions by introducing a one-dimensional model equation. This equation can be integrated numerically quite efficiently on large inertial intervals. They examined a family of Kolmogorov-type solutions depending on the parameters of the equation. The validity of several theoretical

hypotheses was then assessed numerically. Namely, MMT confirmed the random phase and quasi-gaussian approximations. They also showed the independence of the solutions on the nature of forces, initial conditions, and the size and level of discreteness of the computational domain. However, their simulations surprisingly displayed spectra steeper than the predicted ones. They explained the discrepancy by proposing a new inertial range scaling technique which seems to yield the appropriate exponents. More recently, Cai, Majda, McLaughlin and Tabak [7] revisited their earlier results and found some results which agree with WT theory as well.[1] They considered two kinds of Hamiltonians: Hamiltonians which are the sum of a quadratic term and a quartic term (positive nonlinearity), as in [6], and Hamiltonians which are the difference between a quadratic and a quartic term (negative nonlinearity). For either sign of nonlinearity, they found agreement with MMT theory in some cases and agreement with WT theory in some other cases. Since their computations were performed with a dispersion relation in which the frequency varies like the square root of the wave number, one can see an analogy with deep water waves. Incidentally, the WT theory was recently developed for shallow water waves by Zakharov [8].

As in many other fields, numerical modeling leads to some difficulties, especially when one wants to compare with the theory. Most of these difficulties are related to finite-size effects, i.e. the domain is discretized into a grid of points in computations whereas one assumes an infinite medium in theory. We can mention the bottleneck phenomenon [9] which tends to flatten the slope of the inertial range at small scales. It is commonly observed in problems with a dissipative cutoff. In addition, Pushkarev [10] revealed the phenomenon of frozen turbulence at very low levels of nonlinearity. In this situation, the resonance conditions have very few solutions (or may not be fulfilled at all!) because of the discrete values of wave numbers. As a consequence, there is no energy flux due to the lack of resonating wave vectors. The power-law regime only takes place at moderate levels of nonlinearity where quasi-resonant interactions come into play. Pushkarev concluded that weak turbulence in bounded systems combines the features of both frozen and Kolmogorov-type turbulence. The beauty of the MMT model equation is that the above mentioned difficulties can be controlled completely.

After introducing the model equation, the paper is divided into two parts. In the first part, the MMT equation is studied analytically. A weak turbulence description of the equation is provided (see [6]). We find the Kolmogorov solutions of the kinetic equation and determine the set of parameters for which such solutions can be realized. Then we discuss the coherent structures which can compete with weak turbulence. The most simple coherent structures are solitons similar to the soliton solutions of the Nonlinear Schrödinger Equation (NLS).

Solitons for the MMT equation exist only if nonlinearity is negative. In the cases of interest, they are shown to be unstable (see Section 7) and cannot play an important role in the wave dynamics.

As an alternative to soliton coherent structures, there are wave collapses described by self-similar solutions of the MMT equation. These solutions can exist in a certain parameter regime for both signs of nonlinearity. Theoretically speaking, both solitons and collapses can coexist with weak turbulence.

Another type of coherent structures are quasisolitons, or envelope solitons. They were discussed recently by Zakharov and Kuznetsov [11]. In the MMT model quasisolitons exist at positive nonlinearity only. Their stability remains an open question.

The main new theoretical results of the first part are a careful tabulation of the signs

[1]These three papers were kindly given to us when the present manuscript was essentially completed. Some of the results are similar to ours, but their interpretation is different.

of the fluxes for the MMT model equation, the existence and possible role of quasisolitons for positive nonlinearity, and an analogy with Phillips spectrum associated with the formation of collapses.

In the second part, we describe the results of the numerical study of the MMT equation. We find that the wave turbulence described by the MMT equation is different both quantitatively and qualitatively for both signs of nonlinearity. Since the predictions of WT theory are identical for both signs of nonlinearity, WT theory can be applied at best for one sign of nonlinearity. Our analysis of the results leads to somewhat contradictory results.

For positive nonlinearity the balance of energy and particle fluxes as well as the level of turbulence are in good agreement with WT theory. Meanwhile the slope of the spectrum in the window of transparency is steeper than predicted by WT theory.

In the case of negative nonlinearity the picture of turbulence is quite different from the WT predictions, both qualitatively and quantitatively. First of all, the turbulence is stabilized on a level which is one order of magnitude less than predicted by WT theory. Then the sign of the flux of particles is opposite to the one predicted by WT theory. Both these facts lead to a conjecture on the existence of a strong and essentially nonlinear mechanism which competes successfully with WT quartic resonances. In our opinion, this mechanism is the wave collapse, described by self-similar solutions of the MMT equations. At the same time, the high-frequency tail of the spectrum has a slope which coincides exactly with the slope predicted by WT theory. This leads to the conclusion that in spite of the presence of wave collapses, the high-frequency asymptotics of spectra is governed by the WT processes which are responsible for carrying only a small part of the energy. The coexistence of wave collapses and weak turbulence was already described in the context of the 2D NLS [12].

Wave collapse is an example of an essentially nonlinear coherent structure arising in wave turbulence under certain conditions. As said above, another important type of coherent structures are quasisolitons or envelope solitons living for a finite time. Such structures can arise in the MMT model in the case of positive nonlinearity. We believe that these structures are responsible for the deviation of the spectra from the ones predicted by WT theory.

2 Model equation

We investigate the family of dynamical equations

$$\mathrm{i}\frac{\partial\psi}{\partial t} = \left|\frac{\partial}{\partial x}\right|^{\alpha}\psi + \lambda\left|\frac{\partial}{\partial x}\right|^{\beta/4}\left(\left|\left|\frac{\partial}{\partial x}\right|^{\beta/4}\psi\right|^{2}\left|\frac{\partial}{\partial x}\right|^{\beta/4}\psi\right), \quad \lambda = \pm 1, \tag{2.1}$$

where $\psi(x,t)$ denotes a complex wave field and α, β are real parameters.

If $\lambda = +1$, one exactly recovers the MMT model which was treated in [6]. Note that our parameter β is the opposite of the parameter β in MMT. The extension $\lambda = \pm 1$ in Eq. (2.1), which was also treated in [7], raises an interesting problem because the balance between nonlinear and dispersive effects may change according to λ.

Besides the Hamiltonian

$$H = H_L + H_{NL} = \int\left(\left|\left|\frac{\partial}{\partial x}\right|^{\alpha/2}\psi\right|^{2} + \frac{\lambda}{2}\left|\left|\frac{\partial}{\partial x}\right|^{\beta/4}\psi\right|^{4}\right)dx, \tag{2.2}$$

the system (2.1) preserves two other integrals of motion: wave action and momentum, respectively

$$N = \int |\psi|^2 \, dx \qquad \text{and} \qquad M = \frac{\mathrm{i}}{2} \int \left(\psi \frac{\partial \psi^*}{\partial x} - \frac{\partial \psi}{\partial x} \psi^* \right) dx \, .$$

As usual, it is convenient to work in Fourier space. Let us write Eq. (2.1) as

$$\mathrm{i} \frac{\partial \hat{\psi}_k}{\partial t} = \omega(k) \hat{\psi}_k + \int T_{123k} \, \hat{\psi}_1 \hat{\psi}_2 \hat{\psi}_3^* \, \delta(k_1 + k_2 - k_3 - k) \, dk_1 dk_2 dk_3 \, , \tag{2.3}$$

where $\hat{\psi}_k = \hat{\psi}(k,t)$ denotes the k-th component in the Fourier decomposition of $\psi(x,t)$ and $(*)$ stands for complex conjugation.

In this form, Eq. (2.3) looks like the so-called one-dimensional Zakharov's equation determined by the linear dispersion relation

$$\omega(k) = |k|^\alpha \, , \quad \alpha > 0 \, , \tag{2.4}$$

and the simple interaction coefficient

$$T_{123k} = T(k_1, k_2, k_3, k) = \lambda \, |k_1 k_2 k_3 k|^{\beta/4} \, . \tag{2.5}$$

One easily sees that the kernel T_{123k} possesses the symmetry required by the Hamiltonian property

$$T_{123k} = T_{213k} = T_{12k3} = T_{3k12} \, . \tag{2.6}$$

Moreover, the absolute values in Eqs (2.4) and (2.5) ensure the basic assumptions of isotropy and scale invariance. In other words, $\omega(k)$ and T_{123k} are invariant with respect to rotations $(k \to -k)$ and they are homogeneous functions of their arguments with degrees α and β respectively, i.e.

$$T(\xi k_1, \xi k_2, \xi k_3, \xi k) = \xi^\beta \, T(k_1, k_2, k_3, k) \, , \quad \xi > 0 \, . \tag{2.7}$$

Following MMT, we fix $\alpha = 1/2$ by analogy with gravity waves whose dispersion relation reads as $\omega = (g\,k)^{1/2}$ (g being the acceleration due to gravity). The power β takes the value $+3$ if the analogy is extended to the nonlinear term but we will consider a wider range of values for β.

Eq. (2.3) describes four-wave interaction processes obeying the resonant conditions

$$k_1 + k_2 = k_3 + k \, , \tag{2.8}$$

$$\omega_1 + \omega_2 = \omega_3 + \omega \, . \tag{2.9}$$

For $\alpha > 1$ these equations only have the trivial solution $k_3 = k_1, k = k_2$ or $k_3 = k_2, k = k_1$. For $\alpha < 1$ there is also a nontrivial solution. Note that in this case the signs of k_i must be different. For instance, $k_1 < 0$ and $k_2, k_3, k > 0$. If $\alpha = 1/2$, Eqs (2.8)-(2.9) can be parametrized by two parameters A and ξ

$$k_1 = -A^2 \xi^2 \, , \quad k_2 = A^2 (1 + \xi + \xi^2)^2 \, , \quad k_3 = A^2 (1 + \xi)^2 \, , \quad k = A^2 \xi^2 (1 + \xi)^2 \, . \tag{2.10}$$

In the case $\alpha = 2$ and $\beta = 0$, Eq. (2.1) becomes the NLS equation

$$\mathrm{i} \frac{\partial \psi}{\partial t} = -\frac{\partial^2 \psi}{\partial x^2} + \lambda \, |\psi|^2 \, \psi \tag{2.11}$$

(note here that $|\frac{\partial}{\partial x}|^2 = -\frac{\partial^2}{\partial x^2}$).

Positive nonlinearity $\lambda = +1$ corresponds to the *defocusing* NLS, while negative nonlinearity corresponds to the *focusing* NLS.

3 Weak turbulence description of the model equation

If one only considers small nonlinear effects, then the statistical behavior can be mainly described by the evolution of the two-point correlation function

$$\langle\hat{\psi}(k,t)\hat{\psi}^*(k',t)\rangle = n(k,t)\,\delta(k-k')\,,$$

where brackets denote ensemble averaging. We introduce also the four-wave correlation function

$$\langle\hat{\psi}(k_1,t)\hat{\psi}(k_2,t)\hat{\psi}^*(k_3,t)\hat{\psi}^*(k,t)\rangle = J_{123k}\,\delta(k_1+k_2-k_3-k)\,. \tag{3.1}$$

On this basis, WT theory leads to the kinetic equation for $n(k,t)$ and provides tools for finding stationary power-law solutions. For details, see [6]. Here we explain the main steps of the procedure applied to our model.

The starting point is the original equation for $n(k,t)$. From Eq. (2.3), we have

$$\frac{\partial n_k}{\partial t} = 2\int \mathrm{Im}\,J_{123k}\,T_{123k}\,\delta(k_1+k_2-k_3-k)\,dk_1dk_2dk_3\,. \tag{3.2}$$

Due to the Quasi-Gaussian Random Phase approximation

$$\mathrm{Re}\,J_{123k} \simeq n_1n_2\left[\delta(k_1-k_3)+\delta(k_1-k)\right]\,. \tag{3.3}$$

The imaginary part of J_{123k} can be found through an approximate solution of the equation imposed on this correlator. The result is (see [13])

$$\mathrm{Im}\,J_{123k} \simeq 2\,\pi\,T^*_{123k}\,\delta(\omega_1+\omega_2-\omega_3-\omega)(n_1n_2n_3+n_1n_2n_k-n_1n_3n_k-n_2n_3n_k)\,. \tag{3.4}$$

This gives

$$\begin{aligned}\frac{\partial n_k}{\partial t} &= 4\,\pi\int |T_{123k}|^2\,(n_1n_2n_3+n_1n_2n_k-n_1n_3n_k-n_2n_3n_k) \\ &\times\ \delta(\omega_1+\omega_2-\omega_3-\omega)\,\delta(k_1+k_2-k_3-k)\,dk_1dk_2dk_3\,.\end{aligned} \tag{3.5}$$

Since the square norm cancels the sign of T_{123k}, it is clear that the WT approach is independent on λ. Here we point out that MMT mistakenly wrote a factor 12π instead of 4π in Eq. (3.5) and the right hand side of Eq. (3.5) with the opposite sign. This fact is particularly important when determining the fluxes of wave action and energy.

Assuming that $n(-k)=n(k)$ (similarly to an angle averaging in higher dimensions), one gets

$$\begin{aligned}\frac{\partial\mathcal{N}(\omega)}{\partial t} &= \frac{4\pi}{\alpha^4}\int(\omega_1\omega_2\omega_3\omega)^{\frac{\beta/2-\alpha+1}{\alpha}}\,(n_1n_2n_3+n_1n_2n_\omega-n_1n_3n_\omega-n_2n_3n_\omega) \\ &\times\ \delta(\omega_1+\omega_2-\omega_3-\omega)\,\Big[\delta(\omega_1{}^{\frac{1}{\alpha}}+\omega_2{}^{\frac{1}{\alpha}}-\omega_3{}^{\frac{1}{\alpha}}+\omega^{\frac{1}{\alpha}}) \\ &+\ \delta(\omega_1{}^{\frac{1}{\alpha}}+\omega_2{}^{\frac{1}{\alpha}}+\omega_3{}^{\frac{1}{\alpha}}-\omega^{\frac{1}{\alpha}})+\delta(\omega_1{}^{\frac{1}{\alpha}}-\omega_2{}^{\frac{1}{\alpha}}-\omega_3{}^{\frac{1}{\alpha}}-\omega^{\frac{1}{\alpha}}) \\ &+\ \delta(-\omega_1{}^{\frac{1}{\alpha}}+\omega_2{}^{\frac{1}{\alpha}}-\omega_3{}^{\frac{1}{\alpha}}-\omega^{\frac{1}{\alpha}})\Big]\,d\omega_1d\omega_2d\omega_3\,,\end{aligned} \tag{3.6}$$

where $\mathcal{N}(\omega) = n\,(k(\omega))\,dk/d\omega$, n_ω stands for $n\,(k(\omega))$ and ω is given by Eq. (2.4).

The next step consists in inserting the power-law ansatz

$$n(\omega) \propto \omega^{-\gamma}\,, \tag{3.7}$$

and then performing the Zakharov's conformal transformations [6, 12, 13]. Finally, the kinetic equation becomes

$$\frac{\partial \mathcal{N}(\omega)}{\partial t} \propto \omega^{-y-1}\, I(\alpha,\beta,\gamma)\,, \tag{3.8}$$

where

$$\begin{aligned} I(\alpha,\beta,\gamma) \;=\; & \frac{4\pi}{\alpha^4}\int_\Delta (\xi_1\xi_2\xi_3)^{\frac{\beta/2+1}{\alpha}-1-\gamma}\,(1+{\xi_3}^\gamma-{\xi_1}^\gamma-{\xi_2}^\gamma)\;\delta(1+\xi_3-\xi_1-\xi_2) \\ & \times\delta({\xi_1}^{\frac{1}{\alpha}}+{\xi_2}^{\frac{1}{\alpha}}+{\xi_3}^{\frac{1}{\alpha}}-1)\;(1+{\xi_3}^y-{\xi_1}^y-{\xi_2}^y)\;d\xi_1 d\xi_2 d\xi_3\,, \end{aligned} \tag{3.9}$$

with

$$\Delta = \{0<\xi_1<1\,,\,0<\xi_2<1\,,\,\xi_1+\xi_2>1\} \quad \text{and} \quad y = 3\gamma+1-\frac{2\beta+3}{\alpha}\,.$$

The nondimensionalized integral $I(\alpha,\beta,\gamma)$ is obtained by using the change of variables $\omega_j \to \omega\,\xi_j \quad (j=1,2,3)$.

The ansatz (3.7) makes sense if the integral in (3.6) converges. It could diverge both at low and high frequencies. The condition of convergence at low frequencies coincides with the condition of convergence of the integral in (3.9) and can be easily found. It reads

$$2\gamma < -1+\frac{\beta+4}{\alpha}\,. \tag{3.10}$$

The condition of convergence at high frequencies can be found after substituting (3.7) into (3.6). Omitting the details, we get the result

$$\gamma > \frac{\beta+\alpha-1}{\alpha}\,. \tag{3.11}$$

In all the cases discussed in this article, both conditions (3.10) and (3.11) are satisfied.

For the case $\alpha = 1/2$, one can transform Eq. (3.6) into the form

$$\frac{\partial \mathcal{N}(\omega)}{\partial t} = 64\pi\,\omega^{4(\beta+1)}\,[S_1+S_2+S_3+S_4]\;,$$

where

$$
\begin{aligned}
S_1 &= 2\int_0^1 \frac{u^{2\beta+2}(u+1)^{2\beta+1}}{(1+u+u^2)^{3\beta+4}}\left[n\left(\frac{u}{1+u+u^2}\omega\right)n\left(\frac{u(u+1)}{1+u+u^2}\omega\right)n\left(\frac{u+1}{1+u+u^2}\omega\right)\right.\\
&+ n(\omega)\,n\left(\frac{u(u+1)}{1+u+u^2}\omega\right)n\left(\frac{u+1}{1+u+u^2}\omega\right) - n(\omega)\,n\left(\frac{u}{1+u+u^2}\omega\right)n\left(\frac{u+1}{1+u+u^2}\omega\right)\\
&- \left. n(\omega)\,n\left(\frac{u}{1+u+u^2}\omega\right)n\left(\frac{u(u+1)}{1+u+u^2}\omega\right)\right]du\,,\\
S_2 &= \int_0^1 \frac{(1+u+u^2)^{\beta+1}(u+1)^{2\beta+1}}{u^{2\beta+3}}\left[n\left(\frac{1+u+u^2}{u}\omega\right)n\left((u+1)\omega\right)n\left(\frac{u+1}{u}\omega\right)\right.\\
&+ n(\omega)\,n\left((u+1)\omega\right)n\left(\frac{u+1}{u}\omega\right) - n(\omega)\,n\left(\frac{1+u+u^2}{u}\omega\right)n\left(\frac{u+1}{u}\omega\right)\\
&- \left. n(\omega)\,n\left(\frac{1+u+u^2}{u}\omega\right)n\left((u+1)\omega\right)\right]du\,,\\
S_3 &= \int_0^1 \frac{u^{2\beta+2}(1+u+u^2)^{\beta+1}}{(1+u)^{2\beta+3}}\left[n(u\omega)\,n\left(\frac{1+u+u^2}{1+u}\omega\right)n\left(\frac{u}{1+u}\omega\right)\right.\\
&+ n(\omega)\,n\left(\frac{1+u+u^2}{1+u}\omega\right)n\left(\frac{u}{1+u}\omega\right) - n(\omega)\,n(u\omega)\,n\left(\frac{1+u+u^2}{1+u}\omega\right)\\
&- \left. n(\omega)\,n(u\omega)\,n\left(\frac{u}{1+u}\omega\right)\right]du\,,\\
S_4 &= \int_0^1 \frac{(1+u+u^2)^{\beta+1}}{u^{2\beta+3}(1+u)^{2\beta+2}}\left[n\left(\frac{\omega}{u}\right)n\left(\frac{1+u+u^2}{u(1+u)}\omega\right)n\left(\frac{\omega}{1+u}\omega\right)\right.\\
&+ n(\omega)\,n\left(\frac{1+u+u^2}{u(1+u)}\omega\right)n\left(\frac{\omega}{u}\right) - n(\omega)\,n\left(\frac{\omega}{u}\right)n\left(\frac{\omega}{1+u}\right)\\
&- \left. n(\omega)\,n\left(\frac{\omega}{u}\omega\right)n\left(\frac{1+u+u^2}{u(1+u)}\omega\right)\right]du\,.
\end{aligned}
$$

This equation can be used for the numerical simulation of weak turbulence.

4 Kolmogorov solutions

The aim is to look for stationary solutions of the kinetic equation. From Eq. (3.8) we easily find that the solution

$$\frac{\partial \mathcal{N}(\omega)}{\partial t} = 0 \iff I(\alpha,\beta,\gamma) = 0\,, \tag{4.1}$$

is satisfied only for $\gamma = 0, 1$ and $y = 0, 1$.

In terms borrowed from statistical mechanics, the cases $\gamma = 0, 1$ represent the thermodynamic equilibrium solutions

$$n(\omega) = c\,, \tag{4.2}$$

where c is an arbitrary constant and

$$n(\omega) \propto \omega^{-1} \propto |k|^{-\alpha}\,, \tag{4.3}$$

which stem from the more general Rayleigh-Jeans distribution

$$n_{RJ}(\omega) = \frac{c_1}{c_2 + \omega}\,. \tag{4.4}$$

They correspond respectively to equipartition of particle number N and quadratic energy E

$$N = \int n(k)dk = \int \mathcal{N}(\omega)\,d\omega\,, \tag{4.5}$$

$$E = \int \omega(k)n(k)dk = \int \omega\,\mathcal{N}(\omega)\,d\omega\,. \tag{4.6}$$

The cases $y = 0, 1$ give the non-equilibrium Kolmogorov-type solutions, respectively

$$n(\omega) \propto \omega^{\frac{-2\beta/3-1+\alpha/3}{\alpha}} \propto |k|^{-2\beta/3-1+\alpha/3}\,, \tag{4.7}$$

and

$$n(\omega) \propto \omega^{-\frac{2\beta/3+1}{\alpha}} \propto |k|^{-2\beta/3-1}\,, \tag{4.8}$$

which exhibit typical dependence on the parameter β of the interaction coefficient. The latter solutions are more interesting since realistic sea spectra are of Kolmogorov-type by analogy.

For the case $\alpha = 1/2$ and $\beta = 0$, the Kolmogorov-type solutions are

$$n(\omega) \propto \omega^{-5/3} \propto |k|^{-5/6}\,, \tag{4.9}$$

$$n(\omega) \propto \omega^{-2} \propto |k|^{-1}\,. \tag{4.10}$$

Both exponents satisfy the conditions of locality (3.10)-(3.11).

5 Nature and sign of the fluxes

The stationary non-equilibrium states are related to fluxes of integrals of motion, namely the quantities N and E in our four-wave interaction problem. We define the flux of particles (or wave action) and energy as, respectively

$$Q(\omega) = -\int_0^\omega \frac{\partial \mathcal{N}(\omega')}{\partial t}\,d\omega'\,, \tag{5.1}$$

$$P(\omega) = -\int_0^\omega \omega' \frac{\partial \mathcal{N}(\omega')}{\partial t}\,d\omega'\,. \tag{5.2}$$

Here, Eq. (4.7), resp. Eq. (4.8), is associated with constant flux Q_0, resp. P_0, of particles, resp. energy. Let us now mention a physical argument which plays a crucial role in deciding the realizability of the Kolmogorov-type spectra. A more detailed justification is provided below in Section 11 – see also [6] and [13]. Suppose that pumping is performed at some frequencies around $\omega = \omega_f$ and damping at ω near zero and $\omega \gg \omega_f$. Weak turbulence theory then states that the energy is expected to flow from ω_f to higher ω's (direct cascade with $P_0 > 0$) while the particles mainly head for lower ω's (inverse cascade with $Q_0 < 0$). Accordingly, we need to evaluate the fluxes in order to select, among the rich family of power laws (4.7) and (4.8), those which are likely to result from numerical simulations of Eq. (2.1) with damping and forcing.

By inserting Eq. (3.8) into Eqs (5.1) and (5.2), we obtain

$$Q_0 \propto \lim_{y\to 0} \frac{\omega^{-y}}{y} I\,, \quad P_0 \propto \lim_{y\to 1} \frac{\omega^{-y+1}}{1-y} I\,, \tag{5.3}$$

which become

$$Q_0 \propto \left.\frac{\partial I}{\partial y}\right|_{y=0}\,, \quad P_0 \propto \left.\frac{\partial I}{\partial y}\right|_{y=1}\,. \tag{5.4}$$

Using Eq. (3.9), the derivatives in Eq. (5.4) can be expressed as

$$\begin{aligned} -\left.\frac{\partial I}{\partial y}\right|_{y=0} &= \int_\Delta S\,(\xi_1,\xi_2,\xi_3)\;(1+{\xi_3}^\gamma-{\xi_1}^\gamma-{\xi_2}^\gamma)\;\delta(1+\xi_3-\xi_1-\xi_2) \\ &\quad\times \ln\left(\frac{\xi_1\xi_2}{\xi_3}\right)\,\delta({\xi_1}^{\frac{1}{\alpha}}+{\xi_2}^{\frac{1}{\alpha}}+{\xi_3}^{\frac{1}{\alpha}}-1)\,d\xi_1 d\xi_2 d\xi_3\,, \end{aligned}$$

$$\begin{aligned} \left.\frac{\partial I}{\partial y}\right|_{y=1} &= \int_\Delta S\,(\xi_1,\xi_2,\xi_3)\;(1+{\xi_3}^\gamma-{\xi_1}^\gamma-{\xi_2}^\gamma)\;\delta(1+\xi_3-\xi_1-\xi_2) \\ &\quad\times\left[\xi_1\ln(1/\xi_1)+\xi_2\ln(1/\xi_2)-\xi_3\ln(1/\xi_3)\right] \\ &\quad\times\delta({\xi_1}^{\frac{1}{\alpha}}+{\xi_2}^{\frac{1}{\alpha}}+{\xi_3}^{\frac{1}{\alpha}}-1)\,d\xi_1 d\xi_2 d\xi_3\,, \end{aligned}$$

with

$$S\,(\xi_1,\xi_2,\xi_3) = \frac{4\pi}{\alpha^4}\,(\xi_1\xi_2\xi_3)^{\frac{\beta/2+1}{\alpha}-1-\gamma}\,.$$

The sign of each integral above is determined by the factor (see [12])

$$f(\gamma) = 1+{\xi_3}^\gamma-{\xi_1}^\gamma-{\xi_2}^\gamma\,.$$

It is found that $f(\gamma)$ is positive when

$$\gamma<0 \quad \text{or} \quad \gamma>1\,. \tag{5.5}$$

For the same values of β as those considered by MMT and the additional value $\beta=+3$, Table 1 displays the corresponding frequency slopes from Eqs. (4.7), (4.8) and the signs of Q_0, P_0 according to the criterion (5.5).

β	-1	$-3/4$	$-1/2$	$-1/4$	0	$+3$
γ_Q	$1/3$	$2/3$	1	$4/3$	$5/3$	$17/3$
sign of Q_0	$+$	$+$	0	$-$	$-$	$-$
γ_P	$2/3$	1	$4/3$	$5/3$	2	6
sign of P_0	$-$	0	$+$	$+$	$+$	$+$

Table 1: Signs of the fluxes for the Kolmogorov-type solutions.

Our calculations show that WT theory should work most successfully for $\beta=0$ (instead of $\beta=-1$ in [6]) at which they yield both $Q_0<0$ and $P_0>0$. Incidentally, MMT reported the smallest difference between numerics and theory for $\beta=0$. The cases with spectral slopes

less steep than the Rayleigh-Jeans distribution (i.e. $\gamma < 1$) are non-physical. At best, a thermodynamic equilibrium is expected in the conservative regime. Hence, we cannot strictly rely on the Kolmogorov-type exponents for $\beta = -1, -3/4$ to compare with the numerical results in forced regimes. Note that for $\beta = -1/2$, although we find $P_0 > 0$, a pure thermodynamic equilibrium state (i.e. $\gamma = 1$) is predicted instead of the inverse cascade. This is however not valid because of the necessity for a finite flux of particles towards $\omega = 0$. The direct cascade may then be influenced one way or another, possibly making the theory not applicable to the whole spectrum. Using both criteria (5.5), we deduce that the fluxes of particles and energy simultaneously have the correct signs in the region of parameter

$$\beta < -\frac{3}{2} \quad \text{and} \quad \beta > 2\alpha - \frac{3}{2}, \tag{5.6}$$

or

$$\beta < -\frac{3}{2} \quad \text{and} \quad \beta > -\frac{1}{2} \quad \text{if} \quad \alpha = \frac{1}{2}. \tag{5.7}$$

Since the strength of nonlinearity decreases with β, the case $\beta < -3/2$, which is close to a linear problem, is not that interesting from a general viewpoint and may raise some difficulties in numerical studies.

Restricting again to $\alpha = 1/2$ and $\beta = 0$, one has for the spectrum

$$n(\omega) = a\, P^{1/3}\, \omega^{-2}, \tag{5.8}$$

where P is the flux of energy towards high frequencies and

$$a = \left(\left. \frac{\partial I}{\partial y} \right|_{y=1} \right)^{-1/3}, \tag{5.9}$$

is the Kolmogorov constant. Numerical calculations give for a

$$a = 0.376\,. \tag{5.10}$$

An important question is the stability of the stationary spectra. This question was studied by Balk and Zakharov in [14] from a general point of view. The particular situation discussed in the present paper requires an additional study based on the work [14]. However, one should note that instability of the present spectra is unlikely. The reason is that the stationary spectra are solutions of the kinetic equation, which is not sensitive to changing the sign of the nonlinearity in the dynamical equation. In other words, if the Kolmogorov solution was unstable, it would be unstable in both cases. Since we observe the Kolmogorov spectrum in the numerical simulation for one of the signs of nonlinearity, instability is unlikely.

6 Solitons and quasisolitons

Besides random radiative waves, solitons are the most interesting features of nonlinear Hamiltonian models such as the focusing NLS. These localized coherent structures can naturally emerge and persist as the result of the stable competition between nonlinear and dispersive mechanisms. It is known that they act as statistical attractors to which the system relaxes and they can influence the dynamics in a substantial way.

Equally important coherent structures are *quasisolitons*. They could be defined as solitons having finite but long enough life time. Solitons and quasisolitons can be compared with stable and unstable elementary particles. Formally, both solitons and quasisolitons are defined as solutions of Eq. (2.3) of the form

$$\hat{\psi}_k(t) = e^{i(\Omega - kV)t}\,\hat{\phi}_k\,. \tag{6.1}$$

Here Ω and V are constants. In the x-space,

$$\psi(x,t) = e^{i\Omega t}\,\xi(x - Vt)\,, \tag{6.2}$$

where $\xi(x)$ is the inverse Fourier transform of $\hat{\phi}_k$ and V is the soliton velocity. The amplitude $\hat{\phi}_k$ satisfies the integral equation

$$\hat{\phi}_k = -\frac{1}{\Omega - kV + \omega(k)} \int T_{123k}\,\hat{\phi}_1\hat{\phi}_2\hat{\phi}_3^*\,\delta(k_1 + k_2 - k_3 - k)\,dk_1dk_2dk_3\,. \tag{6.3}$$

The "classical" or "true" soliton is a localized solution of Eq. (6.3). In this case,

$$|\xi(x)|^2 \to 0\,, \quad \text{as } |x| \to \infty\,. \tag{6.4}$$

This implies that $\hat{\phi}_k$ is a continuous function which has no singularities for real k. Thus the denominator in Eq. (6.3) should not vanish on the real axis

$$\Omega - kV + \omega(k) \neq 0\,, \quad -\infty < k < +\infty\,. \tag{6.5}$$

For $\omega(k) = |k|^\alpha$ and $\alpha < 1$, the last condition is violated for any $V \neq 0$. So "true solitons" can exist only if $V = 0$.

Next we show that "true" solitons can only exist for $\lambda = -1$. Eq. (6.3) can be rewritten in the variational form

$$\delta(H + \Omega N) = 0\,. \tag{6.6}$$

Obviously, $\Omega > 0$ should hold (otherwise, the denominator (6.5) has zeroes). Since

$$T_{123k} = \lambda\,|k_1k_2k_3k|^{\beta/4}\,, \quad \lambda = \pm 1\,, \tag{6.7}$$

the Hamiltonian is positive for $\lambda = +1$ and the condition (6.6) can be achieved only if $\hat{\phi}_k \equiv 0$. There are no solitons in this case. Meanwhile, solitons can exist for $\lambda = -1$. A rigorous proof of existence is beyond the frame of this article.

Quasisolitons are a more sophisticated object. Let us allow the denominator (6.5) to have a zero at $k = k_0$ and suppose that $\hat{\phi}_k$ is a function which is sharply localized near the wave number $k = k_m$. Let the width of $\hat{\phi}_k$ near $k = k_m$ be κ. One can introduce

$$T(k) = \int T_{123k}\,\hat{\phi}_1\hat{\phi}_2\hat{\phi}_3^*\,\delta(k_1 + k_2 - k_3 - k)\,dk_1dk_2dk_3\,. \tag{6.8}$$

We might expect that

$$T(k_0) \simeq e^{-C\frac{|k_0 - k_m|}{\kappa}}\,|\hat{\phi}(k_m)|^2\hat{\phi}(k_m)\,. \tag{6.9}$$

In other words, $\hat{\phi}_k$ has a pole at $k = k_0$ but the residue at this pole is exponentially small. It means that the soliton (6.2) is not exactly localized and goes to a very small-amplitude monochromatic wave with wave number $k = k_0$ as $x \to -\infty$.

If one eliminates the pole from $\hat{\phi}_k$, one gets a quasisoliton, which is a stationary solution of (2.3) only approximately. Such a quasisoliton lives for a finite time. If this time is long enough, the quasisoliton could become the basic unit of wave turbulence. This is what we believe may happen in the MMT model with positive nonlinearity.

7 Soliton stability and collapse

Coherent structures can play a role in wave turbulence only if they are stable. For $\lambda = -1$, a soliton satisfies the equation

$$(\Omega + |k|^\alpha)\,\hat{\phi}_k = \int |k_1 k_2 k_3 k|^{\beta/4}\;\hat{\phi}_1\hat{\phi}_2\hat{\phi}_3^*\,\delta(k_1 + k_2 - k_3 - k)\,dk_1 dk_2 dk_3\,. \tag{7.1}$$

The free parameter Ω can be eliminated by the scaling

$$\hat{\phi}_k = \Omega^{-\frac{\beta-\alpha+2}{2\alpha}}\,\chi\left(\Omega^{-\frac{1}{\alpha}}k\right)\,, \tag{7.2}$$

where $\chi(\xi)$ satisfies the equation

$$(1 + |\xi|^\alpha)\,\chi(\xi) = \int |\xi_1\xi_2\xi_3\xi|^{\beta/4}\;\chi_1\chi_2\chi_3^*\,\delta(\xi_1 + \xi_2 - \xi_3 - \xi)\,d\xi_1 d\xi_2 d\xi_3\,. \tag{7.3}$$

Let us calculate the total wave action in the soliton

$$N = \int |\hat{\phi}_k|^2\,dk = \Omega^{-\frac{\beta-\alpha+1}{\alpha}}\,N_0\,, \tag{7.4}$$

where

$$N_0 = \int |\chi|^2\,d\xi\,. \tag{7.5}$$

The stability question can be answered by computing $\partial N/\partial\Omega$. As is well-known (see [15]), a soliton is stable if $\partial N/\partial\Omega > 0$. In our case,

$$\frac{\partial N}{\partial\Omega} = -\left(\frac{\beta-\alpha+1}{\alpha}\right)\frac{N}{\Omega}\,. \tag{7.6}$$

The soliton is stable if

$$\beta < \alpha - 1\,, \tag{7.7}$$

otherwise the soliton is unstable. For $\alpha = 1/2$, the condition of soliton instability reads

$$\beta > -\frac{1}{2}\,. \tag{7.8}$$

This condition is satisfied in all the cases we studied.

The soliton instability leads us to guess that the typical coherent structure in the case of negative nonlinearity is a collapsing singularity. Typically, the formation of such singularities is described by self-similar solutions of the initial equations. Eq. (2.3) has the following family of self-similar solutions

$$\hat{\psi}(k,t) = (t_0 - t)^{p+i\epsilon}\,\chi\left[k(t_0 - t)^{\frac{1}{\alpha}}\right]\,, \tag{7.9}$$

where $p = \frac{\beta-\alpha+2}{2\alpha}$ and ϵ is an arbitrary constant. $\chi(\xi)$ satisfies the equation

$$\mathrm{i}\,(p + \mathrm{i}\epsilon)\,\chi + \frac{\mathrm{i}}{\alpha}\,\xi\,\chi' + |\xi|^\alpha\,\chi + \lambda\int |\xi_1\xi_2\xi_3\xi|^{\beta/4}\;\chi_1\chi_2\chi_3^*\,\delta(\xi_1 + \xi_2 - \xi_3 - \xi)\,d\xi_1 d\xi_2 d\xi_3 = 0\,. \tag{7.10}$$

The soliton (7.9) should stay finite when $t \to t_0$. This requirement imposes the following asymptotic behavior on $\chi(\xi)$

$$\chi(\xi) \to C\,\xi^{\frac{-\beta+\alpha-2}{2}}\,,\ \ \xi \to 0\,. \tag{7.11}$$

At time $t = t_0$, Eq. (7.9) turns to the powerlike function

$$\hat{\psi}_k \to C\,k^{-\nu}\,,\quad \nu = \frac{\beta-\alpha+2}{2}\,. \tag{7.12}$$

In reality, the self-similar solution is realized in x-space in a finite domain of order L. Hence the solution (7.12) should be cut off at $k \simeq 1/L$. In k-space, Eq. (7.9) represents the formation of a powerlike "tail" (7.12). The wave action concentrated in this tail must be finite. Therefore the integral

$$\int_0^\infty |\hat{\psi}_k|^2\,dk\,, \tag{7.13}$$

should converge as $k \to \infty$. It leads to the condition on parameters

$$\beta > \alpha - 1\,, \tag{7.14}$$

which coincides with the condition for soliton instability.

Let us plug (7.9) into the Hamiltonian in Fourier space

$$\begin{aligned} H &= \int \omega(k)\,|\hat{\psi}_k|^2 dk + \int T_{123k}\,\hat{\psi}_1\hat{\psi}_2\hat{\psi}_3^*\hat{\psi}_k^*\,\delta(k_1+k_2-k_3-k)\,dk_1dk_2dk_3dk\,, \\ &= (t_0-t)^{\frac{\beta-2\alpha+1}{\alpha}}\,H_0\,, \end{aligned}$$

where

$$H_0 = \int |\xi|^\alpha\,|\chi|^2\,d\xi + \lambda\int |\xi_1\xi_2\xi_3\xi|^{\beta/4}\,\chi_1\chi_2\chi_3^*\chi^*\,\delta(\xi_1+\xi_2-\xi_3-\xi)\,d\xi_1d\xi_2d\xi_3d\xi\,. \tag{7.15}$$

If $\alpha - 1 < \beta < 2\alpha - 1$, then $H \to \infty$ as $t \to t_0$, unless

$$H_0 = 0\,. \tag{7.16}$$

Apparently, this condition can be satisfied only for $\lambda = -1$ (negative nonlinearity). The condition (7.16) imposes implicitly a constraint on the constant ϵ. In fact, it can be realized only at one specific value of ϵ, which is an eigenvalue of the boundary problem (7.10) with the boundary conditions

$$\begin{aligned} &\chi(\xi) \to C\,\xi^{\frac{-\beta+\alpha-2}{2}}\,,\ \ \xi \to 0\,, \\ &\chi(\xi) \to \infty\,,\ \ |\xi| \to \infty\,. \end{aligned}$$

In the case $\beta > 2\alpha - 1$, $H \to 0$ as $t \to t_0$. There is no limitation on the value of H_0 and the singularity can take place for either sign of λ. If $\nu < 1$ in Eq. (7.15) or $\alpha - 1 < \beta < \alpha$, a collapse is the formation of an integrable singularity in x-space. If $\nu > 1$ or $\beta > \alpha$, the singularity is the formation of a discontinuity of the function $\psi(x)$ or its derivatives.

The formation of singularities leads to the formation in k-space of a powerlike spectrum

$$n_k \simeq |\hat{\psi}_k|^2 \simeq |k|^{-2\nu} \simeq |k|^{-\beta+\alpha-2}\,. \tag{7.17}$$

For $\alpha = 1/2$ and $\beta = 0$, one obtains

$$n_k \simeq |k|^{-3/2} \simeq \omega^{-3}\,. \tag{7.18}$$

This spectrum can be called Phillips spectrum by analogy to the well-known "ω^{-5} spectrum" for deep water waves. As $\omega \to \infty$, it decays faster than Kolmogorov spectra.

8 More on quasisolitons

Let us consider again the case of negative nonlinearity $\lambda = -1$ and denote

$$F = -\Omega + kV - \omega(k) = -\Omega + kV - |k|^\alpha . \tag{8.1}$$

If $V = 0$ and $\Omega > 0$, $|F|$ has a minimum at $k = 0$. The Fourier transform of the solution $\hat{\phi}_k$ is concentrated near this minimum in a domain of width

$$\kappa \simeq \Omega^{1/\alpha} . \tag{8.2}$$

Assuming that the soliton is smooth in x-space, $\hat{\phi}_k$ decays very fast outside of the domain (8.2). So far we assumed that $V = 0$. Let now V be positive but very small. Then the denominator F has a zero at $k = k_0 \simeq V^{\frac{1}{\alpha-1}}$. For small V, the wavenumber k_0 is much larger than κ and this zero occurs very far from the domain which supports the soliton. This means that $\hat{\phi}_k$ has a pole at $k = k_0$, but the residue at this pole is very small. The presence of this pole means that the stationary solution (6.3) looks in the x-space like a soliton, which is not completely localized. As $x \to +\infty$, it becomes a monochromatic wave with wave number k_0 and negligibly small amplitude.

If this "wave tail" is cut off in the initial data, one has a "quasisoliton" which slowly decays due to radiation of energy in the right direction. If V is small enough, the lifetime of the quasisoliton is very long and its shape is close to the shape of "real" solitons.

It is unlikely that quasisolitons play an important role in wave turbulence at negative nonlinearity. If V is not small, their lifetime is too short; if V is small, they are unstable like real solitons. Quasisolitons are more relevant in the case of positive nonlinearity $\lambda = +1$.

Let us choose an arbitrary $k = k_m > 0$ and plug in Eq. (6.3)

$$V = \alpha k_m^{\alpha-1} , \quad \Omega = -(1-\alpha) k_m^\alpha - \frac{1}{2} \alpha (1-\alpha) k_m^{\alpha-2} q^2 . \tag{8.3}$$

Then

$$F = k_m^\alpha - |k|^\alpha + \alpha k_m^{\alpha-1}(k - k_m) + \frac{1}{2} \alpha (1-\alpha) k_m^{\alpha-2} q^2 . \tag{8.4}$$

Note that if $\alpha < 1$ then F has a zero at $k = k_0 < 0$ for any k_m. Hence, $1/F$ always has a pole on the negative real axis, and the soliton (6.3) cannot be a real soliton. But if $q^2 \ll k_m^\alpha$, $1/F$ has a sharp minimum at $k \simeq k_m$. Introducing

$$\kappa = |k - k_m| , \tag{8.5}$$

one has approximately

$$F \simeq \frac{1}{2} \alpha (1-\alpha) k_m^{\alpha-2} \left[\kappa^2 + q^2\right] , \tag{8.6}$$

and one gets for the width of the maximum

$$\kappa \simeq q . \tag{8.7}$$

If $\kappa \ll |k_0|$, one can construct a quasisoliton which is supported in k-space near k_m. In the general case, $|k_0| \simeq k_m$. If $\alpha = 1/2$ and $q = 0$, one can easily find

$$k_0 = -(\sqrt{2} - 1)^2 k_m . \tag{8.8}$$

The quasisoliton moves to the right direction with the velocity $V(k_m)$ and radiates backward monochromatic waves of wavenumber k_0. The shape of the quasisoliton can be found explicitly in the limit $q \to 0$. Now $\kappa \ll k_m$ and one has approximately

$$\int |k_1 k_2 k_3 k|^{\beta/4}\ \hat{\phi}_1 \hat{\phi}_2 \hat{\phi}_3^*\, \delta(k_1 + k_2 - k_3 - k)\, dk_1 dk_2 dk_3 \tag{8.9}$$

$$\simeq k_m^\beta \int \hat{\phi}_1 \hat{\phi}_2 \hat{\phi}_3^*\, \delta(\kappa_1 + \kappa_2 - \kappa_3 - \kappa)\, d\kappa_1 d\kappa_2 d\kappa_3\,.$$

Taking into account Eq. (8.6), one can rewrite Eq. (6.3) as

$$\frac{1}{2}\,\alpha\,(1-\alpha)\,k_m^{\alpha-2}(\kappa^2+q^2)\,\hat{\phi}_\kappa = k_m^\beta \int \hat{\phi}_1 \hat{\phi}_2 \hat{\phi}_3^*\, \delta(\kappa_1 + \kappa_2 - \kappa_3 - \kappa)\, d\kappa_1 d\kappa_2 d\kappa_3\,. \tag{8.10}$$

With the help of inverse Fourier transform, one can transform (8.10) into the stationary NLS

$$\frac{1}{2}\,\alpha\,(1-\alpha)\,k_m^{\alpha-2}\left[-\frac{\partial^2\phi}{\partial x^2} + q^2\,\phi\right] = k_m^\beta\,|\phi|^2\,\phi\,, \tag{8.11}$$

which has the soliton solution

$$\phi(x) = \sqrt{\frac{\alpha\,(1-\alpha)}{k_m^{\beta-\alpha+2}}}\,\frac{q}{\cosh q\,x}\,. \tag{8.12}$$

It gives the following approximate quasisoliton solution of Eq. (2.1) with $\lambda = +1$:

$$\begin{aligned} \psi(x,t) &= \phi(x - Vt)\, e^{i\Omega t + i k_m (x - Vt)}\,, \\ \Omega &= -(1-\alpha)\,k_m^\alpha - \frac{1}{2}\,\alpha\,(1-\alpha)\,k_m^{\alpha-2}\,q^2\,, \\ V &= \alpha\,k_m^{\alpha-1}\,. \end{aligned} \tag{8.13}$$

The quasisoliton (8.13) is an "envelope soliton", which can be obtained directly from Eq. (2.1). Simply inject

$$\psi(x,t) = U(x,t)\, e^{-i(1-\alpha)k_m^\alpha t + i k_m (x - Vt)}\,, \tag{8.14}$$

and use the binomial expansion

$$\left|\frac{\partial}{\partial x}\right|^a e^{ikx}\,U = e^{ikx}\left[|k|^a\,U + a\,|k|^{a-1}\left(-\mathrm{i}\frac{\partial}{\partial x}\right)U + \frac{1}{2}\,a\,(a-1)\,|k|^{a-2}\left(-\mathrm{i}\frac{\partial}{\partial x}\right)^2 U + \cdots\right]. \tag{8.15}$$

Plugging Eq. (8.15) into Eq. (2.1) with $\lambda = +1$, one obtains a differential equation of infinite order

$$\begin{aligned} \mathrm{i}\left(\frac{\partial U}{\partial t} + V\,\frac{\partial U}{\partial x}\right) &= L_2\,U + L_3\,U + \cdots\,, \\ V &= \alpha\,k_m^{\alpha-1}\,. \end{aligned} \tag{8.16}$$

Here

$$L_2\,U = \frac{1}{2}\,\alpha\,(1-\alpha)\,k_m^{\alpha-2}\,\frac{\partial^2 U}{\partial x^2} + k_m^\beta\,|U|^2\,U\,, \tag{8.17}$$

$$L_3\,U = \mathrm{i}\left[\frac{1}{6}\,\alpha\,(\alpha-1)(\alpha-2)\,k_m^{\alpha-3}\,\frac{\partial^3 U}{\partial x^3} - \beta\,k_m^{\beta-1}|U|^2\,\frac{\partial U}{\partial x}\right], \tag{8.18}$$

$$L_4\,U = \cdots\,. \tag{8.19}$$

Taking into consideration only the first nontrivial term $L_2 U$, one gets the nonstationary NLS

$$\mathrm{i}\left(\frac{\partial U}{\partial t} + V\,\frac{\partial U}{\partial x}\right) = \frac{1}{2}\,\alpha\,(1-\alpha)\,k_m^{\alpha-2}\,\frac{\partial^2 U}{\partial x^2} + k_m^{\beta}\,|U|^2\,U\,. \tag{8.20}$$

It has a soliton solution

$$U(x,t) = \phi(x - Vt)\,e^{-\frac{1}{2}i\alpha(1-\alpha)k_m^{\alpha-2}q^2 t}\,. \tag{8.21}$$

To find the shape of the quasisoliton more accurately, one should keep in the right hand side of Eq. (8.15) a finite (but necessary odd!) number of terms. The expansion in Eq. (8.16) runs in powers of the parameter q/k_m. Note that one cannot find the lifetime of the quasisoliton. The lifetime grows as $e^{|k_0|/q}$ and its calculation is beyond the perturbation expansion.

As a matter of fact, the parameter

$$\epsilon = \frac{q}{k_m} \tag{8.22}$$

is crucial for quasisolitons. The smaller it is, the closer the quasisoliton is to a "real soliton". The amplitude of a quasisoliton is proportional to ϵ. Quasisolitons of small amplitude satisfy the integrable NLS and are stable. It is not obvious for quasisolitons of finite amplitude. One can guess that at least in the case $\beta > 0$, when collapse is not forbidden, there is a critical value of the amplitude of a quasisoliton ϵ_c such that for $\epsilon > \epsilon_c$ it is unstable and generates a singularity at a finite time. Our numerical experiments confirm this conjecture for $\beta = +3$.

Quasisolitons move with different velocities and collide. If the amplitudes of the quasisolitons are small and their velocities are close, they obey the NLS and their interaction is elastic. One can guess that the same holds for small-amplitude quasisolitons even if their velocities are quite different. This is not obvious for quasisolitons of moderate amplitude. One can think that their interaction is inelastic and leads to the merging and formation of a quasisoliton of larger amplitude.

9 Nonlinear frequency shift

Let us consider one more important nonlinear effect. In a linear system, the harmonic of wavenumber k oscillates with the frequency ω_k. In the presence of nonlinearity, the frequency changes due to the interaction with other harmonics. In a weakly nonlinear system, the frequency is modified by a functional depending linearly on the spectrum

$$\omega(k) \to \omega(k) + \int T_{1k}\,n_1\,dk_1\,. \tag{9.1}$$

It is easy to show that T_{1k} can be expressed in terms of the coefficient T_{123k} in Eq. (2.3) as

$$T_{1k} = 2\,T_{1k1k}\,. \tag{9.2}$$

For the MMT model,

$$T_{1k} = 2\,\lambda\,(k_1 k)^{\beta/2}\,. \tag{9.3}$$

For $\beta = 0$,

$$T_{1k} = 2\,\lambda = \pm 2\,, \tag{9.4}$$

and

$$\omega^{\pm}(k) = \omega(k) \pm 2N\,, \tag{9.5}$$

where $N = \int |\hat{\psi}_k|^2 dk$ is the total number of particles.

In the general case $\beta \neq 0$, renormalization of the frequency leads to modified resonance conditions (2.8)-(2.9). But in the particular case $\beta = 0$, renormalization terms in Eq. (2.9) cancel and the resonance conditions in the first nonlinear approximation remain unchanged. At the same time, the difference of frequencies for different signs of nonlinearity has the form

$$\omega^{+}(k) - \omega^{-}(k) = 4N\,. \tag{9.6}$$

In our case, it does not depend on the wave number.

10 On the MMT model spectrum

In [6], MMT found that in the case of positive nonlinearity the spectrum of wave turbulence is well described by the formula (MMT spectrum)

$$n_k \simeq k^{-\frac{\beta+\alpha}{2}-1}\,. \tag{10.1}$$

They checked this result for $\alpha = 1/2$ and different values of β. Our experiments are in agreement with (10.1). In [7], it was found that the MMT spectrum can appear for either sign of nonlinearity. So far there is no proper theoretical derivation of the MMT spectrum. In this section, we offer some heuristic derivation of (10.1).

Assuming formula (3.2) to be exact, the problem of closure for the equation on particle number lies in the expression of $\mathrm{Im}\, J_{123k}$ in terms of n_k. This expression should a priori satisfy the conditions of symmetry

$$\mathrm{Im}\, J_{123k} = \mathrm{Im}\, J_{213k} = \mathrm{Im}\, J_{12k3} = -\mathrm{Im}\, J_{3k12}\,. \tag{10.2}$$

Moreover, one can assume that the nonlinearity is weak and that the wave energy is roughly

$$E \simeq \int \omega(k)\, n_k\, dk\,. \tag{10.3}$$

From conservation of energy, one obtains

$$\int T_{123k}\, (\omega_1 + \omega_2 - \omega_3 - \omega)\, \mathrm{Im}\, J_{123k}\, dk_1 dk_2 dk_3 dk = 0\,. \tag{10.4}$$

Hence one must have

$$\mathrm{Im}\, J_{123k} \simeq \delta(\omega_1 + \omega_2 - \omega_3 - \omega)\,. \tag{10.5}$$

For Gaussian wave turbulence, the real part of J_{123k} is given by Eq. (3.3) and dimensional analysis gives

$$\mathrm{Re}\, J_{123k} \simeq \frac{n_k^2}{k}\,. \tag{10.6}$$

Up to this point, our consideration was more or less rigorous. Now we present a heuristic conjecture. We suppose that the imaginary part of the four-wave correlator has the same scaling as the real part. In other words, it is quadratic in n_k.

If one takes into account the necessary conditions (10.2), (10.4) and the scaling (10.6) for $\mathrm{Im}\, J_{123k}$, there are not that many possibilities for the construction of $\mathrm{Im}\, J_{123k}$. We offer the following closure

$$\mathrm{Im}\, J_{123k} = a \left(\frac{\partial \omega_1}{\partial k_1} + \frac{\partial \omega_2}{\partial k_2} + \frac{\partial \omega_3}{\partial k_3} + \frac{\partial \omega}{\partial k} \right) \delta \left(\omega_1 + \omega_2 - \omega_3 - \omega \right) \left(n_1 n_2 - n_3 n_k \right) , \qquad (10.7)$$

where $a \ll 1$ is a dimensionless constant. The closure leads to the kinetic equation

$$\begin{aligned} \frac{\partial n_k}{\partial t} &= 2\, a \int T_{123k} \left(n_1 n_2 - n_3 n_k \right) \left(\frac{\partial \omega_1}{\partial k_1} + \frac{\partial \omega_2}{\partial k_2} + \frac{\partial \omega_3}{\partial k_3} + \frac{\partial \omega}{\partial k} \right) \\ &\times \delta \left(\omega_1 + \omega_2 - \omega_3 - \omega \right) \delta \left(k_1 + k_2 - k_3 - k \right) dk_1 dk_2 dk_3 . \end{aligned} \qquad (10.8)$$

It is easy to check that the Kolmogorov solution of Eq. (10.8) leads to the MMT spectrum. Eq. (10.8) resembles the Boltzmann's equation for interacting particles. Apparently, it can make sense only if $a\, T_{123k} > 0$. Otherwise, the H-theorem and the second law of thermodynamics will be violated. We must stress that the formula (10.7) is heuristic and has no rigorous justification.

11 Particle and energy balance

In the presence of damping and linear instability, Eq. (2.3) can be written in the form

$$\mathrm{i} \frac{\partial \hat{\psi}_k}{\partial t} = \frac{\delta H}{\delta \hat{\psi}_k^*} + \mathrm{i}\, D(k)\, \hat{\psi}_k , \qquad (11.1)$$

where

$$H = \int \omega(k) \left| \hat{\psi}_k \right|^2 dk + \frac{1}{2} \int T_{123k}\, \hat{\psi}_1 \hat{\psi}_2 \hat{\psi}_3^* \hat{\psi}_k^*\, \delta(k_1 + k_2 - k_3 - k)\, dk_1 dk_2 dk_3 dk , \qquad (11.2)$$

is the Hamiltonian, $D(k)$ is the damping or the growth rate of instability depending on its sign.

Let $N = \int |\hat{\psi}_k|^2 dk$ be the total number of particles in the system. From (11.1), one can obtain the exact equation for the particle balance

$$\frac{dN}{dt} = Q = 2 \int D(k) \left| \hat{\psi}_k \right|^2 dk . \qquad (11.3)$$

After averaging, one has

$$\frac{d\langle N \rangle}{dt} = 2 \int D(k)\, n_k\, dk = \langle Q \rangle . \qquad (11.4)$$

The flux of particles Q is a linear functional of n_k at any level of nonlinearity.

For the energy flux, one has the exact identity

$$\begin{aligned} P &= \frac{dH}{dt} = 2 \int \omega(k)\, D(k) \left| \hat{\psi}_k \right|^2 dk \\ &+ \frac{1}{2} \int \left[D(k_1) + D(k_2) + D(k_3) + D(k) \right] T_{123k}\, \hat{\psi}_1 \hat{\psi}_2 \hat{\psi}_3^* \hat{\psi}_k^* \\ &\times \delta(k_1 + k_2 - k_3 - k)\, dk_1 dk_2 dk_3 dk . \end{aligned} \qquad (11.5)$$

For the averaged density of energy, one has

$$\begin{aligned}\langle P\rangle &= 2\int \omega(k)\, D(k)\, n_k\, dk \\ &+ \frac{1}{2}\int [D(k_1)+D(k_2)+D(k_3)+D(k)]\, T_{123k}\, \mathrm{Re}\, J_{123k} \\ &\times \delta(k_1+k_2-k_3-k)\, dk_1 dk_2 dk_3 dk\,. \end{aligned} \tag{11.6}$$

Assuming that Gaussian statistics holds, one can write

$$\mathrm{Re}\, J_{123k} \simeq n_1 n_2 \left[\delta(k_1-k_3)+\delta(k_1-k)\right]\,, \tag{11.7}$$

and one obtains after simple calculations

$$\langle P\rangle = 2\int \widetilde{\omega}(k)\, D(k)\, n_k\, dk\,, \tag{11.8}$$

where $\widetilde{\omega}(k) = \omega(k) + \int T_{1k}\, n_1\, dk_1$ is the renormalized frequency.

In the case $\beta = 0$ and $T_{1k} = \pm 2$,

$$\langle P\rangle = 2\int \omega(k)\, D(k)\, n_k\, dk + 2\,\lambda\, N\, \langle Q\rangle\,. \tag{11.9}$$

In the stationary state, $\langle Q\rangle = 0, \langle P\rangle = 0$ and the balance equations are

$$\int D(k)\, n_k\, dk = 0\,, \tag{11.10}$$

$$\int \omega(k)\, D(k)\, n_k\, dk = 0\,. \tag{11.11}$$

In this particular case, renormalization of the frequency does not influence the balance equations.

The balance equations (11.10)-(11.11) can be rewritten as

$$Q_0 = Q^+ + Q^-\,, \tag{11.12}$$

$$P_0 = P^+ + P^-\,, \tag{11.13}$$

where P_0 and Q_0 are the input of particles and energy in the area of instability $\omega \simeq \omega_0$. Q^+ and P^+ are the sinks of particles and energy in the high frequency region $\omega \sim \omega^+$. Q^- and P^- are the sinks in the low frequency region $\omega \sim \omega^-$.

Roughly speaking,

$$P_0 \simeq \omega_0\, Q_0\,, \tag{11.14}$$

$$P^+ \simeq \omega^+\, Q^+\,, \tag{11.15}$$

$$P^- \simeq \omega^-\, Q^-\,, \tag{11.16}$$

and the balance equations can be written as

$$Q_0 = Q^+ + Q^-\,, \tag{11.17}$$

$$\omega_0\, Q_0 \simeq \omega^+\, Q^+ + \omega^-\, Q^-\,. \tag{11.18}$$

Hence

$$\frac{Q^+}{Q^-} \simeq \frac{\omega_0 - \omega^-}{\omega^+ - \omega_0}, \quad \frac{P^+}{P^-} \simeq \frac{\omega^+}{\omega^-} \frac{\omega_0 - \omega^-}{\omega^+ - \omega_0}. \tag{11.19}$$

For $\omega^- \sim \omega_0 \ll \omega^+$, one has

$$\frac{Q^+}{Q^-} \simeq \frac{\omega_0 - \omega^-}{\omega^+}, \quad \frac{P^+}{P^-} \simeq \frac{\omega_0 - \omega^-}{\omega^-}. \tag{11.20}$$

In other words, if $\omega_0 \ll \omega^+$, almost all particles are absorbed at low frequencies. The amounts of energy absorbed in both ranges have the same order of magnitude. These conclusions are valid only under the hypothesis of approximate Gaussianity of wave turbulence.

and for the quadratic part of energy

$$E = \sum_{n=-\frac{N}{2}+1}^{\frac{N}{2}} \omega(k_n) \, |\hat{\psi}_n|^2 \, . \tag{12.5}$$

The linear frequency term is treated exactly by an integrating factor technique, removing it from the timestepping procedure. As emphasized by MMT, we thus avoid the natural stiffness of the problem as well as possible numerical instabilities. Consequently, we do not need to shorten the inertial interval by downshifting the cutoff of ultraviolet absorption (as in [4]). The nonlinear term is calculated through the Fast Fourier Transform by first transforming to real space where a multiplication is computed and then transforming back to spectral space. For the multiplication operation, twice the effective number of grid points are required in order to avoid aliasing errors. A fourth-order Runge-Kutta scheme integrates the conservative model in time, giving a solution to which the diagonal factor

$$e^{[F(k)+D(k)]\,\Delta t}$$

is applied at each time step Δt.

13 Numerical results for $\beta = 0, \lambda = \pm 1$

A series of numerical simulations of Eq. (12.1) with resolution up to 2048 de-aliased modes has been performed. We choose the case $\beta = 0$ as the candidate for testing weak turbulence in our experiments. Both cases $\lambda = \pm 1$ are examined, providing an additional test of the theory, and the study is focused on the direct cascade. Forcing is located at large scales and the inertial interval is defined by the right transparency window $k_f \ll k \ll k_d$ (where k_f and k_d are the characteristic wave numbers of forcing and ultraviolet damping respectively). As displayed in Table 1, the theoretical spectrum which can be realized in this window is

$$n_k \propto k^{-1} \, . \tag{13.1}$$

Typically, initial conditions are given by the random noise in the spectral space. Simulations are run until a quasi-steady regime is established which is characterized by small fluctuations of the energy and the number of particles around some mean value. Then time averaging begins and continues for a length of time which significantly exceeds the characteristic time scale of the slowest harmonic from the inertial range (free of the source and the sink). In turn, the time-step of the integration has to provide, at least, accurate enough resolution of the fastest harmonic in the system. As our experiments show, one has to use an even smaller time-step than defined by the last condition : the presence of fast nonlinear events in the system requires the use of a time-step $\Delta t = 0.005$, which is 40 times smaller than the smallest linear frequency period. Time averaging with such a small time step leads to a computationally time-consuming procedure despite the one-dimensionality of the problem.

From now on, we will present numerical results in the specific situations $\nu^- = 196.61$ ($\lambda = \pm 1$), $\nu^+ = 5.39 \times 10^{-48}$ ($\lambda = +1$) or $\nu^+ = 2.16 \times 10^{-47}$ ($\lambda = -1$), and $f_j = 0.2$, nonzero only for $k_j \in [6, 9]$ ($\lambda = \pm 1$).

The numerical simulations clearly display the development of dynamical chaos and statistically uniform turbulence. Both the amplitude and the phase of each harmonic fluctuate independently of each other. Fig. 1-4 show the behavior of the seventh and eighth harmonics.

Fig. 5-8 show the behavior of the real and imaginary parts of the amplitude of the harmonic $k = 200$. One sees amplitude-modulated oscillations with carrying frequency close to the corresponding linear frequency of the harmonic $\omega \simeq 14$.

Fig. 9-12 represent Fourier transforms in time of the evolution of the harmonic $k = 200$ from the previous pictures. One can see that the maximum of the spectra corresponds to the linear frequency shifted in accordance with the nonlinearity sign $\lambda = \pm 1$.

Fig. 13-14 demonstrate the behavior of the fourth and sixth-order moments as functions of the second-order moment. They fit the Gaussian laws very well. They provide a justification of the initial conjecture that the statistics of the turbulence is close to Gaussian.

Fig. 15 represents the time evolution of the quadratic energy E for $\lambda = \pm 1$ with the same amplitude of forcing. The curves are plotted over the interval $t \in [5000, 10000]$ where the time averaging actually takes place. One obviously sees that the systems have already reached the steady state. Their energies moderately fluctuate about mean values which are $E_m \simeq 19$ $(\lambda = +1)$ and $E_m \simeq 9$ $(\lambda = -1)$. This significant difference with respect to the sign of λ is quite unexpected from the viewpoint of the WT theory since the same rate of forcing is imposed in both systems. We can make the same remarks about the evolution of the number of particles N. In Fig. 16, the mean values stay near $N_m \simeq 3$ $(\lambda = +1)$ and $N_m \simeq 1$ $(\lambda = -1)$ so that their relative difference is even bigger than for E. Fluctuations also spread much more in the case $\lambda = +1$.

In Fig. 17, the stationarity as well as the gap between both signs of λ are verified again in the time evolution of the average nonlinearity ϵ. We define the average nonlinearity in the system as the ratio of the nonlinear part to the linear part of the Hamiltonian $\epsilon = |H_{NL}/H_L|$, each part being calculated over the whole field. Of course, this definition does not really make sense when external forces are applied but it provides a relatively good estimation of the level of nonlinearity once the systems reach the steady state. Note here that the mean values $\epsilon_m \simeq 0.4$ $(\lambda = +1)$ and $\epsilon_m \simeq 0.2$ $(\lambda = -1)$ are relatively small. Thus, the condition of small nonlinearity required by the theory holds for both systems. This conclusion is also supported by comparing Fig. 10 and Fig. 12. It is seen that the difference of frequencies caused by nonlinearity is relatively small. We point out that in our numerical experiments ϵ could not be taken too small (that is, $\epsilon \leq 10^{-3}$) for two reasons. First, the nonlinear turnover time grows longer and the energy flux is too weak to act effectively. Second, one may catch the undesirable frozen turbulence [10] due to the disappearance of quasiresonances. One should note that, in general, frozen turbulence arises more easily in one-dimensional problems due to fewer degrees of freedom than in higher-dimensional problems.

The difference between the cases $\lambda = \pm 1$ is especially conspicuous if one considers the dissipation rates of particles and quadratic energy in the left transparency window

$$Q^- = 2\int_0^{k_f} \nu^- |k|^{-d^-} |\hat{\psi}_k|^2 \, dk \quad , \quad P^- = 2\int_0^{k_f} \nu^- |k|^{-d^-} \omega(k) |\hat{\psi}_k|^2 \, dk \, ,$$

and in the right transparency window

$$Q^+ = 2\int_{k_f}^{k_{max}} \nu^+ |k|^{d^+} |\hat{\psi}_k|^2 \, dk \quad , \quad P^+ = 2\int_{k_f}^{k_{max}} \nu^+ |k|^{d^+} \omega(k) |\hat{\psi}_k|^2 \, dk \, ,$$

where k_{max} corresponds to the highest mode in the spectrum. Fig. 18-21 represent the time evolution of these quantities and their time-averaged values are collected in Table 2.

One can see that the case $\lambda = +1$ quantitatively fits WT theory. Indeed, in this case $Q^+/Q^- \simeq 0.046 \ll 1$ and $P^+/P^- \simeq 0.94$. But in the case of negative nonlinearity $\lambda = -1$ the

λ	N	E	Q^-	Q^+	P^-	P^+
$+1$	3	19	0.1957	0.0090	0.276	0.258
-1	1	9	0.0098	0.0478	0.014	1.430

Table 2: Time-averaged values of the wave action, quadratic energy and corresponding fluxes in the stationary state.

situation is opposite. In this case $Q^+/Q^- \simeq 4.9$ and $P^+/P^- \simeq 102$ which means that most of both quadratic energy and particles are transported to high frequencies.

Comparison of the turbulence levels and fluxes of particles Q^+ for both signs of nonlinearity leads to a paradoxal result. At $\lambda = -1$ the total number of particles is three times less than at $\lambda = +1$, while the dissipation rate of particles is higher by one order of magnitude. It can be explained only by the presence in this case of a much more powerful mechanism of nonlinear interactions, which provides very fast wave particles transport to high frequencies. In our opinion, this mechanism is wave collapse, studied theoretically in Section 7. Sporadic collapsing events developing on top of the WT background could send most of particles to high wavenumbers without violation of energy conservation, because in each self-similar collapse structure the amount of total energy is zero.

We observed such collapsing events in our numerical experiments. Fig. 22 displays the collapse event taking place at the point $x = 1.006$ at time $t = 5000.19$. One can conjecture that the collapses are described by self-similar solutions. For such solutions $H \equiv 0$. It means that the collapse can carry particles to high frequencies, *without carrying any energy at that time*! As far as the Hamiltonian is the difference of quadratic and quartic terms and both of them go to infinity, it becomes possible to explain the apparent contradictions of the dissipation rates.

The hypothesis related to the prevailing role of collapses at $\lambda = -1$ is corroborated by the following facts:

1. Intermittency in dissipation rates of quadratic energy and particles for $\lambda = -1$ is much higher than for $\lambda = +1$ in the region of large wave numbers. This intermittency can be explained by outbursts of dissipation when wave collapses occur.
2. The analysis of time Fourier transforms of separate harmonics (we take $k = 200$) shows the presence of two components, see Fig. 9. The peak at $\omega \simeq 13$ corresponds to a linear wave with a moderate nonlinear shift of frequency. This is the "weak turbulence"component of the wave field. Another component is roughly symmetrical with respect to the reflection $\omega \to -\omega$ with the maximum slightly below $\omega = 0$. This is certainly a strongly nonlinear component which could be associated with wave collapses.

Another indication of the difference of the wave dynamics in the cases $\lambda = +1$ and $\lambda = -1$ follows from the following experiment. Fig. 23-24 show the early stages in the conservative evolution of the same isolated initial condition

$$\psi(x) = \psi_0 \, e^{-\frac{(x-\pi)^2}{2\sigma^2}}, \quad \sigma = 0.5 .$$

In the case $\lambda = -1$, a sufficiently large initial condition collapses into a sharp spike, while in the case $\lambda = +1$ it decays. This experiment could serve as an evidence of the finite-time singularity formation for the case $\lambda = -1$.

Now we discuss the stationary isotropic spectra of turbulence which are displayed in Fig. 25-28. We plotted on the same pictures the Kolmogorov spectra calculated by putting either $P = P^+ = 1.430$ ($\lambda = -1$) or $P = P^+ = 0.258$ ($\lambda = +1$) and $a = 0.376$ in Eq. (5.8). In Fig.

27-28, one can see that for both cases this spectrum provides a higher level of turbulence than the observed one. For $\lambda = -1$ this difference is almost of one order of magnitude. For $\lambda = +1$, the observed spectrum almost coincides with the weak turbulence one at low frequencies and then decays faster at higher wave numbers (approximately as MMT spectrum in Fig. 26).

It is interesting that for $\lambda = -1$ the high frequency asymptotics is fairly close to the one predicted by WT theory (Fig. 25). One can explain this fact as follows. In this case, the turbulence is the coexistence of collapsing events and weak turbulence. Collapses carry most of the fluxes of particles and quadratic energy to high frequencies. But their contribution to the high-frequency part of the spectrum is weak, because they produce Phillips-type spectra, decaying very fast as $k \to \infty$. In our case, this spectrum is

$$n_k \simeq k^{-3/2}\,. \tag{13.2}$$

Hence as $k \to \infty$, only the WT component survives. Even $P \simeq 10^{-2}\,P^+$ is enough to provide an observable tail in the WT Kolmogorov spectrum.

We should stress out again that at $\lambda = +1$ the picture of turbulence matches the WT prediction both quantitatively and qualitatively. Meanwhile, the spectrum at high k's is steeper and closer to the MMT formula. So far we cannot give a consistent explanation of this fact. We can just guess that it is somehow connected with quasisolitons. As an illustration, Fig. 29 shows the conservative evolution of the initial quasisoliton (8.13) with parameter $q/k_m = 0.1$, which is small enough to justify the Taylor expansion used in its derivation. As expected, we observe that the solution propagates and persists over a relatively long time. This similarity between quasisolitons and real solitons is verified even better in Fig. 30-33 where two initial quasisolitons with $q/k_m = 0.2$ for the smaller one and $q/k_m = 0.25$ for the bigger one collide almost elastically. Note here that the solution with smaller amplitude moves with a greater velocity.

14 Numerical results for $\beta = +3$ and $\lambda = +1$

Another series of experiments has been performed for the case $\beta = +3$ and $\lambda = +1$. This case is especially attractive due to the fact that the intensity of interaction grows with characteristic wavenumber in Fourier space and one can expect reduced "frozen" turbulence effects compared to the case $\beta = 0$. Another motivation is the fact that the scaling of the interaction kernel reproduces the kernel for gravity water waves. Therefore, Eq. (12.1) with $\alpha = 1/2$, $\beta = +3$ can be considered as a model of turbulence of the ocean surface.

The numerical simulation of Eq. (12.1) was performed on a grid of 2048 points in the real space domain of length 2π. Parameters of the forcing are defined by

$$F(k) = \begin{cases} 0.001 & \text{if } 30 < k < 42\,, \\ 0 & \text{otherwise}\,, \end{cases}$$

and parameters of damping in the "hyperviscosity" form by

$$D(k) = \begin{cases} -0.05(k-4)^8 & \text{if } 0 < k < 4\,, \\ -0.1(k-824)^2 & \text{if } 824 < k < 1024\,, \\ 0 & \text{otherwise}\,. \end{cases}$$

Aliasing effects were not of concern due to the run-time control of the fastness of the spectrum decay toward high wavenumbers.

The time-step of integration was equal to $\frac{1}{50}$ of the inverse fastest linear frequency in the problem. Such a small value was chosen due to the fact that the time dependence of the individual Fourier harmonics corresponding to intermediate range wavenumbers showed the presence of processes of time scale smaller than the smallest linear time in the system. This observation was an initial indication of the significant role of nonlinearity in the problem under consideration.

Equation (12.1) was integrated numerically over long times for different kinds of initial conditions: low level random noise and single harmonic excitation ($k = 30$) initial conditions. While initial stages of computations were quantitatively different, the later stages of evolution were strikingly similar. Starting from big enough times, the wave system was separated into several soliton-like moving structures and low-amplitude quasi-linear waves. Processes of interaction of solitons and waves slowly redistributed the number of waves in a way leading to the growth of initially bigger solitons and the collapse of initially smaller solitons. Finally the system was clearly separated into a state with one moving soliton and quasi-linear waves.

We interpret the observed phenomenon as similar to the "droplet" effect observed earlier in non-integrable NLS equation [16]. The soliton solution turns out to be the statistical attractor for nonlinear non-integrable wave systems: long time evolution leads to the condensation of the integral of total number of waves into the single soliton which minimizes the Hamiltonian.

Fig. 34-35 show snapshots of the final state of the system: the single soliton is moving with constant speed on the background of quasi-linear waves. A quantitative comparison shows that the parameters of the observed object are close to the parameters of the quasisoliton solution (8.13).

One should emphasize that there is a difference between the situation observed in the present work and former observations of "droplet" effects in non-integrable NLS equations. Solitons observed in [16] were exact stable solutions of the corresponding NLS equation. Solitary solutions observed in the present work are "quasisolitons" which are unstable at least in a certain range of parameters.

In Fig. 36 the initial condition is the quasisoliton (8.13) with parameter $q/k_m = 0.1$. Here again, it behaves as the soliton should: it moves without any detectable change of shape. Fig. 37 shows the evolution for $q/k_m = 0.3$. One can interpret such initial condition as a "deformed" quasisoliton. This initial condition rapidly develops moving singularity collapsing, presumably, in finite time.

15 Conclusion

The MMT model with $\alpha < 1$ and either sign of nonlinearity exhibits coherent structures. In the case of negative nonlinearity these structures are weak collapses. These collapses are a powerful mechanism of energy dissipation, which dominates in all our numerical experiments. Weak turbulence coexists with collapses, and is responsible for the formation of Kolmogorov-type tails of wave spectra. But it carries to high wave numbers just a small part of the energy (less than 5%).

One may hope to get "pure" weak turbulence by decreasing the level of nonlinearity. But to achieve an adequate modeling of the continuous medium, one should take a very fine mesh (at least 10^4 harmonics) and apply forcing in a broad range (say $10 < k < 100$). Otherwise effects of "frozen turbulence" will blur the picture. Such experiments would be very time-consuming.

The case of positive nonlinearity is less clear. In this case the picture of turbulence is qualitatively similar to weak turbulence, but the slope of the spectrum fits better the MMT

spectrum. So far we do not have a satisfactory explanation of this phenomenon. Probably it could be explained by the presence of interacting quasisolitons. In this case again, experiments with a larger number of harmonics could give a result closer to WT predictions.

The relative "suppression" of weak turbulence in the MMT model can be explained by a peculiarity of the resonant conditions. In the one-dimensional case with $\alpha = 1/2$, only well-separated waves interact. Indeed, one can see from (2.10) that

$$\left|\frac{k_2}{k_1}\right| = \left(\frac{1}{\xi} + 1 + \xi\right)^2, \quad \xi > 0, \tag{15.1}$$

and therefore $\min |k_2/k_1| = 9$ is reached at $\xi = 1$. This phenomenon can be called "sparsity of resonances". Due to this sparsity, four wave resonances easily lose the competition with coherent structures - collapses and quasisolitons. In this sense the MMT model is not an optimal object for checking the validity of WT theory. We can offer the following model, which includes the interaction of two types of waves

$$\begin{aligned} H &= \int |k|^\alpha \left(|a_k|^2 + s\,|b_k|^2\right) dk \\ &+ \int |k k_1 k_2 k_3|^{\beta/4} \left(a_k^* a_1^* a_2 a_3 + 2\,p_1\, a_k^* b_1^* a_2 b_3 + p_2\, b_k^* b_1^* b_2 b_3\right) \\ &\times \delta(k + k_1 - k_2 - k_3)\, dk dk_1 dk_2 dk_3\,. \end{aligned} \tag{15.2}$$

If $\alpha > 1$ and $\beta < 2\alpha - 1$, the corresponding dynamical system does not describe any coherent structures which could compete with four-wave resonances. Meanwhile, for $s \neq 1$, it describes nontrivial resonant interactions for different waves propagating in the same direction. The system (15.2) looks like a possible object for the simulation of wave turbulence. In the special case $\alpha = 2$ and $\beta = 0$, it describes coupled NLS equations.

Acknowledgements

The authors are grateful to D. McLaughlin, A. Majda, D. Cai and E. Tabak for useful discussions and for providing their results before publication. This work was performed in the framework of the NATO Linkage Grant OUTR.LG 970583. V. Zakharov and A. Pushkarev also acknowledge support of the US Army, under the grant DACA 39-99-C-0018, and of ONR, under the grant N00014-98-1-0439. F. Dias and P. Guyenne acknowledge support of DGA, under the contract ERS 981135. A. Pushkarev wishes to thank F. Dias for his hospitality during a visit to Nice in the fall of 1998.

References

[1] R. E. Peierls, Zur kinetischen Theorie der Wärmeleitungen in Kristallen, Ann. Phys. 3, 1055-1101, 1929.

[2] K. Hasselmann, On the non-linear energy transfer in a gravity-wave spectrum. Part 1. General theory, J. Fluid Mech. 12, 481-500, 1962; K. Hasselmann, On the non-linear energy transfer in a gravity-wave spectrum. Part 2. Conservative theorems; wave-particle analogy; irreversibility, J. Fluid Mech. 15, 273-281, 1963.

[3] V. E. Zakharov, Stability of periodic waves of finite amplitude on a surface of deep fluid, J. Appl. Mech. Tech. Phys. 9, 190-194, 1968.

[4] A. N. Pushkarev and V. E. Zakharov, Turbulence of capillary waves, Phys. Rev. Lett. 76, 3320-3323, 1996.

[5] V. E. Zakharov and N. N. Filonenko, Weak turbulence of capillary waves, J. Appl. Mech. Tech. Phys. 4, 506-515, 1967.

[6] A. J. Majda, D. W. McLaughlin and E. G. Tabak, A one-dimensional model for dispersive wave turbulence, J. Nonlinear Sci. 6, 9-44, 1997.

[7] D. Cai, A. J. Majda, D. W. McLaughlin and E. G. Tabak, Spectral bifurcations in dispersive wave turbulence, Proc. Natl. Acad. Sci. 96, 14216-14221, 1999; D. Cai, D. McLaughlin, A. Majda and E. Tabak, Dispersive wave turbulence in one dimension, Physica D (this volume), 2000; D. Cai and D. McLaughlin, Chaotic and turbulent behavior of unstable one-dimensional nonlinear dispersive waves, J. Math. Phys., 2000 (to appear).

[8] V. E. Zakharov, Statistical theory of gravity and capillary waves on the surface of a finite-depth fluid, Eur. J. Mech. B/Fluids 18, 327-344, 1999.

[9] G. Falkovich, Bottleneck phenomenon in developed turbulence, Phys. Fluids 6, 1411-1414, 1994.

[10] A. N. Pushkarev, On the Kolmogorov and frozen turbulence in numerical simulation of capillary waves, Eur. J. Mech. B/Fluids 18, 345-352, 1999.

[11] V. E. Zakharov and E. A. Kuznetsov, Optical solitons and quasisolitons, ZhETF (JETP) 113, 1892-1913, 1998.

[12] S. Dyachenko, A. C. Newell, A. N. Pushkarev and V. E. Zakharov, Optical turbulence: weak turbulence, condensates and collapsing filaments in the nonlinear Schrödinger equation, Physica D 57, 96-160, 1992.

[13] V. E. Zakharov, V. Lvov and G. Falkovich, Kolmogorov Spectra of Turbulence I, Springer-Verlag, New-York, 1992.

[14] A. M. Balk and V. E. Zakharov, Stability of weak turbulence Kolmogorov spectra, Amer. Math. Soc. Transl. Ser. 2, Vol. 182, 31-81, 1998.

[15] E. A. Kuznetsov, A. M. Rubenchik and V. E. Zakharov, Soliton stability in plasmas and hydrodynamics, Phys. Rep. 142, 103-165, 1986.

[16] V. E. Zakharov, A. N. Pushkarev, V. F. Shvets and V. V. Yan'kov, Soliton turbulence, JETP Letters 48, 83-87, 1988.

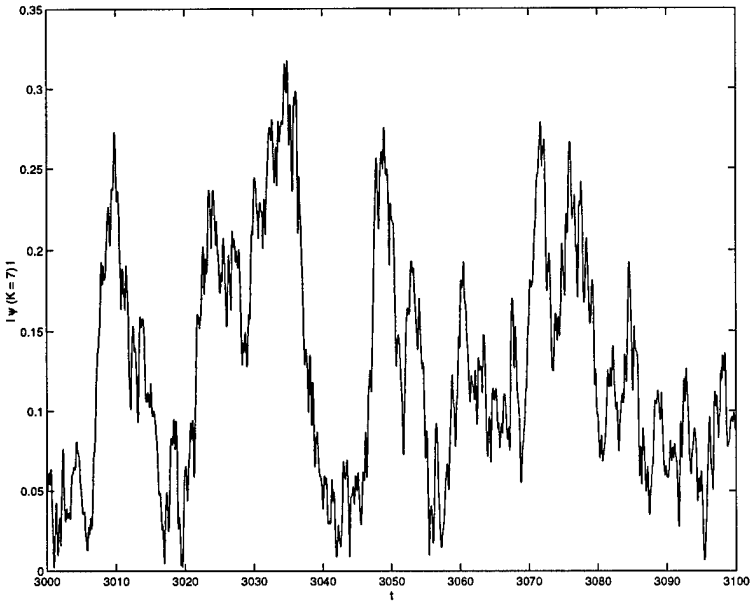

Figure 1: $\beta = 0, \lambda = -1$. Amplitude of the mode $k = 7$ vs. time.

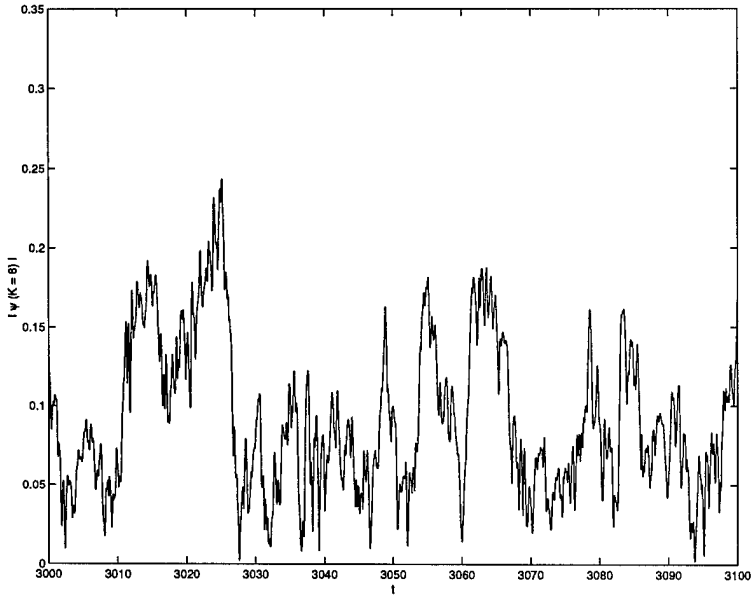

Figure 2: $\beta = 0, \lambda = -1$. Amplitude of the mode $k = 8$ vs. time.

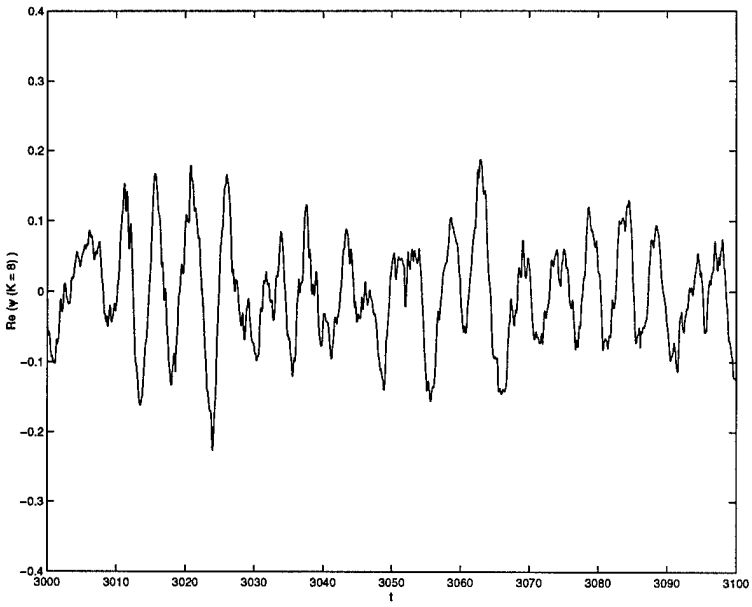

Figure 3: $\beta = 0, \lambda = -1$. Time evolution of the real part of the amplitude for the mode $k = 8$.

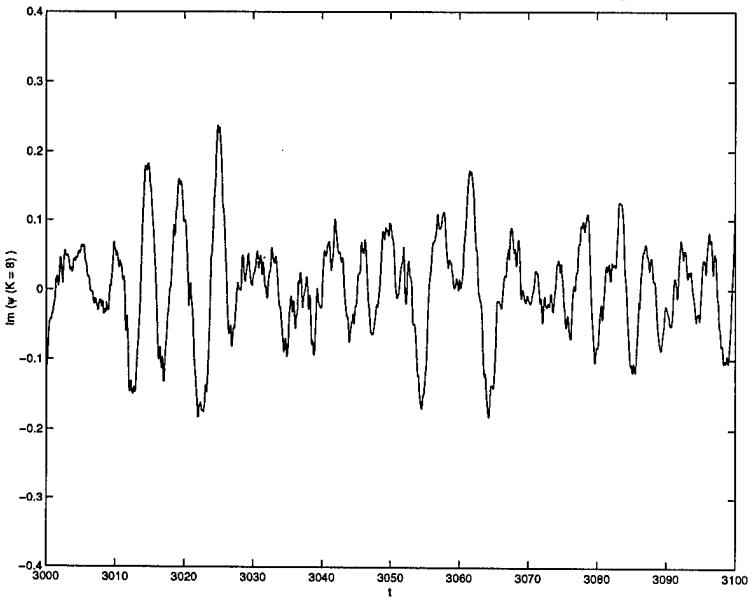

Figure 4: $\beta = 0, \lambda = -1$. Time evolution of the imaginary part of the amplitude for the mode $k = 8$.

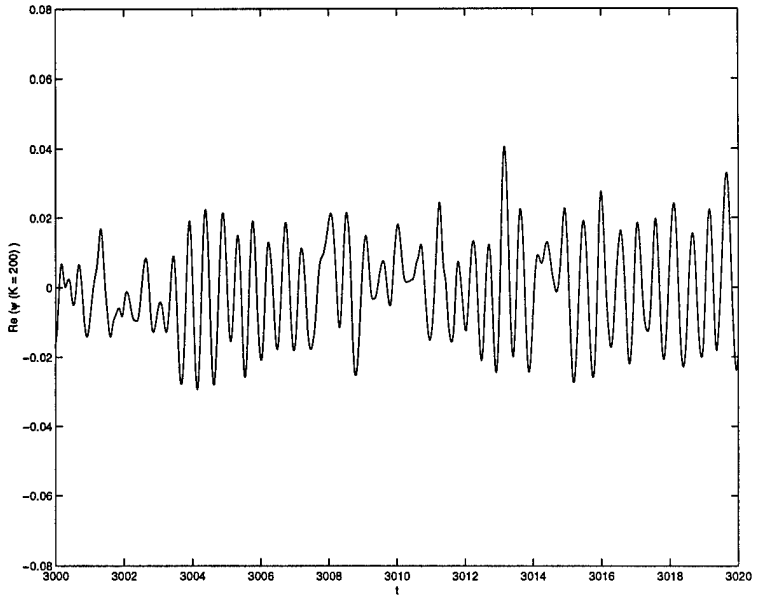

Figure 5: $\beta = 0, \lambda = -1$. Time evolution of the real part of the amplitude for the mode $k = 200$ (time resolution $\tau = 0.015$).

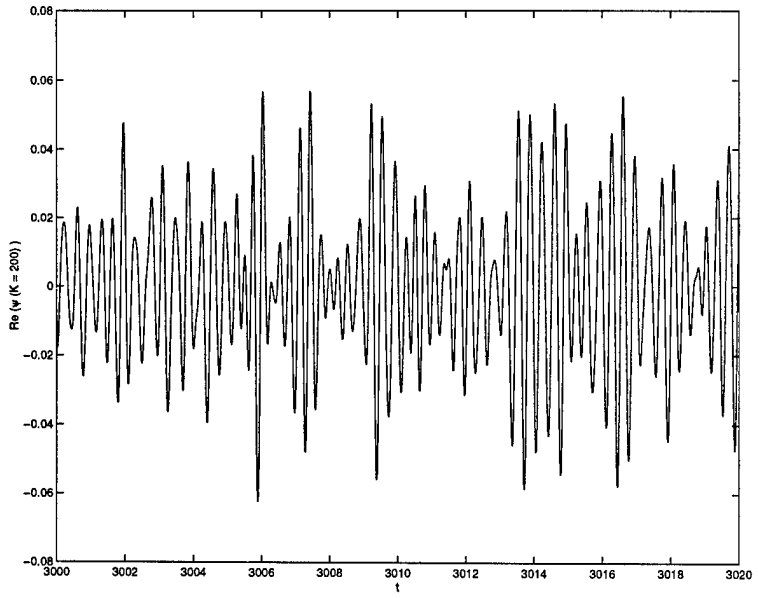

Figure 6: $\beta = 0, \lambda = +1$. Time evolution of the real part of the amplitude for the mode $k = 200$ (time resolution $\tau = 0.015$).

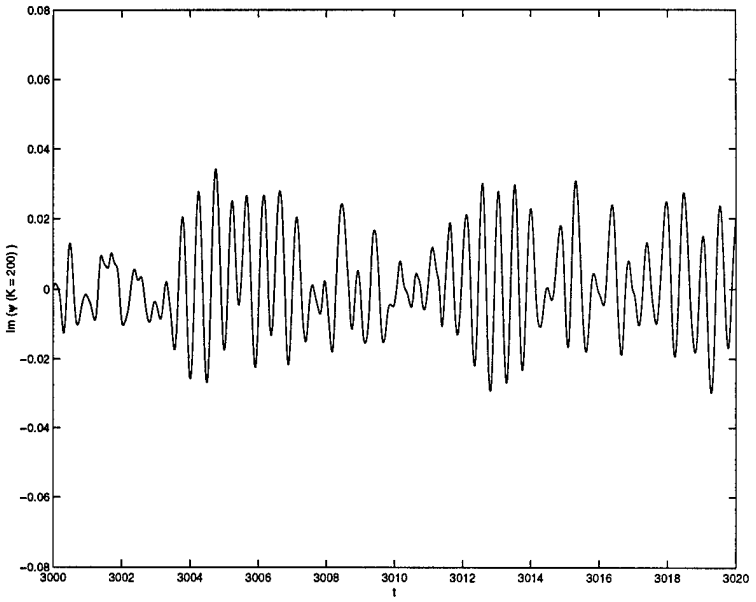

Figure 7: $\beta = 0, \lambda = -1$. Time evolution of the imaginary part of the amplitude for the mode $k = 200$ (time resolution $\tau = 0.015$).

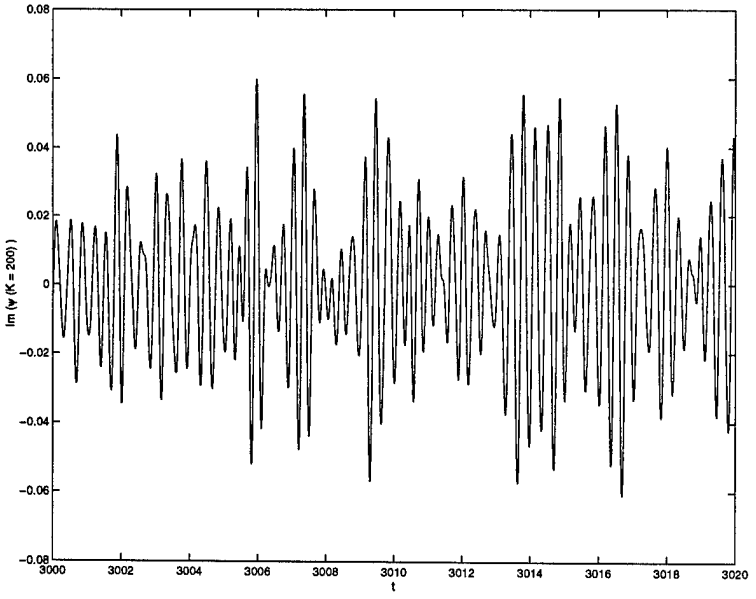

Figure 8: $\beta = 0, \lambda = +1$. Time evolution of the imaginary part of the amplitude for the mode $k = 200$ (time resolution $\tau = 0.015$).

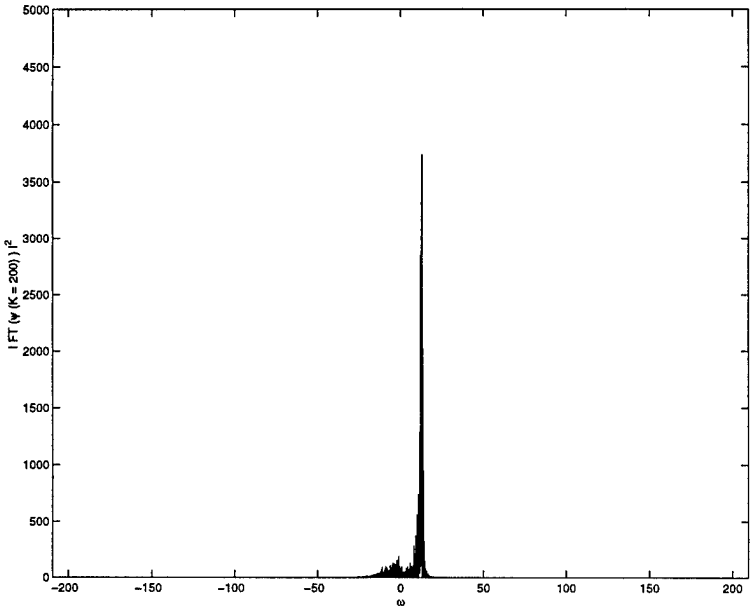

Figure 9: $\beta = 0, \lambda = -1$. Square amplitude of the Fourier transform for the mode $k = 200$ vs. frequency (time resolution $\tau = 0.015$).

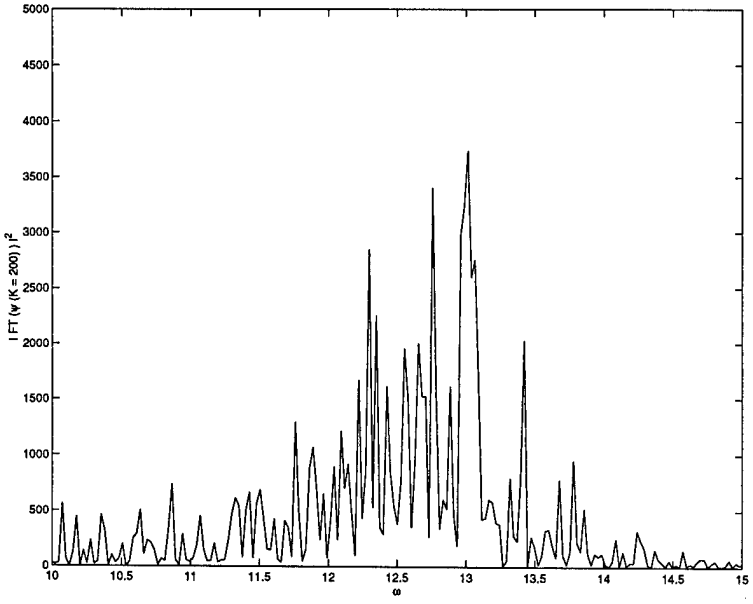

Figure 10: $\beta = 0, \lambda = -1$. Same as before but with a zoom on a smaller frequency window.

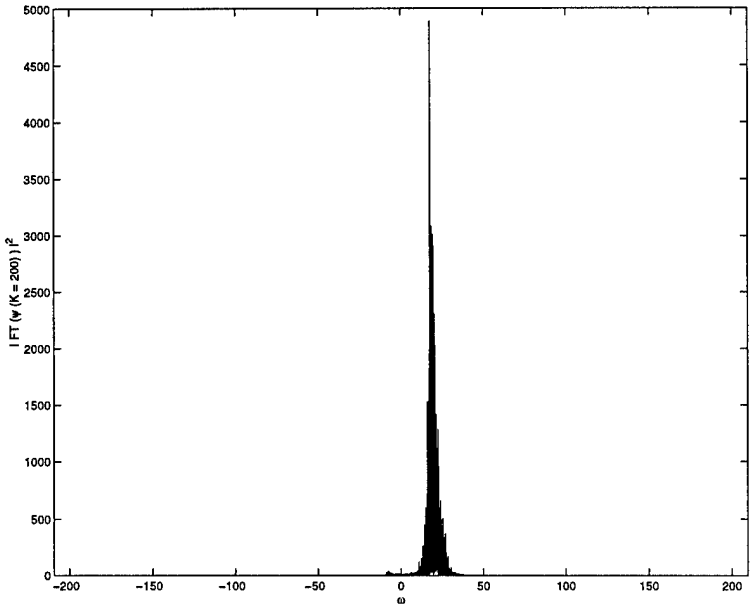

Figure 11: $\beta = 0, \lambda = +1$. Square amplitude of the Fourier transform for the mode $k = 200$ vs. frequency (time resolution $\tau = 0.015$).

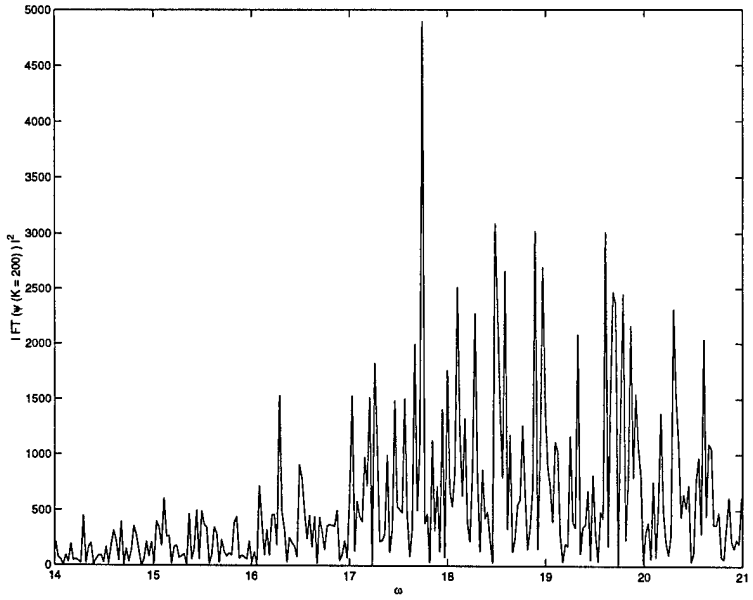

Figure 12: $\beta = 0, \lambda = +1$. Same as before but with a zoom on a smaller frequency window.

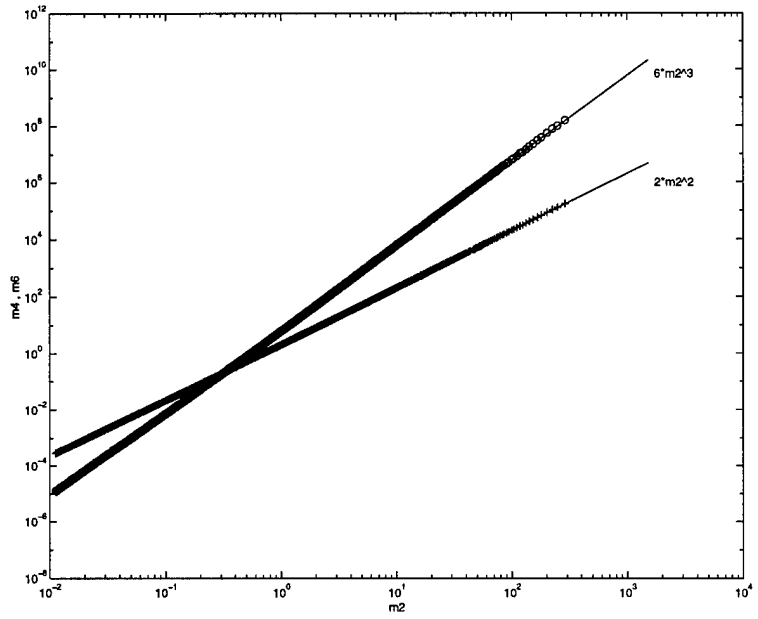

Figure 13: $\beta = 0$, $\lambda = +1$. Fourth (crosses) and sixth-order (circles) moments as functions of the second-order moments. The straight lines are the fitted Gaussian laws.

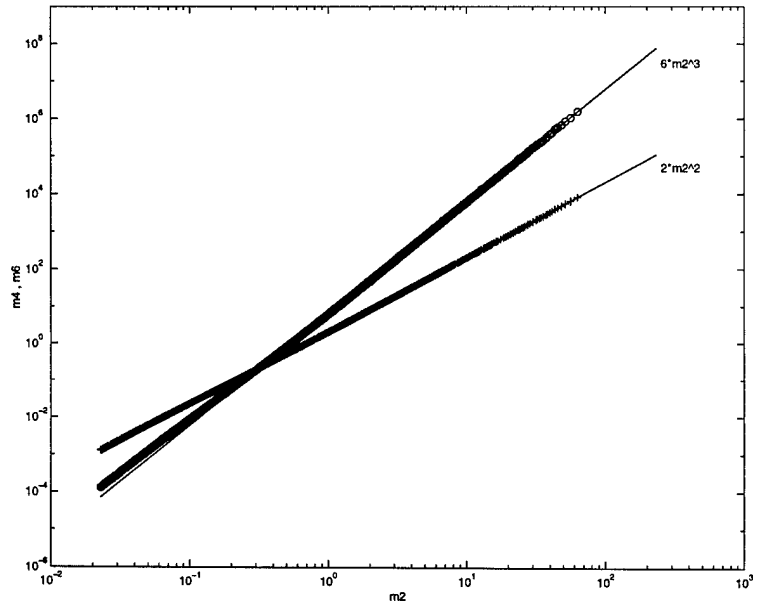

Figure 14: $\beta = 0$, $\lambda = -1$. Fourth (crosses) and sixth-order (circles) moments as functions of the second-order moments. The straight lines are the fitted Gaussian laws.

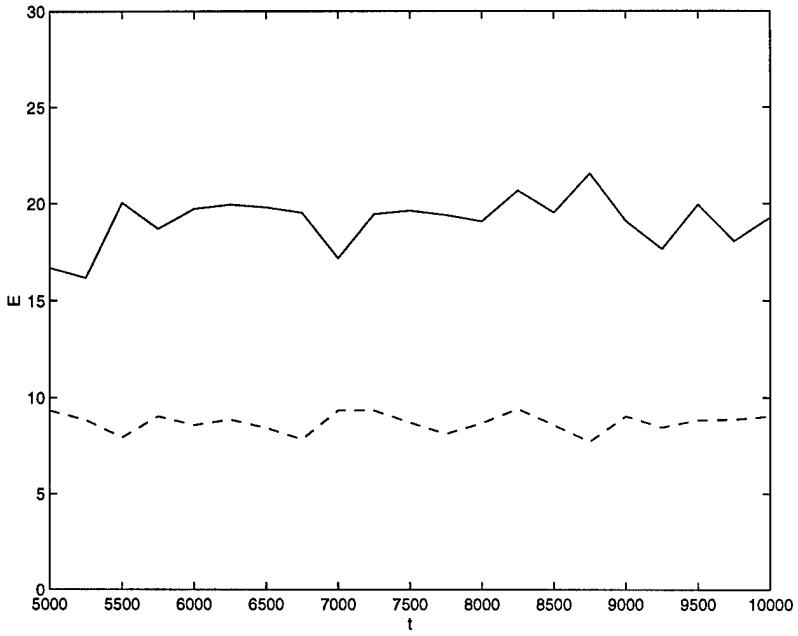

Figure 15: $\beta = 0$. Quadratic energy vs. time. $\lambda = +1$ (solid line), $\lambda = -1$ (dashed line).

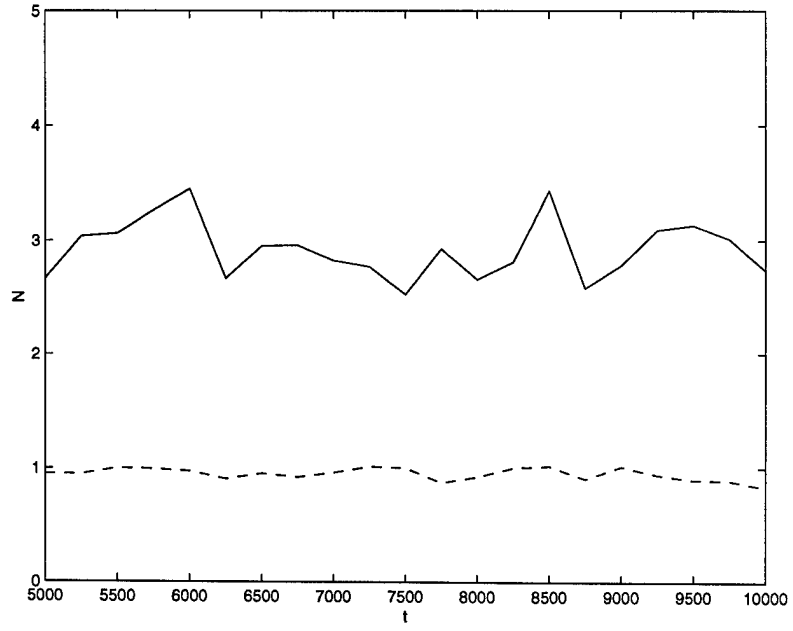

Figure 16: $\beta = 0$. Number of particles vs. time. $\lambda = +1$ (solid line), $\lambda = -1$ (dashed line).

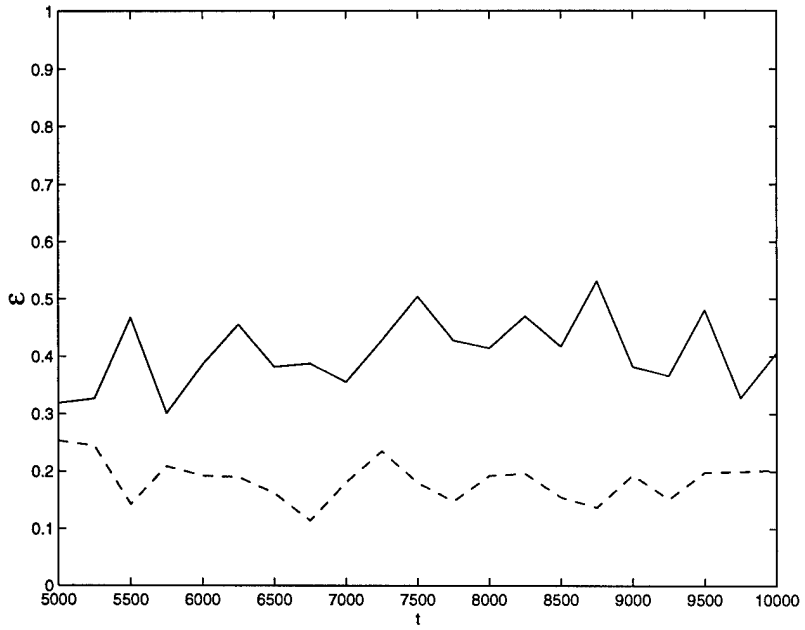

Figure 17: $\beta = 0$. Average nonlinearity $\epsilon = |H_{NL}/H_L|$ vs. time. $\lambda = +1$ (solid line), $\lambda = -1$ (dashed line).

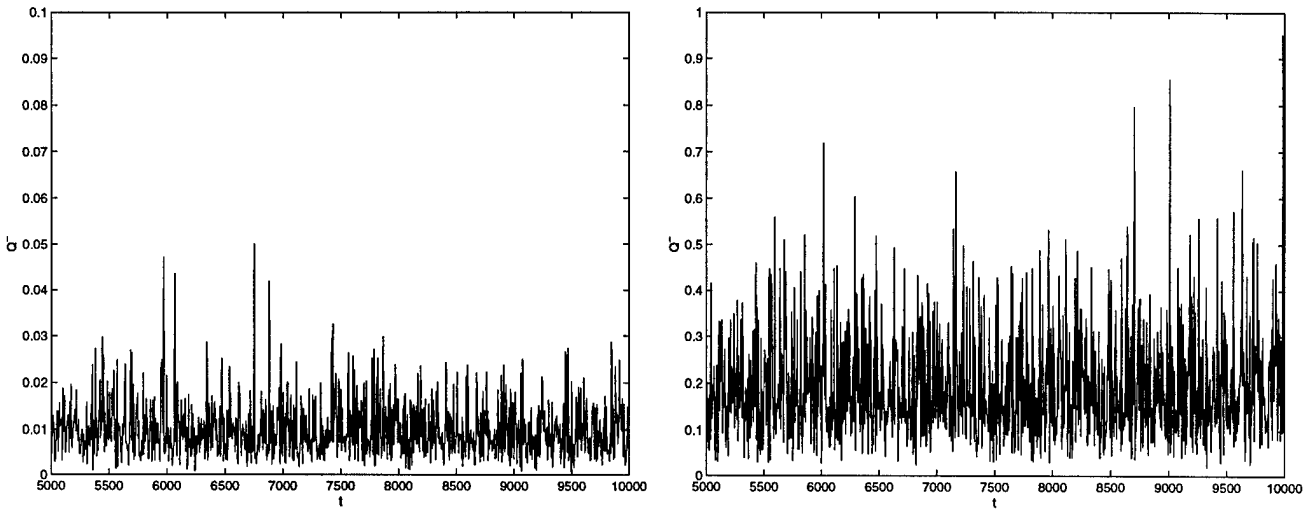

Figure 18: $\beta = 0$, $\lambda = -1$ (left), $\lambda = +1$ (right). Dissipation rate of particles at low wave numbers vs. time.

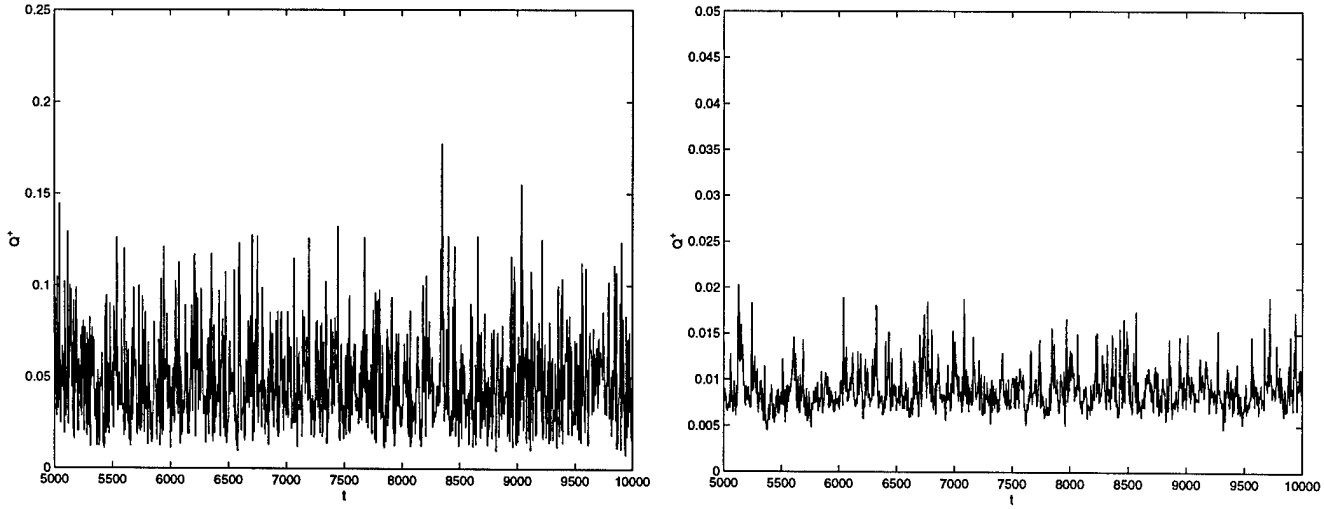

Figure 19: $\beta = 0$, $\lambda = -1$ (left), $\lambda = +1$ (right). Dissipation rate of particles at high wave numbers vs. time.

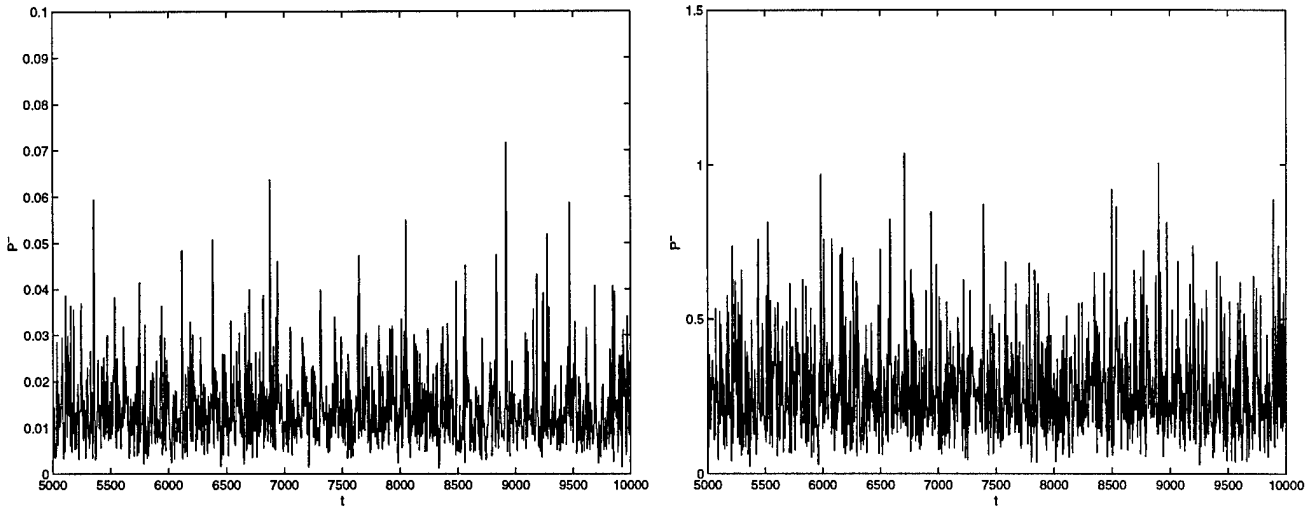

Figure 20: $\beta = 0$, $\lambda = -1$ (left), $\lambda = +1$ (right). Dissipation rate of energy at low wave numbers vs. time.

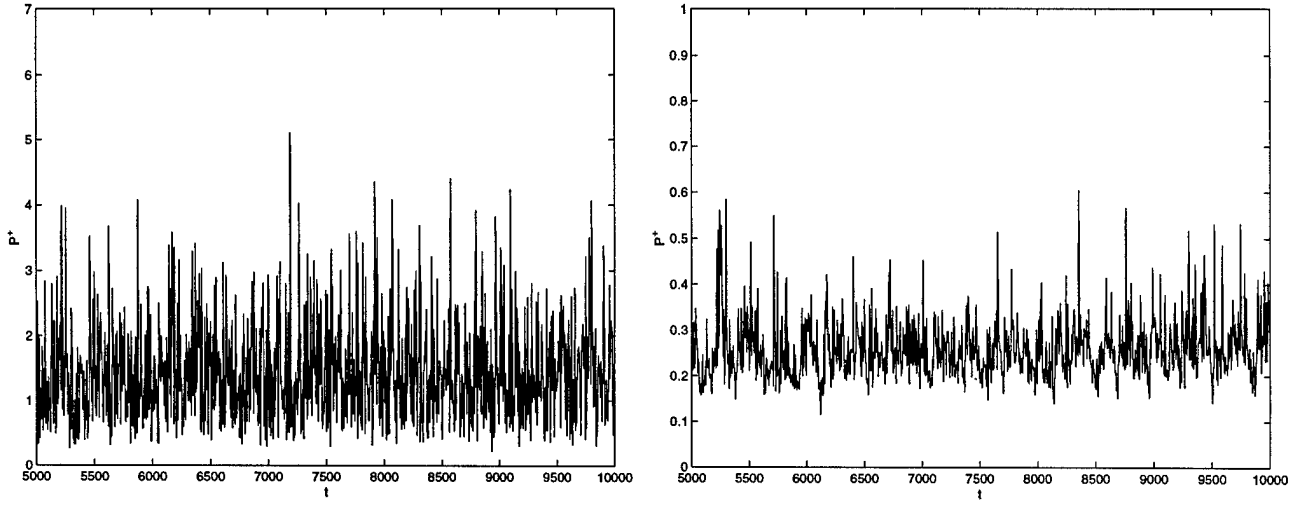

Figure 21: $\beta = 0$, $\lambda = -1$ (left), $\lambda = +1$ (right). Dissipation rate of energy at high wave numbers vs. time.

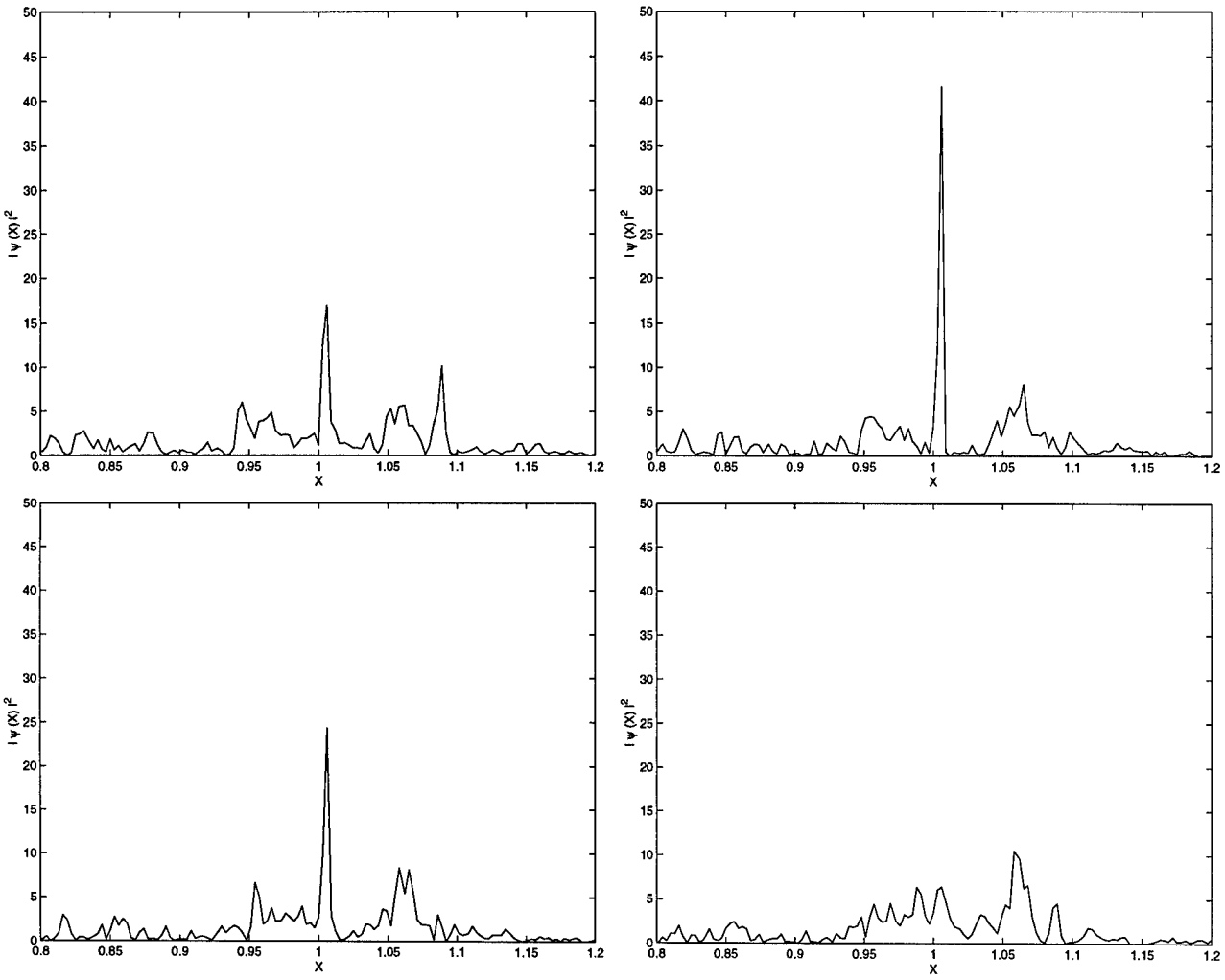

Figure 22: $\beta = 0$, $\lambda = -1$. Evolution of a single collapsing peak at $x \simeq 1.006$ at $t = 4999.98, 5000.19, 5000.295$ and $t = 5000.4$ from left to right and from top to bottom.

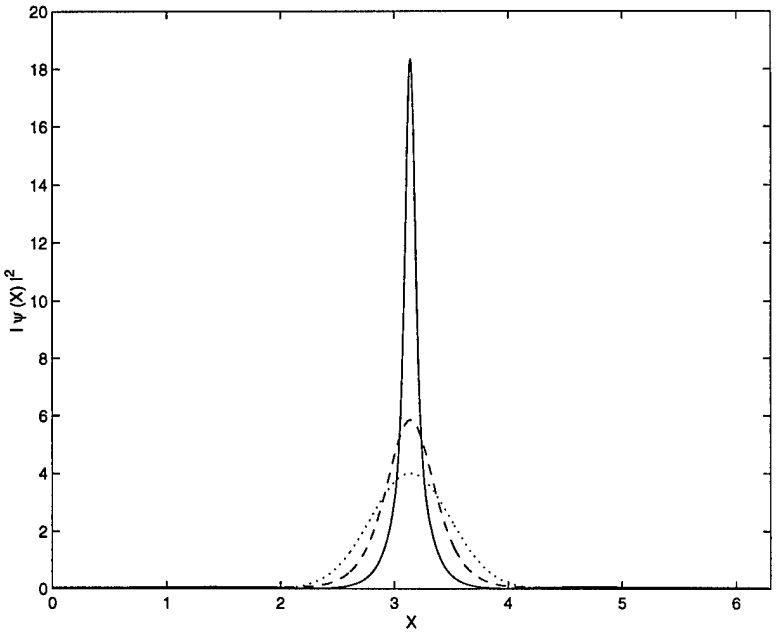

Figure 23: $\beta = 0, \lambda = -1$. Evolution towards a collapsing peak of the isolated solution for the initial amplitude $\psi_0 = 2$. Dotted line $t = 0$, dashed line $t = 0.55$, solid line $t = 1.1$.

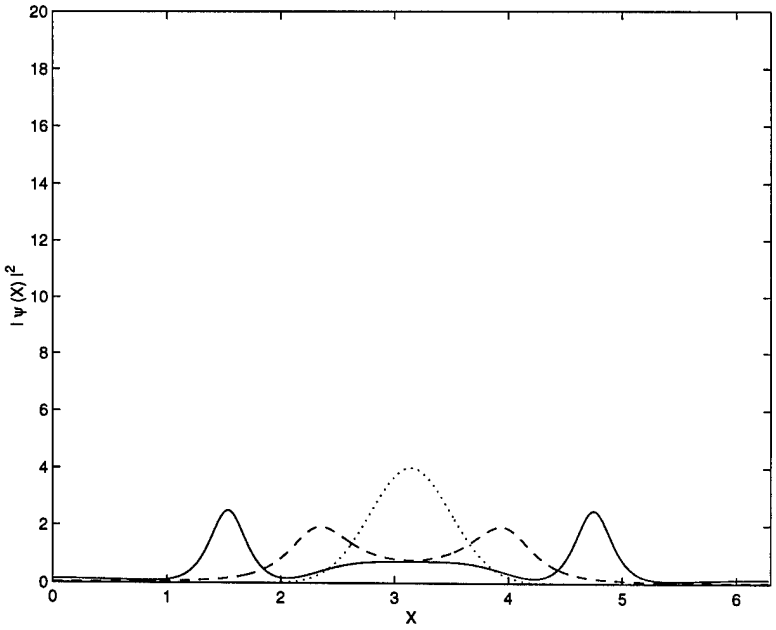

Figure 24: $\beta = 0, \lambda = +1$. Evolution towards decay of the isolated solution for the initial amplitude $\psi_0 = 2$. Dotted line $t = 0$, dashed line $t = 1.65$, solid line $t = 3.85$.

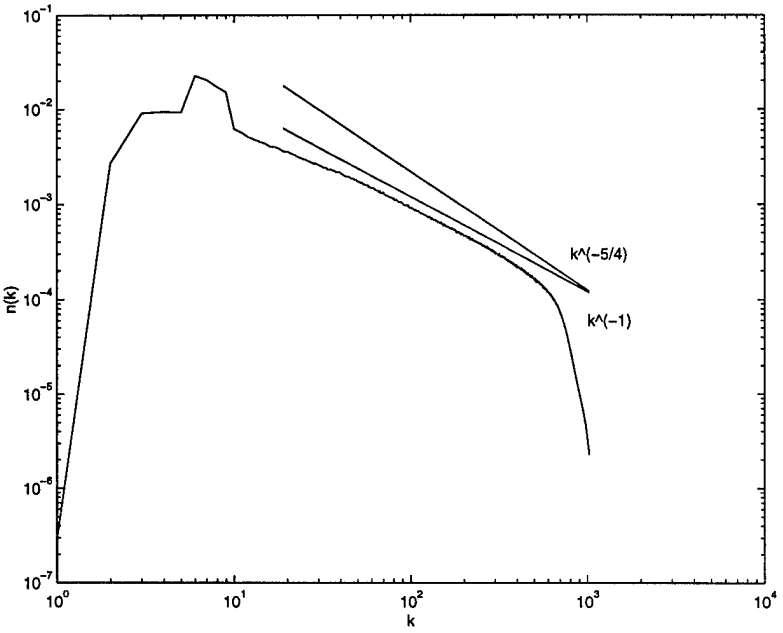

Figure 25: $\beta = 0, \lambda = -1$. Computed spectrum vs. wave number. The theoretical slopes are shown as well (k^{-1} for WT and $k^{-5/4}$ for MMT).

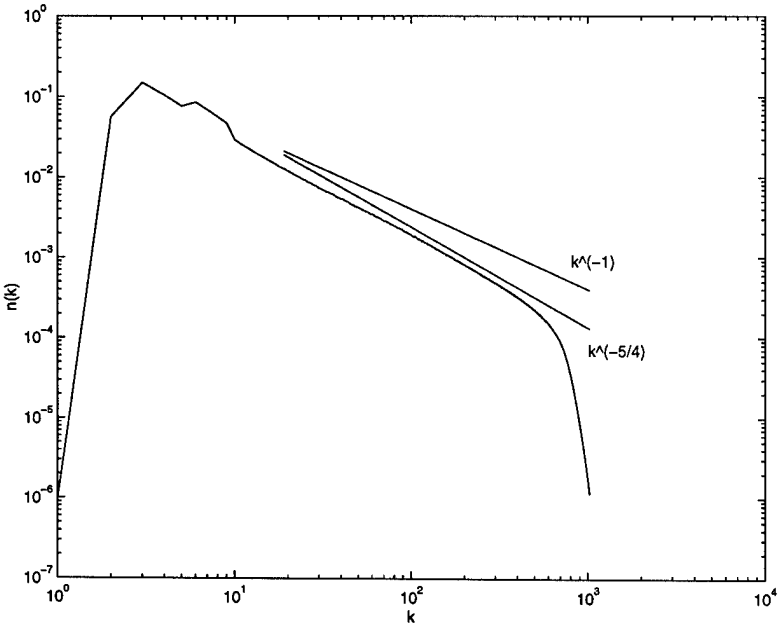

Figure 26: $\beta = 0, \lambda = +1$. Computed spectrum vs. wave number. The theoretical slopes are shown as well (k^{-1} for WT and $k^{-5/4}$ for MMT).

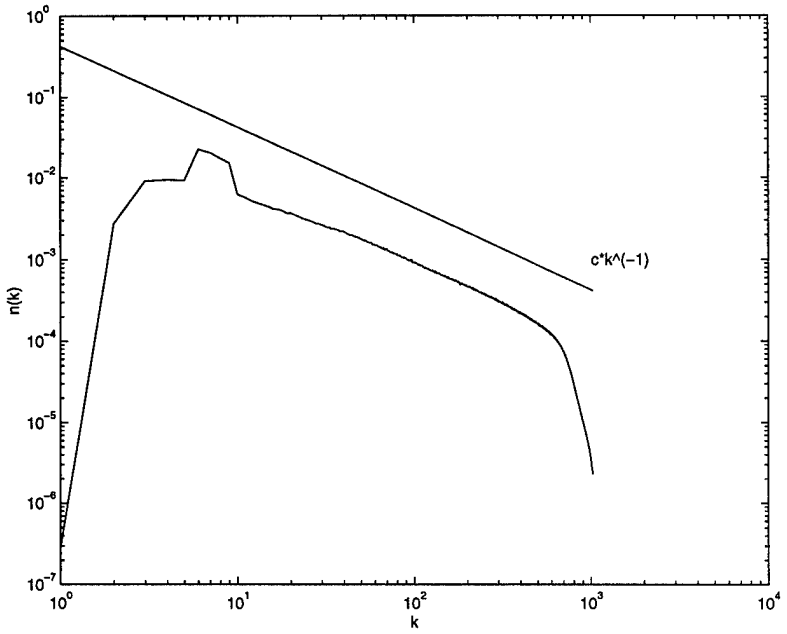

Figure 27: $\beta = 0, \lambda = -1$. Computed spectrum and WT spectrum vs. wave number. The WT spectrum (straight line) is given by $n(k) = c\,k^{-1}$ with $c = a\,P^{1/3} \simeq 0.42$.

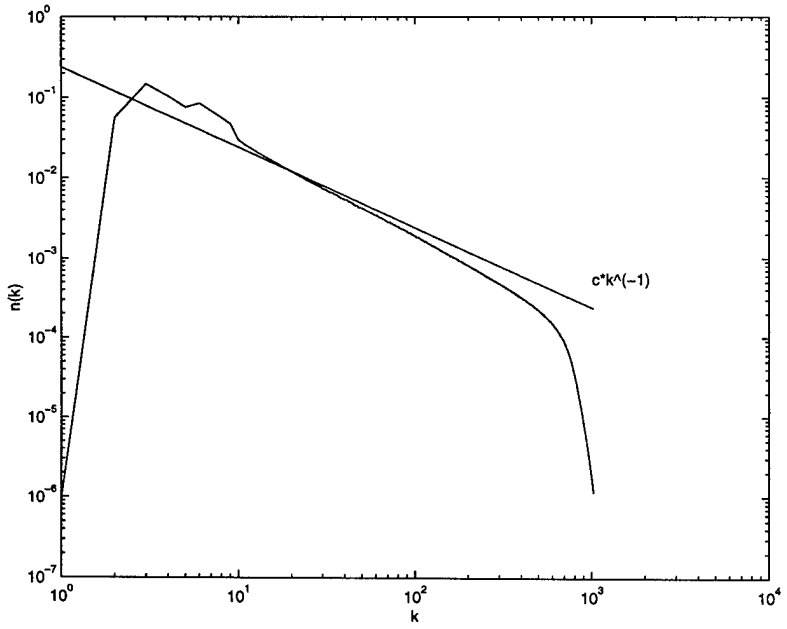

Figure 28: $\beta = 0, \lambda = +1$. Computed spectrum and WT spectrum vs. wave number. The WT spectrum (straight line) is given by $n(k) = c\,k^{-1}$ with $c = a\,P^{1/3} \simeq 0.24$.

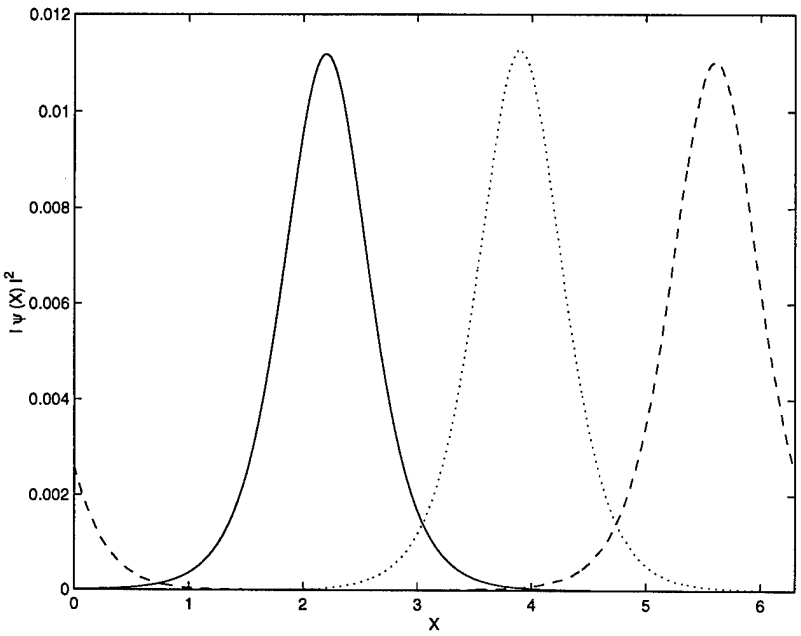

Figure 29: $\beta = 0, \lambda = +1$. Evolution of the initial quasisoliton for $q/k_m = 0.1$. Solid line $t = 0$, dotted line $t = 1250$, dashed line $t = 2500$.

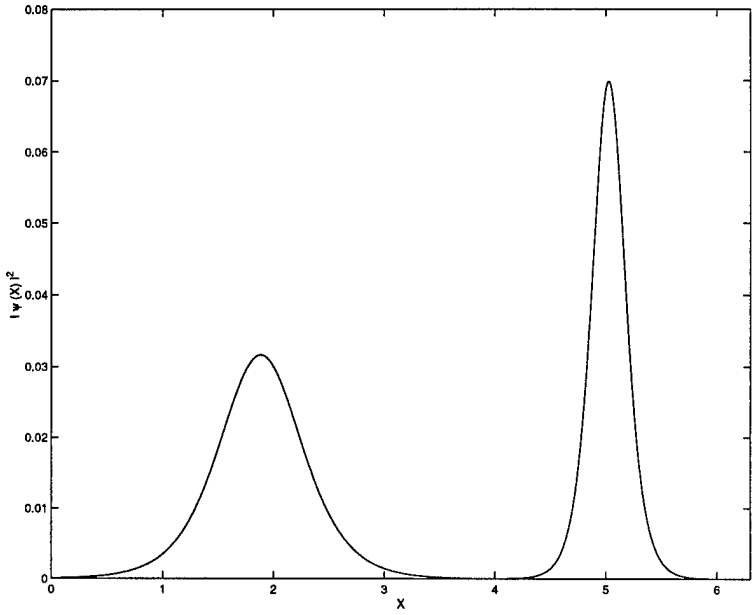

Figure 30: $\beta = 0, \lambda = +1$. Interaction of two initial quasisolitons at $t = 0$. The smaller and bigger ones correspond to $q/k_m = 0.2$ and 0.25 respectively.

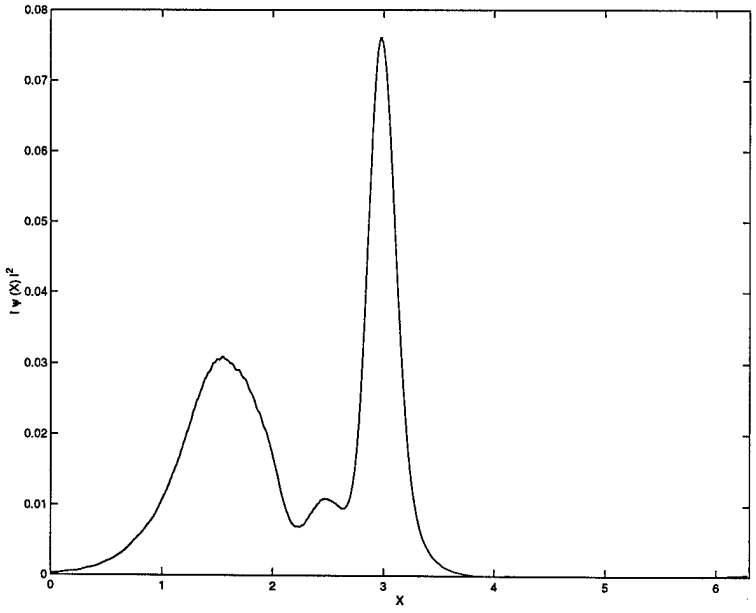

Figure 31: $\beta = 0, \lambda = +1$. Interaction of two initial quasisolitons at $t = 37.5$.

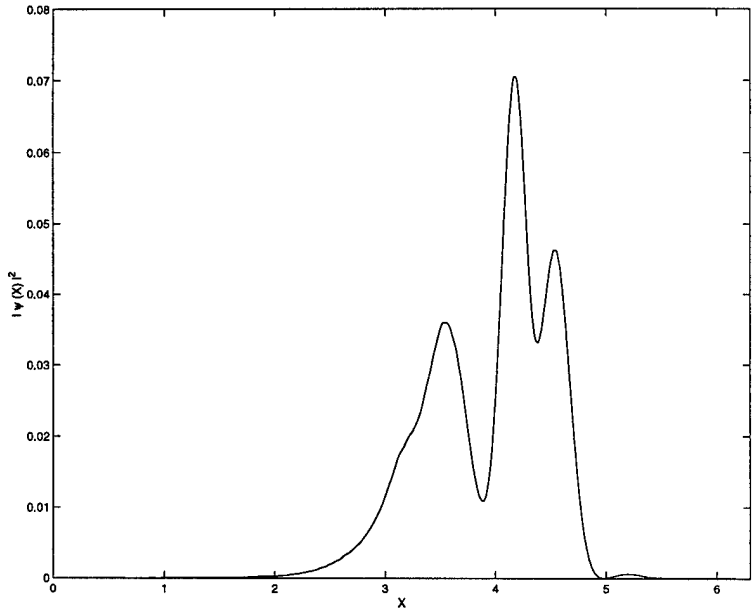

Figure 32: $\beta = 0, \lambda = +1$. Interaction of two initial quasisolitons at $t = 50$.

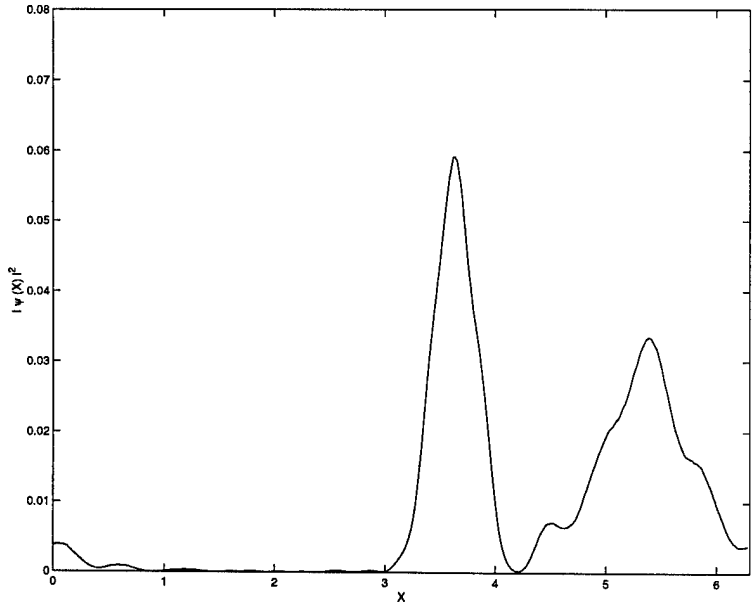

Figure 33: $\beta = 0, \lambda = +1$. Interaction of two initial quasisolitons at $t = 100$.

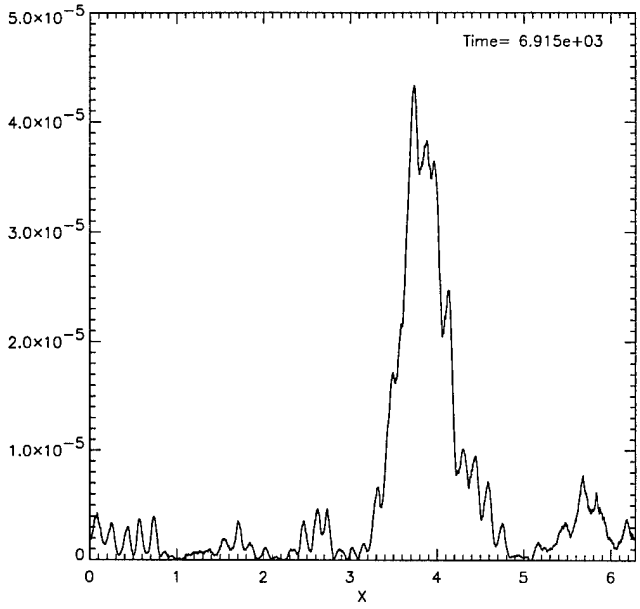

Figure 34: $\beta = 3, \lambda = +1$. Single moving soliton, $t = 6915$.

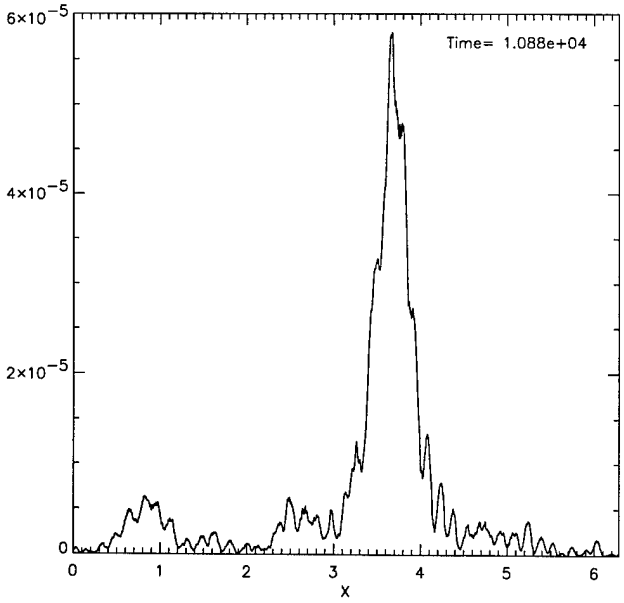

Figure 35: $\beta = 3, \lambda = +1$. Single moving soliton, $t = 10880$.

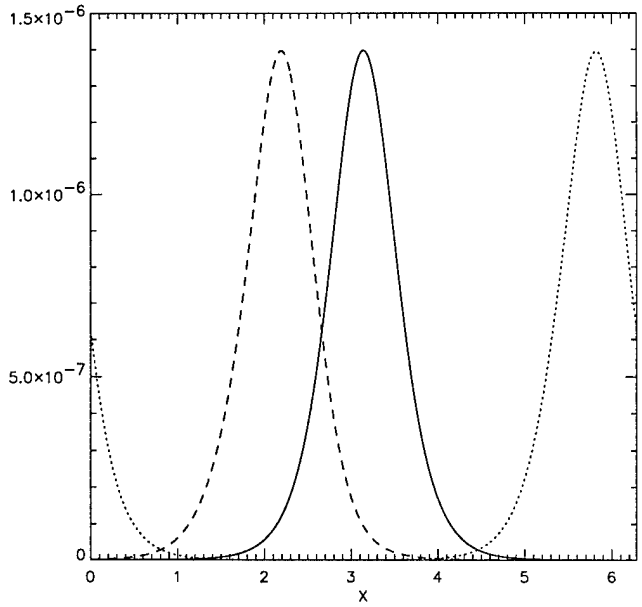

Figure 36: $\beta = 3, \lambda = +1$. Evolution of the initial quasisoliton for $q/k_m = 0.1$. Solid line $t = 0$, dotted line $t = 23.6$, dashed line $t = 47.1$.

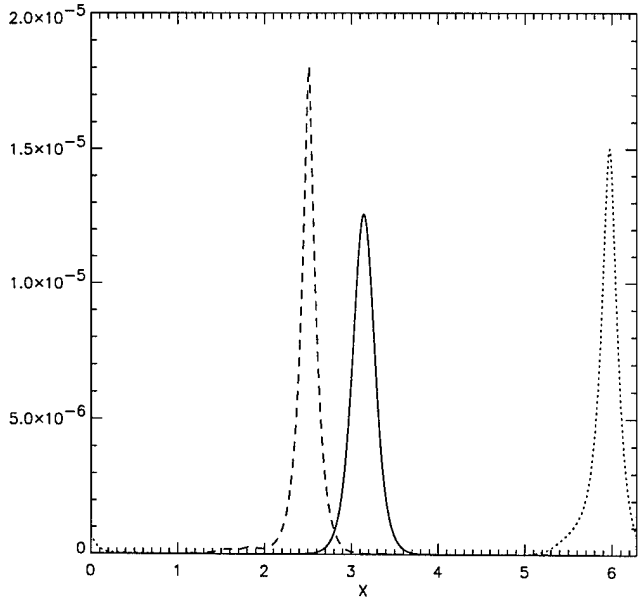

Figure 37: $\beta = 3, \lambda = +1$. Evolution of the initial quasisoliton for $q/k_m = 0.3$. Solid line $t = 0$, dotted line $t = 23.6$, dashed line $t = 47.1$.